1506
UNIVERSITÀ
DEGLI STUDI
DI URBINO
CARLO BO

Department of Biomolecular Science

Ph.D. Programme in Life Sciences, Health and Biotechnology

Cell and organisms biology

XXXIV cycle

FUNCTIONAL PROPERTIES OF PLANT BIOACTIVE COMPOUNDS OF BIOMEDICAL INTEREST

SSD: MED/04

Coordinator: Prof. Marco Bruno Luigi Rocchi

Supervisor: Prof. Maria Cristina Albertini

Ph.D. student: Sofia Coppari

ACADEMIC YEAR
2020/2021

To strive, to seek, to find

and not to yield.

Alfred Tennyson, 1833

Table of contents

Abstract

Plant bioactive compounds are good candidates in biomedicine and the investigation of their functional activities deserves particular attention for their clinical application. This study exploits innovative *in silico*, *in vitro* and *in vivo* approaches to investigate the functional properties of plant secondary metabolites of biomedicine interest.

The *in silico* analyses were supported by bioinformatics tools that have been used to study the ability of biomaterials surface to modulate cellular pathways. Other tools have been used to find food-containing miRs involved in the modulation of the inflammatory process.

In vitro analyses were used to study antimicrobial, antioxidant, anti-inflammaging, wound healing and hypoglycaemic abilities of bioactive compounds. Using *P. Spinosa* L. fruit extract, based on the secondary metabolites analysed (through quali- and quantitative analyses performed with HPLC-DAD and HPLC/MS), the investigation has been performed in microorganisms, cell free and cell based systems.

In vivo analyses were performed in the model organism *C. elegans* to determine antioxidant and anti-aging activities of the *P. Spinosa* L. fruit extract.

Finally, leucosomes loaded with *P. Spinosa* L. fruit extract were used as biomimetic nanosystems to analyse the anti-inflammatory and wound healing properties.

Overall, our data suggest that the use of secondary plant metabolites may be an adjuvant therapeutic treatment to counteract the pro-inflammatory and pro-oxidative conditions induced by aging and the associated diseases. These properties can also be exploited in biomedicine, both for the functionalization of biomaterials and for drug delivery.

1. INTRODUCTION

There is a growing interest in associating “biological” and “material” systems to advance biomedical researchers in innovative opportunities related to biomaterials. A biomaterial is a material designed to take a form that can direct, through interactions with living systems, the course of any therapeutic or diagnostic procedure [1]. Biomaterials are required to act harmoniously with the host. Investigating cellular *in vitro* or *in vivo* phenotypic responses to the material surface helps to determine the associated biocompatibility [2]. The study of biomaterials has focused mainly on the nanofibers scaffold, a three-dimensional substrate that mimics the extracellular matrix (ECM) favouring cell adhesion, proliferation and differentiation. Among the methods for the production of nanofibers, electrospinning is the most efficient and versatile and allows the production of nano-structured fibers that can be used in the process of wound repair, encapsulation of active substances, controlled release systems and functional food [3, 4]. The nanofibrous scaffolds have a very high surface/volume ratio and adjustable porosity and in this way, it is possible to obtain a 3D culture with a high structural similarity to the ECM which influences the behaviour of the cells and which adopt morphologies similar to those assumed *in vivo*. The architecture of the scaffold governs the cellular response leading to changes in intracellular signalling pathways, which results in a modification of gene expression. There are many variables that can influence the interaction of cells with biomaterials such as surface topography [5] and material surface chemistry [6]. In recent years, biomaterials and natural molecules coordination has attracted considerable interest in engineering functional materials [7]. Surface functionalization is a useful and versatile procedure for making multifunctional materials, combining the properties of both substrates and grafted molecules. The coupling between biomaterials and polyphenols extracts allows combining their properties, with

possible benefits on human health. Scientific literature has shown that functionalization of biomaterials with polyphenols improves the performance of final medical devices [8]. For example, the polyphenols extracted from green tea coupled with bioactive glasses have been shown to preserve the viability and proliferation rate and of healthy osteoblastic progenitor cells [9].

Plant polyphenols are usually referred to as a diverse group of compounds containing multiple phenolic functionalities, which are produced as secondary metabolites by most of higher plants [10]. Phenolic compounds have been documented to possess potent antioxidant, antimicrobial, enzyme inhibitory, anti-inflammatory, antimutagenic, anticarcinogenic, anti-aging effects and complexing properties towards proteins, stimulating antioxidant enzymes in the human body [11]. These properties depend on the potential of polyphenols to reduce the production of reactive oxygen species (ROS) through the inhibition of oxidase, decreasing the production of superoxide, improving the mitochondrial oxidative process and inhibiting the formation of oxidized low-density lipoproteins [12]. These abilities make polyphenols interesting for the treatment of various diseases like inflammation or cancer, but also for anti-aging purposes and for nutraceutical applications.

In recent years, numerous studies have highlighted the role of inflammaging defined as a systemic, chronic, low-grade inflammatory state associated with aging [13]. This phenomenon is characterized by the increased production of pro-inflammatory factors by senescent cells in the tissue microenvironment. This secretory phenotype is defined SASP (Senescence-Associated Secretory Phenotype**)** and involves the secretion of different molecules, including interleukin (IL)-1α/β, IL-6, IL-8, transforming growth factor (TGF)-β and tumor necrosis factor (TNF)-α [14]. MicroRNAs have also been reported to play a role in SASP and its systemic spread [15]. These microRNAs have been recently defined as inflamma-miRs and they are involved in inflammation and oxidative stress. It has been

documented that the interaction between inflamma-miRs and the intestinal microbiome can participate to the balance between pro- and anti-inflammatory factors potentially contributing to the development of some diseases [16]. Notably, inflamma-miRs may integrate signals from food and gut microbiota by modulating common signalling pathways [17, 18].

Of great interest is the role played by miR-126 which regulates the expression of the VCAM-1 (Vascular Cell Adhesion Molecule 1) and ICAM-1 (Intercellular Adhesion Molecule 1) proteins responsible for the endothelial adhesion process [19]. The partial interaction that is established between this miRNA and the 3 'UTR region inhibits the translation of the proteins. Another important miRNA is miR-146a which is involved in the inhibition of the expression of its targets IRAK-1 (Interleukin-1 receptor-associated kinases 1) and TRAF-6 (TNF Receptor Associated Factor-6), two proteins involved in the signal transduction of TLR4 (Toll-Like Receptor 4). The TLR4 signaling pathway, through the IRAK-1 mediator, promotes the activation of the NF-κB transcriptional complex, which is responsible for the production of pro-inflammatory cytokines, including IL-6. The miR-146a also regulates TLR4 pathway activation through a negative feedback loop. Hence, during a pro-inflammatory condition, miR-146a is down-regulated and allows the expression of IRAK-1 and IL-6 [20].

The release of SASP factors, including proteins and nucleic acids, at the paracrine and systemic levels, fuels inflammation and induces the recruitment of immune cells to eliminate damaged cells from tissues [21]. Thus, senescence appears to have evolved as a protective mechanism against damage induced by a variety of stressors and play a physiological role in promoting wound healing, reducing the expansion of transformed cells, limiting fibrosis and aiding cell reprogramming *in vivo* [22–24]. However, a chronic SASP is associated with the spread of senescence and a higher pro-inflammatory state leading to increased tissue injury and poor healing [25]. This condition depends not only by the persisting inflammatory cells

and generation of pro-inflammatory cytokines, but also by increased ROS that can lead to direct damage of cells or extracellular matrix molecules [26]. SASP is also related to the development of Age-Related Diseases (ARDs) associated with a chronic inflammatory state including type 2 Diabetes Mellitus, cancer, cardiovascular and neurodegenerative diseases (Alzheimer's and Parkinson's). Type 2 Diabetes Mellitus is a chronic disease characterized by high levels of glucose in the blood due to insulin-resistance where the chronic hyperglycemia is a condition that fosters oxidative stress and pro-inflammatory signals, both involved in the promotion of cellular senescence.

Since SASP exerts pro-oxidant and pro-inflammatory activities, it is likely that bioactive compounds found in food with antioxidant or anti-inflammatory properties could serve as anti-SASP agents and promote health beneficial effects [27]. In recent years there has been a growing interest in the isolation of bioactive compounds from natural sources, in particular from fruits, vegetables, cereals and seeds [28]. As illustrated by Li et al. [29] wild fruits, including *P. spinosa* L. fruits, are a source of important bioactive compounds, such as anthocyanins and flavonoids. Many studies have shown that wild fruits have various health benefits such as anti-inflammatory, antimicrobial, antitumor and antioxidant activities, which include free radical scavenging. For this reason they can potentially be used as functional foods and a source of new therapeutic preparations to prevent and treat various chronic diseases [30, 31]. Natural products such as plants and their extracts have been used for thousands of years for their beneficial effects, and today an increasing attention is paid to the search for natural extracts that are potentially active in inflammatory states and microbial infections. The *Prunus spinosa* L. commonly called "blackthorn", belonging to the *Rosaceae* family and to the *Prunus* genus, grows spontaneously in uncultivated land as a thorny shrub and all the components of the tree are widely used in phytotherapy. The blackthorn is a deciduous fruit common in all the mountainous wooded places of Italy and other provinces of

Europe, western Asia, north-western Africa and is also naturalized in New Zealand and North America [32]. Each part of the plant, namely the flowers, fruits, leaves and young branches of the blackthorn, have peculiar beneficial properties [33]. In particular, the flowers are used as infusions for their purgative, diuretic and detoxifying properties. The fruits, on the contrary, are used as astringents, and in mild inflammatory states of the oral and pharyngeal mucosa [34]. The beneficial effects of *P. Spinosa* L. are probably attributed to the polyphenols present in the plant which include flavonoids, anthocyanins, phenolic acids, flavonols, tannins and ascorbic acid [35]. These compounds individually or combined are responsible for various health benefits closely related to the phenolic content. The most abundant compounds present in the fruit of *P. Spinosa* L. are anthocyanins, the pigments responsible for the blue-violet colour of the blackthorn, in particular cyanidin-3-O-rutinoside, cyanidin 3-glucoside and peonidin-3-O-rutinoside [36]. Anthocyanins have long been known for some biological properties: they reduce capillary permeability, prevent collagen degradation, reduce oedema and act as free radical scavenger. The other phenolic compounds present are hydroxycinnamic acids, hydroxybenzoic acids, and especially flavonols, such as some derivatives of quercetin (quercetin-3-O-rutinoside, quercetin-3-O-hexoside-O-pentoside, quercetin-3-O-glucoside, quercetin-3-O-pentoside and quercetin-3-O-rhamnoside) [37]. Specifically, flavonols can play a role as antioxidants, positively regulating blood and lymphatic microcirculation, strengthening the immune system and preventing diseases associated with chronic inflammation. Other active components of the plant include phenolic acids such as chlorogenic acid, gallic acid, trans-caftaric acid, trans-coutaric acid, caffeic acid, sirginic acid, p-coumaric acid and flavanols such as procyanidin B2, (+)-catechin, (-)-epicatechin and hyperoside [32, 38].

The main disadvantage of using natural extracts is their low bioavailability [39]. Effective concentration of these substances are unlikely to be found in the bloodstream and therefore

hardly exert biological properties in the site of action they have to reach. In the context of biomaterials, these are used in nanomedicine for the drug delivery system (DDS). The DDS are developed in order to improve the pharmacokinetics and pharmacodynamics of substances for therapeutic use and to allow their desired dose delivery in the targeted site. To meet the most advanced therapeutic needs, innovative DDSs such as nanoparticles have been developed. The nanodelivery systems can carry the drug adsorbed or conjugated to the surface of the particles, encapsulated inside or can even be released in the matrix. When the nanoparticles are loaded with a drug, they can also be directed towards a specific pathological site. Different types of nanocarriers are used in drug delivery formulations such as liposomes, polymer micelles, dendrimers, polymer-drug conjugates, inorganic nanoparticles and carbonaceous nanomaterials. Liposomes are the most common and studied nanocarriers, while polymeric nanoparticles represent one of the most innovative approaches for drug delivery. An innovative biomimetic nanosystem, which combines nutraceutical active ingredients, purified membrane proteins, and fully biocompatible synthetic lipids, represents a possible effective adjuvant therapy for the treatment of wound healing. Furthermore, biomimetic nanovesicles can be useful for the encapsulation/incorporation of other nutraceutical products, of which pharmacological properties *in vivo* are hindered by their poor chemical stability and low bioavailability.

2. AIM OF THE STUDY

Bioactive compounds of food origin are good candidates in biomedicine and the investigation of their functional activities deserves particular attention for their clinical application. This study exploits innovative *in silico*, *in vitro* and *in vivo* approaches to investigate the functional properties of plant secondary metabolites of interest for biomedicine.

The *in silico* analyses were supported by bioinformatics tools that have been used to study the ability of biomaterials surface to modulate cellular pathways. Other tools have been used to find food-containing miRs involved in the modulation of the inflammatory process.

With the aim to identify natural bioactive compounds useful for biomaterials functionalization, we focused the attention on *P. Spinosa* L. fruit extract, curcumin, polydatin and quercetin functional activities (i.e.: antimicrobial, antioxidant, anti-inflammaging, wound healing and hypoglycaemic abilities).

In vitro analyses were used to study antimicrobial, antioxidant, anti-inflammaging, wound healing and hypoglycaemic abilities of bioactive compounds. Using *P. Spinosa* L. fruit extract, based on the secondary metabolites analysed (through quali- and quantitative analyses performed with HPLC-DAD and HPLC/MS), the investigation has been performed in microorganisms, cell free and cell based systems.

In vivo analyses were performed in the model organism *C. elegans* to determine antioxidant and anti-aging activities of the *P. Spinosa* L. fruit extract.

Finally, leucosomes loaded with *P. Spinosa* L. fruit extract were used as biomimetic nanosystems to analyse the anti-inflammatory and wound healing properties.

3. SYMBIOTIC RELATIONSHIP BETWEEN CELL SIGNALLING AND BIOMATERIALS

Through the Reactome bioinformatics analysis, the pathways that are modulated by topographies on different biomaterials have been evaluated. Novel molecular mechanisms modulated during cell and matrix interactions have been identified. Independently from the biomaterial considered, the pathways modulated by topography were the 'Developmental biology (Axon guidance)' and the 'Metabolism of protein' pathways. With these analyses it has been evidenced that nanofibers may have the suitable topography that more closely mimics extracellular matrix components.

Original article published in:

Current Opinion in Biomedical Engineering. Volume 17, March 2021, 100246 (doi.org/10.1016/j.cobme.2020.09.002).

Available online at www.sciencedirect.com

ScienceDirect

Current Opinion in Biomedical Engineering

Cell signalling and biomaterials have a symbiotic relationship as demonstrated by a bioinformatics study: The role of surface topography

Sofia Coppari[1], Seeram Ramakrishna[2], Laura Teodori[3,a] and Maria Cristina Albertini[1,a]

Abstract

Cell–substrate interaction is a process influenced by several variables. The topography, the chemical and mechanical properties of a biomaterial can influence significantly specific intracellular signalling cascades that exert control over adhesion, proliferation, self-renewal, migration and cell differentiation. Through a bioinformatics approach, we evaluated the pathways that are modulated by topographies on different biomaterials. Nanofibers are biomaterials with a topography that well mimics naturally occurring extracellular environment able to establish symbiotic-like relationships with the cells. Interactions with the contact area of the cells and the focal contacts represent a link between the extracellular matrix and the cytoskeleton, capable of influencing epigenetic regulation of cell processes. Electrospun fibres are the ideal candidate scaffolding material owing to their surface properties and the ability to promote cell adhesion and to guide intracellular signalling cascades. The use of predictive models can facilitate the rational design of tailored biomaterial substrate–cells interfaces necessary for the improved outcomes of biomaterials science, stem cells, tissue engineering and regenerative medicine.

Addresses

[1] Department of Biomolecular Sciences, University of Urbino Carlo Bo, Urbino, Italy

[2] Center for Nanofibers and Nanotechnology, National University of Singapore, Singapore

[3] Diagnostics and Metrology Laboratory, ENEA C.R. Frascati, Rome, Italy

Corresponding author: Albertini, Maria Cristina (maria.albertini@uniurb.it)

[a] The authors equally contributed.

Current Opinion in Biomedical Engineering 2021, **17**:100246

This review comes from a themed issue on **Biomaterials: Futures of Biomaterials**

Edited by **Aldo Boccaccini, Himansu Sekhar Nanda,Syam Nukavarapu** and **Vinoy Thomas**

For complete overview of the section, please refer the article collection - Biomaterials: Futures of Biomaterials

Received 24 June 2020, revised 25 August 2020, accepted 4 September 2020

https://doi.org/10.1016/j.cobme.2020.09.002

Keywords

Biomaterial, Cell–material interaction, Surface topography, Nanofibers, Bioinformatics.

Introduction

A biomaterial is a material designed to take a form that can direct, through interactions with living systems, the course of any therapeutic or diagnostic procedure [1]. Biomaterials are required to act harmoniously with the host. Investigating cellular *in vitro* or *in vivo* phenotypic responses to the material surface helps to determine the associated biocompatibility [2]. Understanding material surface properties and cellular responses relationship is thus crucial. In the last decade, exploring molecular environment and gene expression interactions, we are gaining new significant insight into the nature of cell–biomaterial interface. Microarrays technology has become a standard powerful tool to investigate global gene expression patterns [3]. Microarrays have been used to investigate how cells can be adapted in response to different biomaterials, including polymers. Polymers are important materials for their chemical versatility, mechanical strength and flexibility, they can be used to control cell function including the assembly of cells into tissues [4].

Additional quantitative information such as omics technologies, cytometry or imaging, have validated these results (Figure 1). Noteworthy, bioinformatics tools have revealed new biological information encompassing modulated pathways and gene ontologies. Indeed, *in silico* bioinformatics analyses is essential to advance biomaterials science and elucidate possible combinations of surface and chemistry properties that far exceed what could realistically be tested *in vitro* or *in vivo*.

Creating biomaterials suitable for clinical application is still hampered by a lack of understanding of the interaction between cells and the biomaterial surface they grow on. Properties such as surface roughness, hydrophobicity, topography, surface charge, functional groups and specific interaction with the cell surface can all affect cell activity and therefore cellular behaviour. In addition, cell types respond differently to the same surface. Another constrain is the lack of appropriate

Figure 1

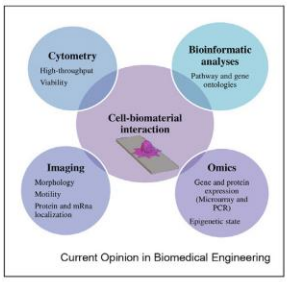

Methods used for the study of cell–biomaterial interaction.

investigation techniques: the research on appropriate analytic devices and protocols is rapidly evolving and goes along with biomaterials research.

To explain the biological mechanisms underlying these cell–biomaterial interactions, we have considered the different studies indicated in 'The Compendium for Biomaterial Transcriptomics (cBiT)' a publicly accessible repository. cBiT is a data warehouse that gives the opportunity to search through biomaterial-based transcriptomics data sets using a web interface [5]. Entering in CBiT, it is possible, through a Dashboard, to get a quick overview of what kind of biomaterial studies cBiT considers (they are showed in a series of graphs). By clicking on a bar or pie slice in these graphs, you are allowed to get access to the corresponding studies in the results section of the Biomaterial Studies page. Each cBiT study contains a wide range of materials, biological and technical properties along with detailed measurements of specific material properties and technical details on the biological material(s) used [5]. We thus used cBiT to retrieve biomaterials published articles with available transcriptomics data. Selecting the *Polymer bar* on the link, '*Biomaterial studies by Material class*' and using different filters, the software shows 13 studies to be exploited for molecular bioinformatics analyses. We selected articles, where the cell growth surface (topography) has been considered (improved topography compared to flat substrate) [6–8]. All these articles offer an overview of differential expressed genes on cells growing on the modified versus unmodified surfaces. The genes were further analysed by Reactome Pathway Database (https://reactome.org). Reactome is a freely available, open source relational database that provides molecular details of signal transduction, transport, DNA replication, metabolism and other cellular processes as an ordered network of molecular transformations in a single consistent data model, an extended version of a classic metabolic map. The Reactome Knowledgebase systematically links human proteins to their molecular functions, providing a resource that functions both as an archive of biological processes and as a tool for discovering novel functional relationships in data such as gene expression studies [9]. We restricted our investigation on the 'symbiotic' relationship between biological systems and biomaterials. We believe that this symbiotic relationship naturally occurs when a biological interaction between extracellular environment and cells can be effective for long-term. Considering topography a crucial issue of this interaction, through the Reactome analysis, we have observed that there are many pathways modulated by genes expressed differentially in the different topographies depending on the biomaterial used. Moreover, some of these pathways have never been described before related to biomaterial topography.

Nanofibers are fibre-shaped nanostructures that have a high surface-area-to-volume ratio, they can easily be functionalized with different molecules. Nanofibers characteristics make them suitable for many applications: energy generation and storage, water and environmental treatment, and healthcare and biomedical engineering applications [10]. We focused this study on the nanofibers developed with the electrospinning technique as promising biomaterials to mimic tissue microenvironment interactions.

Cell–biomaterial interactions

Attachment of anchorage growing cell is the first step in the process of cell–surface interactions which in turn can affect subsequent cellular and tissue responses. Cells attach to substrates through contact sites, which are classified as focal contacts. Adhesion phase involves various biological molecules such as extracellular matrix (ECM) proteins, transmembrane proteins and cytoskeletal proteins. Initially, the cells synthesize and deposit on the substrate the ECM proteins such as fibronectin, collagen or laminin. The minimum adhesion motif on ECM molecules should contain at least three amino acids, which are often represented by Arg-Gly-Asp [11]. These motifs assist the initial interaction of the cellular integrin receptor with the complementary ligand on the surface of the material. After ligand binding, the integrin receptors are grouped into focal adhesion complexes that send specific signals to the associated proteins of cytoskeleton such as talin, α-actinin, paxillin, or vinculin. These proteins mediate the interaction between the integrin receptors and the cytoplasmatic actin cytoskeleton, which is associated with nuclear membrane and membranes of cellular organelles which interact together to induce signal transduction, promoting the action of transcription factors and consequently regulating gene expression. This mechanism influences intracellular processes important for cell behaviour and directs cell migration, proliferation and differentiation [11].

Transfer of signals from the substratum into the cells also depends on the physicochemical nature of the material (Figure 2) that are able to create a symbiotic association (close relationship with the coexistence of interpenetration of signals).

Many variables related to topography influence the cell interaction with the biomaterial [12]: material surface chemistry, surface energy and wettability, electrical charge and conductivity of the material surface, rigidity and deformability of the cell adhesion substrate. Surface energy is a critical component of cell response to a biomaterial and this depends on the terminal groups of the molecules at the interface of the solid which can be hydrophilic or hydrophobic (surface chemistry) [12]. The material surface energy can be calculated from the contact angle measured between the material surface and liquids of various polarity (wettability). When the contact angle between the surface and the liquid is high, the surface of the material will be hydrophobic. Although, a low contact angle indicates a good diffusion of the liquid to the surface of the material, and therefore the hydrophilicity of the material. Many studies have shown that cell adhesion is mediated by surface hydrophobicity as described by Bacakove et al. [12]. If the material is too hydrophobic, the adhesion proteins are adsorbed in a denatured and rigid state. Hence, their geometric conformation is inappropriate for binding to cell adhesion receptors. The electrical charge and conductivity of the material surface are also important because the ECM molecules mediating the adhesion process are negatively charged and therefore preferably interact with positively charged substrates [12]. The rigidity and flexibility of the substrate are features to be considered because they mediate the balance between the cellular traction forces and the resistance of ECM, necessary for cell adhesion.

Among the polymeric materials, polystyrene and polyamide are the most used for cell growth because of their chemical versatility, processability and biomechanical strength. The performance of the polymeric materials largely depends on their surface properties, polystyrene has a poor biocompatibility linked to the hydrophobicity of the material [13], whereas, polyamide exhibits good biocompatibility, probably because of its similarity to collagen proteins in the chemical structure and active groups [14]. Polylactic acid (PLA) is one of the most promising biopolymers because of its excellent biocompatibility and biodegradability since structural monomers can be produced from nontoxic renewable raw materials and natural organic acid [15]. It is also characterized by a high versatility in mechanical properties but has limitations such as slow degradation rate and hydrophobicity.

Biomaterials and topographical modification

The variables influencing the adhesion of a cell to a substrate could be grouped into physical and chemical surface properties, all of which play an important role in directing cellular behaviour. The literature provides experimental evidence that surface topography, particularly microscale or nanoscale topography, is one of the most important physical properties that provide control

Figure 2

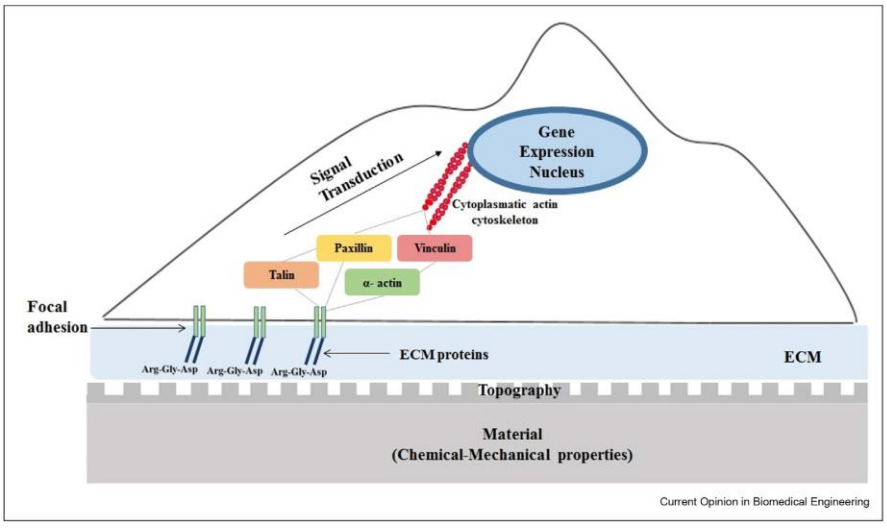

The physical and chemical properties of a material and the adhesion phase of the cell on a substrate can influence gene expression in the nucleus.

over fundamental cellular behaviours such as proliferation, migration and differentiation. Topographical modifications range from random, simple, and homogeneous to highly specific, ordered treatments. Cells can recognize different models of nanoscale and submicron topography such as roughness, grating, wrinkle and pillar [16].

The molecular mechanisms induced by topography allow the change of the cellular shape, the reorganization of the cytoskeleton and therefore of the intracellular signals through force-mediated proteins [17]. Furthermore, it has been shown that both the microscale and nanoscale topography of a substrate can induce changes in the gene expression of cells by altering the nuclear form and histone acetylation pattern [18].

In vitro and *in vivo*, studies are incredibly beneficial to collect data and results on how artificially created microfeatures and nanofeatures perform in realistic applications but the underlying mechanisms of cell–material interactions are only partially understood [19].

For a broader understanding of how intracellular pathways are affected by topographic signals and material properties, we have focused our attention on the articles found in CBiT, describing topographical modifications of different types of materials: polystyrene, polyamide, and dl-lactic acid. From these articles, we have considered the differentially expressed genes between 'flat cultured cells' versus 'topographically improved cultured cells'. The authors also reported the function and pathways of genes differentially regulated (Table 1).

We considered the differentially expressed genes of each Reactome articles to identify all the pathways modulated by these genes, considering only those significantly different (as reported by the p-value calculated by Reactome with the Binomial Test).

In accordance with our Reactome analysis, many other pathways are modulated by topography (data not shown) than those reported in the articles we considered.

'Developmental biology (Axon guidance)' and 'Metabolism of protein' are the common pathways to all the articles considered, meaning that topography has a common effect independently from the material used.

Cells adhere to substratum surfaces mainly through focal contact, and the adhesion phase is facilitated and modified by proteins adsorbed to the substratum surface. Protein adsorption, in turn, is modified by the underlying substratum surface properties including surface chemistry, charge, and free energy [12]. Because discontinuities or curvatures associated with topographic features may represent local changes in surface-free energy, these discontinuities trigger changes in protein adsorption, protein configuration and cellular response [20]. For this reason, it was not surprising to observe that the pathway 'Metabolism of Protein' was modulated. In particular, the Reactome analysis showed that in the topography of polystyrene and polyamide, the modulated pathways were respectively translation termination and post-translation protein phosphorylation. The latter pathway is also modified in the topography of dl-lactic acid. All these pathways deserve more investigations to better understand how polystyrene, polyamide and dl-lactic acid are directly involved in these biochemical mechanisms.

In our Reactome analysis, topographies of polystyrene, polyimide and dl-lactic acid also show the modulation of genes involved in axon guidance. Topographical cues of polymeric surface have garnered the attention of researchers in the field because they have been implicated in differentiating cells into specific types. The focal adhesion points between surfaces and cells seem to play significant roles because several adhesion molecules at these points can trigger intracellular signal cascades for cellular differentiation. Stems cells cultivated on the surface with aligned patterns were shown to differentiate into neuron-like cells, even without specific growth supplements [21].

Table 1

Material, topography and function of differentially expressed genes obtained from CBiT articles.

Reference	Topography and materials	Function of differentially expressed genes
Beijer NRM. et al., 2019 [6]	Micrometric topography on polystyrene	p53-dependent metabolic regulation of the cell cycle Cell growth through protein synthesis
Abagnale G. et al., 2017 [7]	Groove-ridge structures, sub micrometre range on polyamide	Remodelling of the extracellular matrix Tissue morphogenesis Lipid metabolism (ANKRD1)
Unadkat HV. et al., 2012 [8]	Surface roughness, micrometre scale on polylactic acid	Cell adhesion Cellular organization Chondrocyte matrix production

cBIT, Compendium for Biomaterial Transcriptomics.

Electrospun fibres and topography

Experimental evidence indicates that nanoscale scaffolds mimic the ECM. ECM components such as collagen and elastin provide biological and physical support for proliferation, migration, differentiation and cell fate. There are several techniques for developing geometry and dimension-controlled scaffolds including electrospinning. Electrospinning is a simple and versatile technique that can produce a macroporous scaffold comprising randomly oriented or aligned nanofibers with microscale to nanoscale features similar to the hierarchical structure of the ECM [22]. Nanofibers present a topography that more closely mimics naturally occurring ECM than micropatterned features such as ridges or grooves [23]. The reason is that cell growth in a two-dimensional plane compels the unbalanced attack of receptors and the unnatural activation of intracellular signalling. Although the three-dimensional structure resulting from the nanostructured material mimics the morphology of the ECM, increasing the binding sites and orientation signals to cellular receptors [24] (Figure 3).

Electrospun polymer fibrous meshes also offer a higher surface/volume ratio for the adsorption of proteins, for the binding of ligands and finally for cellular anchorage. The ability to mimic the structural organization of the ECM is an important consideration in the rational design of a cell-sensitive scaffold platform on which additional functionality can be incorporated [10].

Electrospinning technology offers many advantages such as the choice of material and the geometry of the scaffold. Indeed, the diameter of the fibres is empirically regulated by modulating the spinning parameters such as flow rate and collection distance and properties of the polymeric solution such as solvent, concentration, conductivity and surface tension [25]. Furthermore, electrospun fibres are easy and cheap to fabricate and are relatively reproducible [26].

Nanofibers can provide nanomechanical and biodegradation properties for cells to proactively interplay with the provisional matrix, functionalize, and remodel it, similar to that of the native cellular remodelling process within the ECM. Nanofibrous scaffold could therefore provide environmental or physical cues to the cells and promote cell growth and function towards the synthesis of genuine extracellular matrices over time [27].

Traditional synthetic biodegradable aliphatic polyesters such as PLA, poly(lactic-coglycolic acid) and polycaprolactone are still the preferred and prevailing choices of materials for constructing nanofibrous scaffolds due to their well known good processability and mechanical performance. Systems based on synthetic polymers have disadvantages in fact they lack cell recognition sites on the surfaces and are also characterized by intrinsic hydrophobicity which will influence cell seeding and subsequent cellular activities [28]. On the other hand, they offer advantages with their adjustable mechanical properties, as well as the ease of surface functionalization through protein coatings or chemical conjugation of specific signalling molecules [28]. For this reason, the research focuses on the use of biofunctional nanofibers which can be directly manufactured from synthetic polymers that can be mixed with natural ECM molecules to form copolymer fibres.

Figure 3

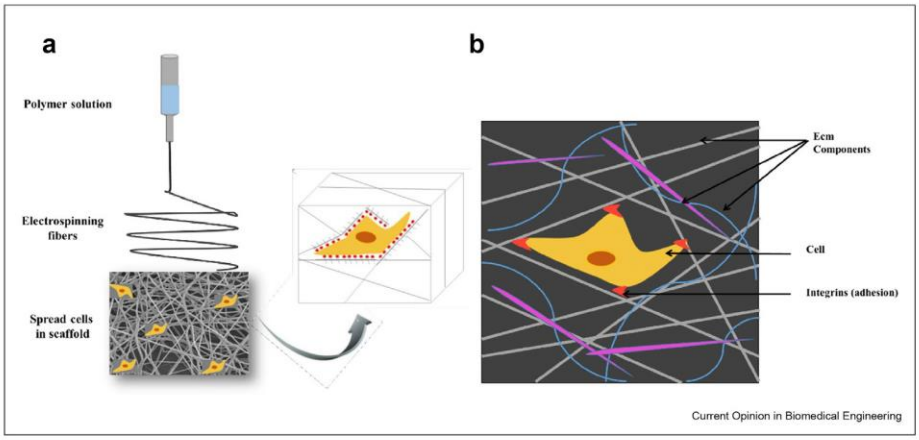

Electrospun nanofiber scaffold. (**a**) Cell adhesion in the 3D system scaffold similar to the ECM and increase of the binding sites of cell and substrate (**b**) Schematic illustration of ECM. ECM components (e.g. collagen, fibrin, elastin) provide the support for the binding of integrins to cells, that mediate cell adhesion. ECM, extracellular matrix.

Figure 4

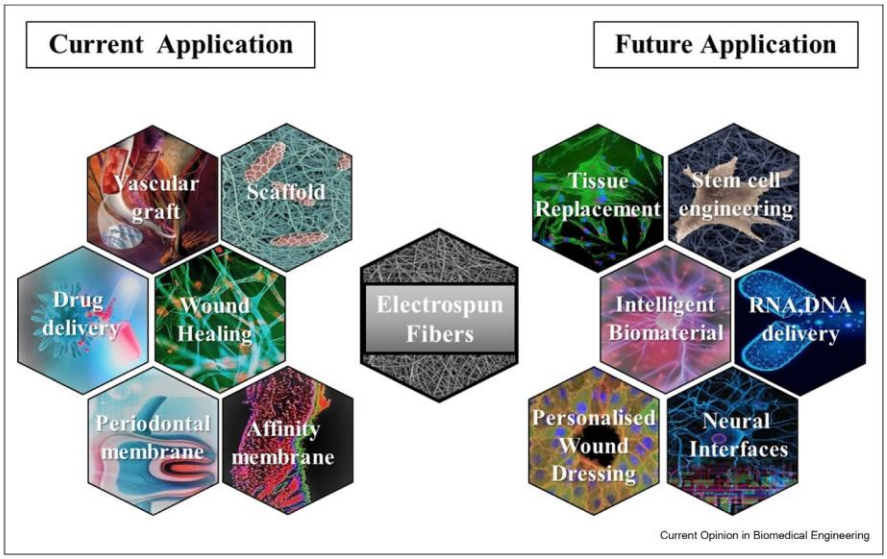

Current applications and future prospective of electrospun fibres.

Blended nanofibers generally benefit from improved physical properties due to the synthetic polymer component and improved bioactivity due to the natural ECM component. The incorporation of ECM molecules or ECM-inspired peptide analogues into electrospun scaffolds is thus a mean of combining the structural features of the scaffolds with the biofunctionality of ECM proteins. Such biologically active nanofibers can better support stem cell attachment and growth. For example, fibres with surface laminin coating are favourable for the attachment, proliferation and differentiation of neural stem cells and progenitor cells. Tian et al. [29] designed scaffold composed of PLA polypyrrole and polyornithine coating to improve the biocompatibility and the initial cell attachment.

Electrospinning is a simple, cost-effective technique with controlled mechanical properties that allow the formation of nanofibers capable of mimicking the extracellular environment and the possibility of adding functional components (biofunctionalization). For these characteristics, most applications of this technique is placed in the biomedical and tissue engineering fields. Electrospinning is used for the development of scaffolds, drug delivery system, for affinity membrane application and in wound healing treatment. Future work will probably be concentrated in the development of 'intelligent biomaterials' to maximize biomimetic and the degree of symbiosis between these systems and the human body. The approach is expected to be applied for a variety of purposes such as: the replacement of all types of tissue on a clinically relevant scale; delivery system for DNA, RNA and hormones for targeted treatment of many diseases [10] and personalization of the dressing based on the individual patients [30] (Figure 4).

Conclusion

In this manuscript, we have reviewed the characteristics of the cell–substrate adhesion process and how it is guided by the different physical and chemical biomaterial surface properties. These affect the fate of the cell, modulating gene expression. Among the physical properties, there are those induced by the topography of the substrate. Indeed, surface topography on different polymeric and biopolymer biomaterials, allows the modulation of numerous genes and cell pathways. In all the works considered, we have observed pathways such as protein metabolism, which demonstrates a change in the processes that take place within the nucleus including the transcription and the Axon guidance pathway, involved in the neuronal differentiation of the cell. The use of Reactome computational model can reveal new unpredictable pathways modulation that often do not appear when *in vitro* studies are performed. In this study different pathways emerged from our bioinformatics analyses and have never been described before related to biomaterial topography representing a noteworthy and novel result.

Numerous solutions have been developed for cell growth to optimize adhesion process including the electrospinning technique to produce scaffolds from microscale to nanoscale features similar to the ECM structure. Currently, no techniques combine control over the structural arrangement, material composition and biofunctionalization to ensure reasonable costs and yield. Promising strategies are needed to allow the construction of optimal polymer scaffolds with the aim of the best use of the cell adhesion process to the substrate.

Declaration of competing interest

The authors declare that they have no known competing financial interests or personal relationships that could have appeared to influence the work reported in this paper.

Acknowledgements

This research did not receive any specific grant from funding agencies in the public, commercial or not-for-profit sectors.

References

Papers of particular interest, published within the period of review, have been highlighted as:

* of special interest
** of outstanding interest

1. Ghasemi-Mobarakeh L, Kolahreez D, Ramakrishna S, Williams D: **Key terminology in biomaterials and biocompatibility**. *Curr Opin Biomed Eng* 2019, **10**:45–50.

2. Power KA, Fitzgerald KT, Gallagher WM: **Examination of cell-host-biomaterial interactions via high-throughput technologies: a re-appraisal**. *Biomaterials* 2010, **31**:6667–6674.

3. Anderson DG, Putnam D, Lavik EB, Mahmood TA, Langer R: **Biomaterial microarrays: rapid, microscale screening of polymer-cell interaction**. *Biomaterials* 2005, **26**:4892–4897.

4. Zhang N, Kohn DH: **Using polymeric materials to control stem cell behavior for tissue regeneration**. *Birth Defects Res Part C Embryo Today - Rev* 2012, **96**:63–81.

5. Hebels DGAJ, Carlier A, Coonen MLJ, Theunissen DH, de Boer J: **cBiT: a transcriptomics database for innovative biomaterial engineering**. *Biomaterials* 2017, **149**:88–97.

6. * Beijer NRM, Nauryzgaliyeva ZM, Arteaga EM, Pieuchot L, Anselme K, van de Peppel J, Vasilevich AS, Groen N, Roumans N, Hebels DGAJ, *et al.*: **Dynamic adaptation of mesenchymal stem cell physiology upon exposure to surface micropatterns**. *Sci Rep* 2019, **9**:1–14.
for findings on the dynamic adaptation of mesenchymal stem cell upon exposure to surface micro patterns

7. * Abagnale G, Sechi A, Steger M, Zhou Q, Kuo CC, Aydin G, Schalla C, Müller-Newen G, Zenke M, Costa IG, *et al.*: **Surface topography guides morphology and spatial patterning of induced pluripotent stem cell colonies**. *Stem Cell Reports* 2017, **9**:654–666.
on Surface Topography Guides

8. * Unadkat HV, Groen N, Doorn J, Fischer B, Barradas AMC, Hulsman M, van de Peppel J, Moroni L, van Leeuwen JP, Reinders MJT, *et al.*: **High content imaging in the screening of biomaterial-induced MSC behavior**. *Biomaterials* 2013, **34**:1498–1505.
on biomaterial-induced MSC behaviour

9. * Fabregat A, Sidiropoulos K, Garapati P, Gillespie M, Hausmann K, Haw R, Jassal B, Jupe S, Korninger F, McKay S, *et al.*: **The reactome pathway knowledgebase**. *Nucleic Acids Res* 2016, **44**:D481–D487.
on Reactome pathway knowledgebase

10. Shahriar SMS, Mondal J, Hasan MN, Revuri V, Lee DY, Lee YK: **Electrospinning nanofibers for therapeutics delivery**. *Nanomaterials* 2019, **9**.

11. * Bačáková L, Filová E, Rypáček F, Švorčík V, Starý V: **Cell adhesion on artificial materials for tissue engineering**. *Physiol Res* 2004, **53**.
on modulation of cell adhesion, proliferation and differentiation on materials designed for body implants

12. Bacakova L, Filova E, Parizek M, Ruml T, Svorcik V: **Modulation of cell adhesion, proliferation and differentiation on materials designed for body implants**. *Biotechnol Adv* 2011, **29**:739–767.

13. Boulares-Pender A, Thomas I, Prager A, Schulze A: **Surface modification of polyamide and poly(vinylidene fluoride) membranes**. *J Appl Polym Sci* 2013, **128**:322–331.

14. Winnacker M: **Polyamides and their functionalization: recent concepts for their applications as biomaterials**. *Biomater Sci* 2017, **5**:1230–1235.

15. Singhvi MS, Zinjarde SS, Gokhale DV: **Polylactic acid: synthesis and biomedical applications**. *J Appl Microbiol* 2019, **127**:1612–1626.

16. Yang L, Gao Q, Ge L, Zhou Q, Warszawik EM, Bron R, Lai KWC, van Rijn P: **Topography induced stiffness alteration of stem cells influences osteogenic differentiation**. *Biomater Sci* 2020, **8**:2638–2652.

17. ** Gao C, Tang L, Hong J, Liang C, Tan LP, Li H: **Effect of laser induced topography with moderate stiffness on human mesenchymal stem cell behavior Recent citations Effect of laser induced topography with moderate stiffness on human mesenchymal stem cell behavior**. *J Phys Mater* 2019, **2**:34006.
for findings on epigenetics and bioengineering

18. Larsson L, Pilipchuk SP, Giannobile WV, Castilho RM: **When epigenetics meets bioengineering—a material characteristics and surface topography perspective**. *J Biomed Mater Res B Appl Biomater* 2018, **106**:2065–2071.
on cellular response to surface morphology

19. Denchai A, Tartarini D, Mele E: **Cellular response to surface morphology: electrospinning and computational modeling**. *Front Bioeng Biotechnol* 2018, **6**.

20. von Recum AF, van Kooten TG: **The influence of micro-topography on cellular response and the implications for silicone implants**. *J Biomater Sci Polym Ed* 1995, **7**:181–198.

21. Cho Y Il, Choi JS, Jeong SY, Yoo HS: **Nerve growth factor (NGF)-conjugated electrospun nanostructures with topographical cues for neuronal differentiation of mesenchymal stem cells**. *Acta Biomater* 2010, **6**:4725–4733.

22. Chew S, Wen Y, Dzenis Y, Leong K: **The role of electrospinning in the emerging field of nanomedicine**. *Curr Pharmaceut Des* 2006, **12**:4751–4770.

23. Beachley V, Wen X: **Polymer nanofibrous structures: fabrication, biofunctionalization, and cell interactions**. *Prog Polym Sci* 2010, **35**:868–892.

24. ** Matellan C, del Rõó Hernández AE: **Engineering the cellular mechanical microenvironment – from bulk mechanics to the nanoscale**. *J Cell Sci* 2019:132.
on engineering related to cellular mechanical microenvironment

25. Tebyetekerwa M, Ramakrishna S: **What is next for electrospinning?** *Matter* 2020, **2**:279–283.

26. Lim SH, Mao HQ: **Electrospun scaffolds for stem cell engineering**. *Adv Drug Deliv Rev* 2009, **61**:1084–1096.

27. Laurencin CT, Ambrosio AMA, Borden MD, Cooper JA: **Tissue engineering: orthopedic applications**. *Annu Rev Biomed Eng* 1999, **1**:19–46.

28. Zhang YZ, Su B, Venugopal J, Ramakrishna S, Lim CT: **Biomimetic and bioactive nanofibrous scaffolds from electrospun composite nanofibers**. *Int J Nanomed* 2007, **2**:623–638.

29. Tian L, Prabhakaran MP, Hu J, Chen M, Besenbacher F, Ramakrishna S: **Synergistic effect of topography, surface chemistry and conductivity of the electrospun nanofibrous scaffold on cellular response of PC12 cells**. *Colloids Surf B Biointerfaces* 2016, **145**:420–429.

30. Yan X, Yu M, Ramakrishna S, Russell SJ, Long YZ: **Advances in portable electrospinning devices for: in situ delivery of personalized wound care**. *Nanoscale* 2019, **11**: 19166–19178.

4. INFLAMM-AGING microRNAs MAY INTEGRATE SIGNALS FROM FOOD AND GUT MICROBIOTA

Through bioinformatics tools (DIANA, PATRIC, DMD database and SID.01), we have demonstrated a relationship between the gut microbiota, human inflammatory microRNAs (miR-155, miR-146a and miR-21) and food. These inflamma-miRs can modulate some pathways (degradation of lysine and elongation of fatty acids) involved in the modulation of the composition of the intestinal microbiota. Furthermore, the same inflamma-miRs are present in several foods, which, if consumed through the diet, could target and modulate the identified pathways associated with inflammation.

Original article published in:

Mechanisms of Ageing and Development. Volume 182, September 2019, 111127 (doi.org/10.1016/j.mad.2019.111127).

Mechanisms of Ageing and Development 182 (2019) 111127

Contents lists available at ScienceDirect

Mechanisms of Ageing and Development

journal homepage: www.elsevier.com/locate/mechagedev

Inflamm-aging microRNAs may integrate signals from food and gut microbiota by modulating common signalling pathways

Laura Teodori[a,*], Ilaria Petrignani[a], Angelica Giuliani[b], Francesco Prattichizzo[c], Felicia Gurău[b], Giulia Matacchione[b], Fabiola Olivieri[b,d], Sofia Coppari[e], Maria Cristina Albertini[e]

[a] Laboratory of Diagnostics and Metrology, Division of Health Physical Sciences (FSN-TECFIS-DIM), ENEA, C.R. Frascati, Rome, 00044, Italy
[b] Department of Clinical and Molecular Sciences, DISCLIMO, Università Politecnica delle Marche, Ancona, Italy
[c] IRCCS MultiMedica, Milano, Italy
[d] Center of Clinical Pathology and Innovative Therapy, IRCCS INRCA National Institute, Ancona, Italy
[e] Department of Biomolecular Sciences, University of Urbino Carlo Bo, Urbino, Italy

ARTICLE INFO

Keywords:
Immune system
miR-21
miR-155
miR-146a
Senescence
Nutrition
Bioinformatics
MicroRNA-repository
Aging

ABSTRACT

Human gut microbiota, which comprises an extremely diverse and complex community of microorganisms inhabiting the intestinal tract, may be associated with inflammation and age-related chronic health conditions. However, the mechanism underlying this association is only recently beginning to emerge. Transfer and modulation of gene expression by diet-derived microRNAs (miRs) in mammals might be involved in this communication. Through a bioinformatics approach, using on line tools and repositories, we searched for evidences that food-containing miRs, actually involved in the modulation of the inflammatory process, (inflamma-miRs), may contribute to mediate the anti-inflammatory effects exerted by some foods through the modulation of aging-related pathways and gut microbiota composition in a bidirectional communication. Supported by a "Pubmed" search and our previous research, a trio of experimentally validated inflamma-miRs were considered: miR-155, miR-146a and miR-21. Our *in silico* study supports the hypothesis that these inflamma-miRs could modulate some pathways, such as lysine degradation and lengthening of fatty acids which are involved in the modulation of microbiota composition, i.e. prevotella, ruminococcus and oscillibacter and *vice versa*. Food homologues to human miR-21, miR-155 and miR-146a were found in cow fat, cow milk, and eggs suggesting that they may be able of targeting, and probably exacerbating, inflammation related pathways. If these data will be experimentally validated, they will further support the relevance of a nutraceutical approach for a healthy aging.

1. Introduction

Although research on nutrition has focused on the interactions between nutrients and organism, it is becoming increasingly meaningful to study the effects of nutrient on host gut microbiota composition. Human organism hosts trillions microbial cells in a symbiotic relationship and, in the normal healthy state, they benefit from each other. Over 1000 different species of microorganism are making up the human microbiota. Ninety % of microbiota is concentrated in the gut, especially intestine. Emerging evidences indicated gut microbiota as an important component of human health preservation. The understanding the interrelationship among nutrient-host-microbiota may lead to the discovery of new mechanisms of disease onset and progression. Recent studies are indicating the microbiota as a principal key of healthy phenotype during aging (Franceschi et al., 2017; Claesson et al., 2012; Forslund et al., 2015). A new intriguing hypothesis of aging is that bacteria influence the degree of systemic inflammation through chronic, low grade endotoxemia, thus promoting and sustaining inflamm-aging (Zhang et al., 2013). Growing evidence suggests chronic low-grade inflammation (LGI) as one of the most relevant possible mechanism underlying the aging process (Custodero et al., 2018). A major negative consequence of aging is immuno-senescence, which can be defined as a decline in the functionality of the immune system (Gruver et al., 2007), causing a chronic low-grade inflammatory status in the gut. Immuno-senescence can therefore cause unfavourable changes in the composition and structure of the gut microbiota in older people (Neish, 2009).

Gut microbiota can modulate the host gene expression, primarily the innate immune response (Tomkovich and Jobin, 2015). Recent evidences suggest that communication between the gut microbiota and

* Corresponding author.
E-mail address: laura.teodori@enea.it (L. Teodori).

https://doi.org/10.1016/j.mad.2019.111127
Received 28 April 2019; Received in revised form 16 July 2019; Accepted 6 August 2019
Available online 08 August 2019
0047-6374/

host may in part occur via microRNAs miRs (Williams et al., 2017; Dalmasso et al., 2011). MiRs are a class of short (18–24 nt) regulatory RNAs that are widely evolutionary conserved among many species. These single-stranded, non-coding molecules mediate gene regulation at different levels. The best characterized function of miRs is the post-transcriptional repression of the targets mRNA by promoting cleavage or inhibiting its translation. In this way, miRs negatively regulate target genes expression, modulating all biological functions, including cell development, apoptosis, proliferation, differentiation and regulate inflammatory pathways (Cătană et al., 2015; Olivieri et al., 2013).

Several evidences showed that nutrients may modulate endogenous miRs (Carotenuto et al., 2016). In addition to endogenous miRs, recent fascinating results demonstrated that food-derived miRs enter the mammals' circulatory system and reach their target thus modulating specific mammalian protein expression (Wang et al., 2012; Sherman et al., 2015). This as an intriguing thesis that may pave the way for novel therapeutic approaches discovery. Recent studies confirmed this hypothesis demonstrating that miRs not only are synthesized endogenously, but also might be obtained from dietary sources (Philip et al., 2015; Baier et al., 2014). We hypothesized that ingested biological matter contributes directly to the miRs arsenal of body compartments or that the diet-derived exogenous miRs (referred as "xenomiRs") can affect total miRs profiles as part of a circulating miRs homeostasis that is altered in many diseases (Witwer, 2012). Epigenetic crosstalk between different kingdoms, has been extensively studied in the interaction between plants and bacteria, while evidences in humans are emerging only recently (Williams et al., 2017; Liu et al., 2016; Hua et al., 2018; Qin and Wade, 2017). Increasing evidence suggests the existence of a miRs-based crosstalk between microbiota, the host, and food (Witwer, 2012; Liu et al., 2016; Philip et al., 2015).

Beyond opposing arguments regarding the cross-kingdom regulation of gene expression by plant miRs, concern on how these molecules can access the gastro-intestinal (GI) tract, enter the circulation and transport to cell have also been raised. Several endogenously originating miRs intercellular carriers have been identified, including microvesicle (MV), which are membrane-derived vesicles released from various cell types (Valadi et al., 2007; Zernecke et al., 2009; Zhang et al., 2015; Turchinovich et al., 2012). Encapsulation of miRs in exosomes and exosome-like particles confers protection against RNA degradation and creates a pathway for intestinal and vascular endothelial transport by endocytosis, as well as delivery to peripheral tissues. Exosome-like nanoparticles present in edible fruits and vegetables can be phagocyted by intestinal macrophages and stem cells (Mu et al., 2014). Thus, considering the recent assumptions and evidences that exogenous miRs might be sufficiently stable to pass through the GI tract and enter circulation without losing functionality, we decided to study whether food-containing miRs, especially those that were identified in serum (exosome), can carry signals to host modulating immune system. For this purpose, we used a bioinformatics approach *(in silico)* that, through web-based tools and supplemental data available in literature, can predict the putative microRNAs involved in health microbiota. In this way, we were able to hypothesize new regulatory mechanisms associated to microbiota driven immune dysregulation and its implication with aging. Indeed, *in silico* biology which refers to computational models and simulations applied to complex biological phenomena is a potent tool to obtain quantitative insights into regulatory networks and processes. Due to the vast amounts of data generated by molecular analyses, computational biology is increasingly exploited to filter big amount of data. *In silico* applied to vast amounts of biological data uses sophisticated algorithms to advance scientific understanding. The retrieved information can then be experimentally validated or serve as a guide for future investigations. We consulted different databases for microRNAs pathway prediction, microbiota integrated pathways, clusters % match with other species (Dietary microRNA Database) and to filter common pathways (SID1.0). The aim of our *in silico* approach is to study the possible miRs-mediated interactions between the healthy microbiota and host and to explore the impact of nutrition on maintaining the health status, with a specific focus on the inflamm-aging process.

2. Materials and methods

2.1. Data collection

We used PubMed free resource (https://www.ncbi.nlm.nih.gov/pubmed/) to collect papers from literature related to food and microbiota impacting to inflamm-aging. This data search helped us to collect miRs information contained in feces relevant for aging and inflammation. For this purpose, the combination of the following terms has been used in the search box: microbiota health interactions, immunity, inflamm-aging, microRNA, food and nutrition. We focused our attention on miRs able of shaping microbiota and of modulating inflamm-aging processes. These collected miRs were all experimentally validated in the papers we have selected.

2.2. Bioinformatics in silico analysis

We exploited different bioinformatics repositories and tools to analyze microbiota (Ruminococcus; Prevotella; Oscillibacter species) associated pathways, microRNAs modulated pathways, dietary microRNAs and common microbiota/microRNAs pathways. These tools are reported below.

DIANA tool (http://snf-515788.vm.okeanos.grnet.gr/) has been used for the prediction of the pathways modulated by microRNAs. Since DIANA can utilize experimentally validated miRNA interactions derived from DIANA-TarBase, we retrieved the KEGG Pathway IDs (strings) modulated by each miRNAs (Annex 1 in Supplementary data) and used them for SID1.0 analysis. MicroRNA nomenclatures used for the analysis were the following: hsa-miR-21-3p; hsa-miR-21-5p; hsa-miR-155-3p; hsa-miR-155-5p; hsa-miR-146a-3p; hsa-miR-146a-5p; hsa-miR-146b-3p; hsa-miR-146b-5p.

PATRIC (https://patricbrc.org/) tool has been used to find the metabolic pathways related to the genomes of Ruminococcus, Prevotella and Oscillibacter species. PATRIC puts together data from sources, data types, molecular entities and organisms. Data are collected from public repositories, for instance NCBI, the United States Department of Agriculture, the Centers for Disease Control (CDC) and other NIAID-funded projects, such as the System Biology for Infectious Disease Centers, as well as from studies published by researchers. The search tool was used to insert the name of each species and the KEGG IDs (Strings) has been used for SID1.0 analysis (Annex 2 in Supplementary data).

DMD database (Dietary microRNA Database: http://sbbi-panda.unl.edu:5000/dmd/browse) has been used to retrieve food containing microRNAs (miR-155, miR-146a and miR-21) with 100% clusters percentage match with human.

SID1.0 tool is a simple string identifier that has been used to filter the common microbiota/microRNAs pathways (strings of KEGG Pathway ID) obtained from PATRIC and DIANA tools retrieving common strings (Annex 3 in Supplementary data). All the information regarding the tools and repositories we used are reported in the webpage of the tools/repositories quoted. In the flow chart in Fig. 1 the followed road map is reported.

3. Results

3.1. MicroRNAs involved in the crosstalk between microbiota and host

From our data search we observed that feces contain miRs relevant for aging and inflammation processes. Based on our previous experiences we selected from the literature three miRs, namely miR-155, miR-21 and miR-146a as markers of inflamm-aging sensing. From the data

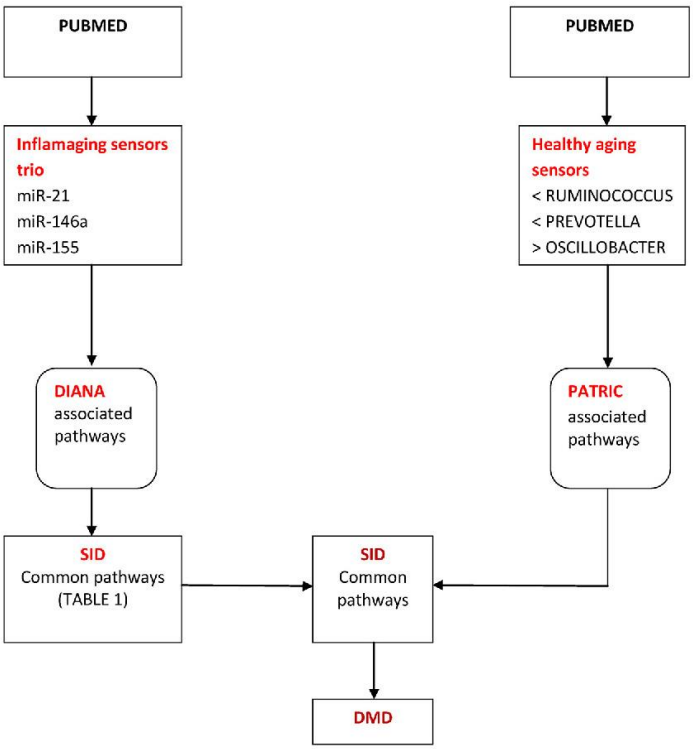

Fig. 1. Flowchart of visual representation of the sequence of steps applied to perform our *in silico* study.

Table 1
MiR-21, miR-155 and miR-146a common pathways analyzed with SID1.0 (the pathways have been retrieved with DIANA tool). Common pathways were found only with the combination of 2 miRs out of three, no common pathways between all the trio-miRs have been found.

KEGG Pathway ID	Pathway name	Common microRNAs
hsa05142	Chagas disease (American trypanosomiasis)	miR-146a; miR-155
hsa05321	Inflammatory bowel disease (IBD)	miR-146a; miR-155
hsa04064	NF-kappa B signaling pathway	miR-146a; miR-155
hsa05161	Hepatitis B	miR-146a; miR-155
hsa05203	Viral carcinogenesis	miR-146a; miR-21
hsa04012	ErbB signaling pathway	miR-146a; miR-21
hsa04520	Adherens junction	miR-155; miR-21
hsa05223	Non-small cell lung cancer	miR-155; miR-21
hsa05219	Bladder cancer	miR-155; miR-21
hsa05212	Pancreatic cancer	miR-155; miR-21
hsa04110	Cell cycle	miR-146a; miR-21
hsa05210	Colorectal cancer	miR-155; miR-21
hsa00310	Lysine degradation	miR-146a; miR-21
hsa05220	Chronic myeloid leukemia	miR-155; miR-21
hsa00062	Fatty acid elongation	miR-155; miR-21

collected, these three candidate miRs were found to be able of modulating inflamm-aging processes (Olivieri et al., 2013) and of shaping microbiota. The pathways associated to each miR of the trio were retrieved using DIANA tool. Subsequently, the search for common pathways was carried out inquiring SID1.0. This analysis demonstrated that common pathways were found with two by two miRs combination only. As indicated in the Table 1, many of the pathways regulated by these miRs are involved in immune system processes indicating that these processes are mainly involved in the crosstalk between microbiota and host.

3.2. Pathways associated to healthy microbiota, miR-21, miR-155 and miR-146a

Literature search evidenced that gut microbiota composition correlates with diet and health in the elderly and it is mainly associated either to a decreased amount of Ruminococcus/Prevotell and to an increased amount of the Oscillibacter as reported by Claesson et al. Thus, these three enterobacters have been taken as indicative of healthy aging.

By inquiring PATRIC tool we were able to find the pathways associated to healthy aging bacteria (Annex 2 in Supplementary data). We combined with that of Table 1 (pathways associated to each of the trio miRs) and inquiring SID1.0 analysis we, thus, retrieved the common pathways to bacteria and miRs as demonstrated in Table 2. As showed from the data reported in Table 2 common pathways to all of them were not found. We found the common pathways with the combination of 5 and 4 out of the six items (Annex 3 in Supplementary data).

Our results indicate that the miRs we selected, and the bacteria considered may modulate: Amino Acid Metabolism, Lipid Metabolism, Cofactors and Vitamins Metabolism, Glycan Biosynthesis and Metabolism.

3.3. Food derived microRNA match with human microRNAs

Based on the fact that the analysis presented in Table 2 demonstrated that miR-21, miR-155 and miR-146a can probably modulate gut associated metabolism and could be involved in inflamm-aging process and on the observation that diet is emerging as the most critical determinant in human health and healthy aging, we inquired into the web platform DMD to retrieve information about foods containing such miRs. The results are reported in Table 3. As indicated in Table 3 cow fat/milk, chicken (and chicken egg), Atlantic salmon and pig possess

Table 2
MiR-21, miR-155, miR-146a, Ruminococcus, Prevotell and Oscillibacter common pathways analyzed with SID1.0 (the pathways have been retrieved with Diana tool, mirpath v.3 for miRS and with PATRIC tool for microbiota). Common pathways to all of them were not found. We found the common pathways with the combination of 5 and 4 of them out of 6 elements (trio-miRs and trio-bacteria).

KEGG Pathway ID	Pathway name/Pathway class	Common microRNAs/microbiota
hsa00310	Lysine degradation/ Amino Acid Metabolism	miR-21; miR-146a/ Ruminococcus; Prevotell; Oscillibacter
hsa00062	Fatty acid elongation in mitochondria/ Lipid Metabolism	miR-21; miR-155/ Ruminococcus; Prevotell; Oscillibacter
hsa00670	One carbon pool by folate/ Metabolism of Cofactors and Vitamins	miR-146a/ Ruminococcus; Prevotell; Oscillibacter
hsa00601	Glycosphingolipid biosynthesis - lacto and neolacto series/ Glycan Biosynthesis and Metabolism	miR-146a/ Ruminococcus; Prevotell; Oscillibacter
hsa00290	Valine, leucine and isoleucine biosynthesis/ Amino Acid Metabolism	miR-21/ Ruminococcus; Prevotell; Oscillibacter
hsa00071	Fatty acid metabolism/ Lipid Metabolism	miR-21/ Ruminococcus; Prevotell; Oscillibacter
hsa00061	Fatty acid biosynthesis/ Lipid Metabolism	miR-21/ Ruminococcus; Prevotell; Oscillibacter
hsa00100	Steroid biosynthesis/ Lipid Metabolism	miR-155/ Ruminococcus; Prevotell; Oscillibacter

Table 3
DMD has been used to find the percentage match between food and human miR-21, miR-155 and miR-146a.

	miR-21	miR-155	miR-146a	% Match (Dietary species in DMD)
Cow microRNA fat (bta-)	bta-miR-21-5p	bta-miR-155	bta-miR-146a	95.65% gga-miR-155 **100 % hsa-miR-155-5p** 100 % ssa-miR-155-5p
Cow microRNA milk (bta-)	bta-miR-21-5p bta-miR-21-3p	bta-miR-155	bta-miR-146a	95.65% gga-miR-155 **100 % hsa-miR-155-5p** 100 % ssa-miR-155-5p
Orange microRNA fruit (csi-)	–	–	–	–
Chicken egg MicroRNA (gga-)	gga-miR-21-5p	–	gga-miR-146a-5p	**100 % hsa-miR-21-5p** 100% ssc-miR-21 **100%hsa-miR-146a-5p** 100% ssc-miR-146a-5p
Chicken MicroRNA (gga-)	gga-miR-21-3p	gga-miR-155	gga-miR-146a-3p	95.45% bta-miR-155 **95.45%hsa-miR-155-p** 95.45% ssa-miR-155-5p
Soybean MicroRNA (gma-)	–	–	–	–
Human MicroRNA, breastmilk (hsa-)	hsa-miR-21-5p hsa-miR-21-3p	hsa-miR-155-5p hsa-miR-155-3p	hsa-miR-146a-5p hsa-miR-146a-3p	100 % gga-miR-21-5p 100 % ssc-miR-21 100 % bta-miR-155 95.65% gga-miR-155 100 % ssa-miR-155-5p 100 % gga-miR-146a-5p 100 % ssc-miR-146a-5p
Apple MicroRNA (mdm-)	–	–	–	–
Banana MicroRNA (msp-)	msp-miR-21 msp-miR-21*	msp-miR-155 msp-miR-155*	msp-miR-146 msp-miR-146*	– –
Rice MicroRNA (osa-)	–	–	–	–
Tomato MicroRNA (sly-)	–	–	–	–
Atlantic salmon MicroRNA (ssa-)	ssa-miR-21a-5p ssa-miR-21a-3p ssa-miR-21a-2-3p ssa-miR-21b-5p ssa-miR-21b-3p	ssa-miR-155-5p ssa-miR-155-3p	ssa-miR-146a-5p ssa-miR-146a-3p ssa-miR-146a-3-3p ssa-miR-146b-5p ssa-miR-146b-3p ssa-miR-146d-5p ssa-miR-146d-3p ssa-miR-146d-2-3p	100% bta-miR-155 95.65% gga-miR-155 **100% hsa-miR-155-5p**
Pig MicroRNA (ssc-)	ssc-miR-21	ssc-miR-155-3p ssc-miR-155-5p	ssc-miR-146a-3p ssc-miR-146b	**100% gga-miR-21-5p** **100% hsa-miR-21-5p** 95.24% hsa-miR-146b-5p
Wheat MicroRNA (tae-)	–	–	–	–
Grape MicroRNA (vvi-)	–	–	–	–
Corn MicroRNA (zma-)	–	–	–	–

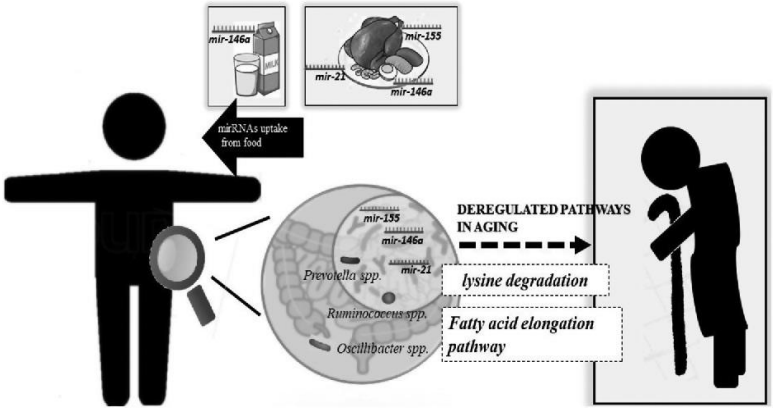

Fig. 2. Graphical representation of the results indicating an interaction among foods, host microbiota and aging through the common pathways lysine degradation and fatty acid elongation.

one or two inflamm-aging miRs with a 100% match with the same human microRNAs. All the other aliments indicated in the Table 3 do not have these microRNAs or do not matches 100% with humans. It must be noted that not many foods have been tested yet for miRs libraries. It's interesting to note that human breast milk used only by neonates, has 100% matches for the 3 inflamm-aging miRs from animal foods. The fact that breast milk is limited to weaning probably indicates that this aliment is not a suitable food for adults, and this represents an interesting observation.

3.4. Gut microbiota, inflamm-aging miRs, diet and signaling pathways

Lysine degradation pathway and fatty acid elongation pathways were the two most representative pathways (five out of six elements in common) as demonstrated in Table 2. Indeed, these pathways are found common to miR-21; miR-146a/ Ruminococcus; Prevotell; Oscillibacter. In Fig. 2 are graphically represented these converging routes, taking together the results from Tables 1–3.

4. Discussion

We demonstrated here, through a bioinformatics *in silico* study, that a cross-talk among i) gut microbiota, ii) human inflamm-aging miRs, and iii) foods might occur. This suggests that diet induces epigenetic modifications and these modifications work together in various combinations with gut microbiota and host, targeting signalling pathways relevant for contrasting or exacerbating inflammation associated senescence. The debate about gut microbiota miRs existence and their capacity to modulate human mRNA transcripts is a hot topic and a controversial issue. However, epigenetic crosstalk between different kingdoms, especially regarding exosome or vesicle like particles cross-talk between kingdoms is becoming more and more evident and it can be relevant for the aging phenotype outcome (Williams et al., 2017). In addition, recent studies suggest that miRs not only are synthesized endogenously, but also might be obtained from dietary sources (Quintanilha et al., 2017). We previously defined a set of miRs, namely: miR-146, miR-155, and miR-21, which play a central role in the interplay among DNA damage response, cell senescence and inflammation and yield a well-recognized role in aging and development of aging related diseases (ARDs) in humans (Olivieri et al., 2015; Carotenuto et al., 2016). We found here that this trio-miRs shows inflammation related pathways in common (Table 1). Noteworthy, the analysis presented in Table 2 demonstrated that miR-21, miR-155 and miR-146a share common molecular pathways with some of gut microbiota demonstrating that this trio-miRs can actually modulate the gut associated metabolism. Among the common molecular pathways, we found that lysine degradation and fatty acid elongation in mitochondria are the most represented being common to 4 out of the five items considered, namely: miR-21; miR-146a; Ruminococcus; Prevotell; Oscillibacter (for lysine degradation pathway) and miR-21; miR-155; Ruminococcus; Prevotell; Oscillibacter (for fatty acid elongation in mitochondria). Vital et al. (2014) demonstrated that acetyl-coenzyme A (CoA) is the microbiota most prevalent pathway (mean, 79.7% of all pathways), followed by the lysine pathway (mean, 11.2%). On the other hand, acetyl-CoA is a lysine degradation pathway product. Indeed, in mammals, lysine is metabolized to acetyl-CoA; an acetyl-CoA rise induces the increase of the overall acetylation of cytoplasmic proteins, as well as the impairment of autophagy (Mariño et al., 2014). Acetyl-CoA is a central molecule connecting the catabolism of glucose, fatty acids, and amino acids, thus it is a key metabolite at the intersection of catabolic and anabolic metabolism being a major acetyl donor in cells.

It is worthwhile to note that the mammalian degradation of lysine proceeds via two distinct routes, the saccharopine and the pipecolic acid route. In mammalian brain an age-dependent lysine degradative pathway occurs, and the pipecolate pathway emerged as the main catabolic pathways, whereas the saccharopine pathway prevails in developing brain (Hallen et al., 2013). Indeed, lysine degradation pathway dysregulation has been associated to neurodegeneration in elderly. In addition, lysine plays several others important roles in humans, like proteinogenesis, crosslinking of collagen polypeptides, uptake of essential mineral nutrients, production of carnitine, which is key element in fatty acid metabolism and elongation. The growing fatty acid chain is elongated by the sequential addition of two-carbon units derived from acetyl-CoAGenes of fatty acid elongation pathway were decreased in intestinal microbiome of patients suffering from neovascular age-related macular degeneration (Zinkernagel et al., 2017). Indeed, it has been suggested that fatty acid chain elongation is decreased with age (Jimenez et al., 1997).

Apart from the above discussed cross-talk between microbiota and host organism, diet is the other key element modulating host response to inflammation. Diet is emerging as the most critical determinant in human health and healthy aging, thus suggesting that the study of the effects of food derived inflamm-aging miRs are urgently needed to elucidate whether some foods should be avoided in the aging people diet since they could harmfully regulate both inflammation related metabolism and healthy gut, thus contributing to unhealthy aging. With this in mind, we inquired the DMD (Dietary MicroRNA Database) web platform to retrieve foods derived miR-21, miR-155 and miR-146a that are 100% homologues to human (Table 3). Our results suggest that cow fat, cow milk, and eggs are rich in this trio-miRs (100% homologues to

human) and thus might target inflammation related pathways. Conversely none of the plant aliments in DMD yielded the inflamma-miRs trio. Thus, the information retrieved by enquiring the DMD repository would suggest restricting cow fat, milk and eggs and increase plant aliments which do not contain any of these trio-miRs. Of note is that human breast milk has 100% matches for the 3 inflamma-miRs from animal foods. Human breast milk is a particular nutrient used from birth to weaning only, and it is interesting that has a 100% match with animals (pig, caws, atlantic salmom, gallus) homologous miRs to be avoided in diet.

In order to uncover the network linking gut microbiota, inflamma-miRs, and diet we speculate on the possible converging signalling pathways. In Fig. 2 are reported some of these converging routes, crossing the results of Tables 1 and 2. As discussed above, lysine degradation pathway and fatty acids elongation pathways were the two most representative pathways (four out of six common elements). A cross talk between these two pathways is also evidenced from biochemical studies, as for example through carnitine production (lysine degradation) and fatty acids elongation (Longo et al., 2016).

Furthermore, some of the direct target of the inflamma-miRs trio are straightforwardly involved in the modulation of oxidative stress and autophagy. As for example miR-21 has as direct target BCL2 an antioxidant proteins family. A reduction of this protein suppresses mitophagy.

5. Conclusions

We demonstrated here, through a bioinformatics *in silico* research, that a cross-talk among gut microbiota, humans inflamm-aging miRs, and foods may occur through the sharing of signalling pathways. These pathways are relevant for contrasting or, *viceversa*, exacerbating inflammation associated senescence. Indeed, we postulate by this computational study that a putative multi-directional communication among i) microbiota; ii) dietary metabolism and iii) host metabolism exists. Dietary microRNAs affect pathways that regulate microbiota composition and gut microbiota affect these pathways as well. MicroRNAs act as a link between the two systems and both tune the host metabolism. Obviously, this observation must be validated experimentally, however we believe that this hypothesis is worthy and pave the way to the study of cross-talk among the systems.

Unfortunately, this scientific approach is still in its infancy, not many nutrimiromics studies are yet carried out and some show contradictory results. In addition a very few miRs food repositories are available as yet (Quintanilha et al., 2017). DMD for example contains miRs library for 15 aliments only. This fact highlights the urgent need for more research devoted to the study of the epigenetic role of foods and microbiota and the importance of nutrition for inflammation related aging.

Ethical statement for solid state ionics – diffusion and reactions

All the authors: Laura Teodori, Ilaria Petrignani, Angelica Giuliani, Francesco Prattichizzo, Felicia Gurău, Giulia Matacchione, Fabiola Olivieri, Sofia Coppari, Maria Cristina Albertini

Testify that:

1) This material has not been published in whole or in part elsewhere.
2) The manuscript is not currently being considered for publication in another journal.
3) All authors have been personally and actively involved in substantive work leading to the manuscript and will hold themselves jointly and individually responsible for its content.

Declaration of Competing Interest

The authors declare no commercial or financial conflict of interest.

Guardare se questa Rivista lo vuole scritto qui o su una dichiarazione a parte

Appendix A. Supplementary data

Supplementary material related to this article can be found, in the online version, at doi:https://doi.org/10.1016/j.mad.2019.111127.

References

Baier, S.R., Nguyen, C., Xie, F., Wood, J.R., Zempleni, J., 2014. MicroRNAs are absorbed in biologically meaningful amounts from nutritionally relevant doses of cow milk and affect gene expression in peripheral blood mononuclear cells, HEK-293 kidney cell cultures, and mouse livers. J. Nutr. 144 (10), 1495–1500. https://doi.org/10.3945/jn.114.196436.

Carotenuto, F., Albertini, M., Coletti, D., Vilmercati, A., Campanella, L., Darzynkiewicz, Z., Teodori, L., 2016. How diet intervention via modulation of DNA damage response through MicroRNAs may have an effect on cancer prevention and aging, an in silico study. Int. J. Mol. Sci. 17 (5), 752. https://doi.org/10.3390/ijms17050752.

Cătană, C., Calin, G.A., Neagoe, I., 2015. Inflamma-miRs in aging and breast cancer: are they reliable players? Front. Med. 2. https://doi.org/10.3389/fmed.2015.00085.

Claesson, M.J., Jeffery, I.B., Conde, S., Power, S.E., O'Connor, E.M., Cusack, S., et al., 2012. Gut microbiota composition correlates with diet and health in the elderly. Nature 488 (7410), 178–184. https://doi.org/10.1038/nature11319.

Custodero, C., Mankowski, R.T., Lee, S.A., Chen, Z., Wu, S., Manini, T.M., et al., 2018. Evidence-based nutritional and pharmacological interventions targeting chronic low-grade inflammation in middle-age and older adults: a systematic review and meta-analysis. Ageing Res. Rev. 46, 42–59. https://doi.org/10.1016/j.arr.2018.05.004.

Dalmasso, G., Nguyen, H.T.T., Yan, Y., Laroui, H., Charania, M.A., Ayyadurai, S., et al., 2011. Microbiota modulate host gene expression via microRNAs. PLoS One 6 (4), e19293. https://doi.org/10.1371/journal.pone.0019293.

Forslund, K., Hildebrand, F., Nielsen, T., Falony, G., Le Chatelier, E., et al., 2015. Disentangling type 2 diabetes and metformin treatment signatures in the human gut microbiota. Nature 528 (7581), 262–266. https://doi.org/10.1038/nature15766.

Franceschi, C., Garagnani, P., Vitale, G., Capri, M., Salvioli, S., 2017. Inflammaging and "Garb-aging". Trends Endocrinol. Metab. 28 (3), 199–212. https://doi.org/10.1016/j.tem.2016.09.005.

Gruver, A., Hudson, L., Sempowski, G., 2007. Immunosenescence of ageing. J. Pathol. 211 (2), 144–156. https://doi.org/10.1002/path.2104.

Hallen, A., Jamie, J.F., Cooper, A.J.L., 2013. Lysine metabolism in mammalian brain: an update on the importance of recent discoveries. Amino Acids 45 (6), 1249–1272. https://doi.org/10.1007/s00726-013-1590-1.

Hua, C., Zhao, J.-H., Guo, H.-S., 2018. Trans-kingdom RNA silencing in plant–fungal pathogen interactions. Mol. Plant 11 (2), 235–244. https://doi.org/10.1016/j.molp.2017.12.001. , http://sbbi-panda.unl.edu:5000/dmd/browse, http://snf-515788.vm.okeanos.grnet.gr/, https://www.ncbi.nlm.nih.gov/pubmed. https://patricbrc.org/.

Jimenez, J.A.L., Bordoni, A., Lorenzini, A., Rossi, C.A., Biagi, P.L., Hrelia, S., 1997. Linoleic acid metabolism in primary cultures of adult rat cardiomyocytes is impaired by aging. Biochem. Biophys. Res. Commun. 237 (1), 142–145. https://doi.org/10.1006/bbrc.1997.7101.

Liu, S., da Cunha, A.P., Rezende, R.M., Cialic, R., Wei, Z., Bry, L., et al., 2016. The host shapes the gut microbiota via fecal microRNA. Cell Host Microbe 19 (1), 32–43. https://doi.org/10.1016/j.chom.2015.12.005.

Longo, N., Frigeni, M., Pasquali, M., 2016. Carnitine transport and fatty acid oxidation. Biochim. Biophys. Acta (BBA) – Mol. Cell Res. 1863 (10), 2422–2435. https://doi.org/10.1016/j.bbamcr.2016.01.023.

Mariño, G., Pietrocola, F., Eisenberg, T., Kong, Y., Malik, S.A., Andryushkova, A., et al., 2014. Regulation of autophagy by cytosolic acetyl-coenzyme A. Mol. Cell 53 (5), 710–725. https://doi.org/10.1016/j.molcel.2014.01.016.

Mu, J., Zhuang, X., Wang, Q., Jiang, H., Deng, Z., Wang, B., et al., 2014. Interspecies communication between plant and mouse gut host cells through edible plant derived exosome-like nanoparticles. Mol. Nutr. Food Res. 58 (7), 1561–1573. https://doi.org/10.1002/mnfr.201300729.

Neish, A.S., 2009. Microbes in gastrointestinal health and disease. Gastroenterology 136 (1), 65–80. https://doi.org/10.1053/j.gastro.2008.10.080.

Olivieri, F., Albertini, M.C., Orciani, M., Ceka, A., Cricca, M., Procopio, A.D., Bonafè, M., 2015. DNA damage response (DDR) and senescence: shuttled inflamma-miRNAs on the stage of inflamm-aging. Oncotarget 6 (34). https://doi.org/10.18632/oncotarget.5899.

Olivieri, F., Rippo, M.R., Procopio, A.D., Fazioli, F., 2013. Circulating inflamma-miRs in aging and age-related diseases. Front. Genet. 4. https://doi.org/10.3389/fgene.2013.00121.

Philip, A., Ferro, V.A., Tate, R.J., 2015. Determination of the potential bioavailability of plant microRNAs using a simulated human digestion process. Mol. Nutr. Food Res. 59 (10), 1962–1972. https://doi.org/10.1002/mnfr.201500137.

Qin, Y., Wade, P.A., 2017. Crosstalk between the microbiome and epigenome: messages from bugs. J. Biochem. 163 (2), 105–112. https://doi.org/10.1093/jb/mvx080.

Quintanilha, B., Reis, B., Duarte, G., Cozzolino, S., Rogero, M., 2017. Nutrimiromics: role of microRNAs and nutrition in modulating inflammation and chronic diseases. Nutrients 9 (11), 1168. https://doi.org/10.3390/nu9111168.

Sherman, J.H., Choudhuri, S., Vicini, J.L., 2015. Transgenic proteins in agricultural biotechnology: the toxicology forum 40th annual summer meeting. Regul. Toxicol. Pharmacol. 73 (3), 811–818. https://doi.org/10.1016/j.yrtph.2015.10.014.

Tomkovich, S., Jobin, C., 2015. Microbiota and host immune responses: a love-hate relationship. Immunology 147 (1), 1–10. https://doi.org/10.1111/imm.12538.
Turchinovich, A., Weiz, L., Burwinkel, B., 2012. Extracellular miRNAs: the mystery of their origin and function. Trends Biochem. Sci. 37 (11), 460–465. https://doi.org/10.1016/j.tibs.2012.08.003.
Valadi, H., Ekström, K., Bossios, A., Sjöstrand, M., Lee, J.J., Lötvall, J.O., 2007. Exosome-mediated transfer of mRNAs and microRNAs is a novel mechanism of genetic exchange between cells. Nat. Cell Biol. 9 (6), 654–659. https://doi.org/10.1038/ncb1596.
Vital, M., Howe, A.C., Tiedje, J.M., 2014. Revealing the bacterial butyrate synthesis pathways by analyzing (meta)genomic data. mBio 5 (2). https://doi.org/10.1128/mbio.00889-14.
Wang, K., Li, H., Yuan, Y., Etheridge, A., Zhou, Y., Huang, D., et al., 2012. The complex exogenous RNA spectra in human plasma: an interface with human gut biota? PLoS One 7 (12), e51009. https://doi.org/10.1371/journal.pone.0051009.
Williams, M.R., Stedtfeld, R.D., Tiedje, J.M., Hashsham, S.A., 2017. MicroRNAs-based inter-domain communication between the host and members of the gut microbiome. Front. Microbiol. 8. https://doi.org/10.3389/fmicb.2017.01896.
Witwer, K.W., 2012. Circulating MiRNA profiles. RNA Biol. 9 (9), 1147–1154.
Zernecke, A., Bidzhekov, K., Noels, H., Shagdarsuren, E., Gan, L., Denecke, B., et al., 2009. Delivery of microRNA-126 by apoptotic bodies induces CXCL12-dependent vascular protection. Sci. Signal. 2 (100). https://doi.org/10.1126/scisignal.2000610.ra81–ra81.
Zhang, C., Li, S., Yang, L., Huang, P., Li, W., Wang, S., et al., 2013. Structural modulation of gut microbiota in life-long calorie-restricted mice. Nat. Commun. 4 (1). https://doi.org/10.1038/ncomms3163.
Zhang, J., Li, S., Li, L., Li, M., Guo, C., Yao, J., Mi, S., 2015. Exosome and exosomal microRNA: trafficking, sorting, and function. Genomics Proteom. Bioinform. 13 (1), 17–24. https://doi.org/10.1016/j.gpb.2015.02.001.
Zinkernagel, M.S., Zysset-Burri, D.C., Keller, I., Berger, L.E., Leichtle, A.B., Largiadèr, C.R., et al., 2017. Association of the intestinal microbiome with the development of neovascular age-related macular degeneration. Sci. Rep. 7 (1). https://doi.org/10.1038/srep40826.

5. FUNCTIONAL ACTIVITIES OF PRUNUS SPINOSA EXTRACT

The chemical composition of P. *Spinosa* L. extract was analysed to investigate its biological properties. Considering the phenolic profile, we evaluated different functional activities. The antimicrobial properties against bacteria and fungi were determined. The antioxidant capacity by in *vitro* assays were evidenced and confirmed *in vivo* using the *C. elegans* model. The anti-inflammatory and anti-aging properties were determined by analysing the expression of microRNAs associated with the inflammation process (TLR4 signalling: IRAK-1, IL-6 and miR-146a and cell adhesion: ICAM-1, VCAM-1 and miR-126) in U937, young and senescent HUVECs. The extract has also been used during HUVEC replicative senescence to demonstrate its ability to improve biological aging. Furthermore, the *C. elegans* model has also been exploited to determine *in vivo* anti-aging property (lifespan and healthspan). Wound healing properties have also been identified supported by inflammation markers analyses (TLR4 signalling: IRAK-1, IL-6 and miR-146a). The extract was encapsulated within biomimetic nanoparticles (leucosomes) with two different formulations (different phospholipid constituents). Thanks to this approach, we identified specific secondary metabolites responsible for the wound healing repair.

Original articles published in:

- Journal of Functional Foods. Volume 67, April 2020, 103885 (doi.org/10.1016/j.jff.2020.103885).
- Nanomaterials. Volume 11, December 2020 (doi.org/10.3390/nano11010036).
- Antioxidants, Volume 10, March 2021 (doi.org/10.3390/antiox10030374).

Journal of Functional Foods 67 (2020) 103885

Contents lists available at ScienceDirect

Journal of Functional Foods

journal homepage: www.elsevier.com/locate/jff

Chemical composition, antioxidant, antimicrobial and anti-inflammatory activity of *Prunus spinosa* L. fruit ethanol extract☆,☆☆

Luigia Sabatini[a,1], Daniele Fraternale[a,1], Barbara Di Giacomo[a], Michele Mari[a], Maria Cristina Albertini[a], Belén Gordillo[b], Marco Bruno Luigi Rocchi[a], Davide Sisti[a], Sofia Coppari[a], Federica Semprucci[a], Loretta Guidi[a], Mariastella Colomba[a,*]

[a] Department of Biomolecular Sciences, University of Urbino Carlo Bo, 61029 Urbino (PU), Italy
[b] Food Colour & Quality Laboratory, Department of Nutrition & Food Science, Universidad de Sevilla, 41012 Sevilla, Spain

ARTICLE INFO

Keywords:
Prunus spinosa
microRNA
Anthocyanins
Functional additives
New foods

ABSTRACT

Prunus spinosa L. (from Italy) fruit ethanol extract (40 μg/mL) was assessed by evaluating the antioxidant, anti-inflammatory and antimicrobial activities against five bacterial and two fungi ATCC strains. Moreover, the phenolic profile was also investigated and results are indicative of an intense anthocyanin accumulation which may be responsible for the antioxidant properties revealed by the DPPH assay. MIC and MBC/MFC values (4.36–8.72 mg/mL; 8.72–17.44 mg/mL, respectively) revealed a wide antibacterial activity and yeast inhibition. No specific inhibitory action was observed against the tested Gram-negative or Gram-positive bacteria. Preliminary data on the effect on both miR-126 and miR-146a expression levels suggested a very interesting anti-inflammatory activity of the extract. A possible mechanism underpinning the observed effects was hypothesized and discussed. Finally, *P. spinosa* fruit extract could be used as supplementary source of functional additives and might be a promising antimicrobial compound of natural origin to be employed to fight microbial resistance.

1. Introduction

Prunus spinosa L. (also known as blackthorn, Rosaceae family), is a thorny shrub growing wild in uncultivated areas of Europe, West Asia and the Mediterranean. The plant, used in phytotherapy for the treatment of cough but also as a diuretic, laxative, antispasmodic and anti-inflammatory (see Fraternale et al., 2009 and references therein), has been widely known since the nineteenth century for its pharmaceutical properties. Because of a very pungent flavour, *P. spinosa* fruits (1–1.5 cm plums) are unsuitable for human direct consumption, but usable for the production of jams and various beverages. Such a tart taste is due to the high content of tannins that, together with the high content of anthocyanins, make these fruits interesting for their potential antioxidant, antibacterial and anti-inflammatory activity (Kubacey et al., 2012; Pinacho, Cavero, Astiasaran, Ansorena, & Calvo, 2015). For this reason, wild *P. spinosa* from different countries has progressively been receiving increasing attention, which is also a good opportunity to recover and maintain local and almost forgotten varieties.

In the last years, biological activity of natural products on human health, food preservation, pharmaceutical application, nutrition and therapy, has been subject of many studies (Bernardini, Tiezzi, Larghezza Masci, & Ovidi, 2018; Georgiev, 2014; Mostafa et al., 2018). In particular, attention has been focused on their potential antimicrobial activity (i.e. the effect on microorganisms growth), especially in view of increasing resistance of pathogenic microbes to common antimicrobials, showing that natural compounds could be also a promising means to fight microbial resistance (Aleksic & Knezevic, 2014; Balouiri, Sadiki, & Ibnsouda, 2016; Hayek, Gyawali, & Ibrahim, 2013). Veličković et al. (2014) reported that *P. spinosa* (from South East Serbia) ripe fruit ethanol extract showed antibacterial activity against some ATCC strains of *Staphylococcus aureus*, *Escherichia coli*, *Pseudomonas aeruginosa*, and *Salmonella abony* NCTC 6017, with the exception

☆ This research did not receive any specific grant from funding agencies in the public, commercial, or not-for-profit sectors.
☆☆ This work has been supported by DISB_Progetti_valorizzazione_2018, University of Urbino Carlo Bo, Urbino (PU), Italy.
* Corresponding author at: Via I. Maggetti 22, 61029 Urbino (PU), Italy.
E-mail address: mariastella.colomba@uniurb.it (M. Colomba).
[1] These authors equally contributed.

https://doi.org/10.1016/j.jff.2020.103885
Received 14 November 2019; Received in revised form 19 February 2020; Accepted 29 February 2020
Available online 06 March 2020

of *Bacillus subtilis*. Moreover, the antifungal activity tested against two pathogenic fungi such as *Aspergillus niger* and *Candida albicans* was significant only against *C. albicans*. Antibacterial and bactericidal activities of *P. spinosa* fruit methanol extract have been tested against Gram negative (*E. coli*, *P. aeruginosa*, *Salmonella enteritidis*, *Shigella sonnei*, *Klebsiella pneumoniae* and *Proteus vulgaris*) and Gram positive bacteria (*Clostridium perfringens*, *B. subtilis*, *S. aureus*, *Listeria innocua*, *Sarcina lutea* and *Micrococcus flavus*) by Radovanović, Milenković Anđelković, Radovanović, and Anđelković (2013) and, in that study, obtained results revealed a high antimicrobial activity of the extract against almost all the tested bacterial strains, with the exclusion of *Klebsiella pneumoniae*. According to available data, such a bacteriostatic and bactericidal properties mainly rely on the presence of polyphenols, in particular anthocyanins (Cisowska, Wojnicz, & Hendrich, 2011; Govardhan Singha, Negib, & Radhaa, 2013; Sikora, Bieniek, & Borczak, 2013; Veličković et al., 2014).

The high quantity of polyphenols reported for *P. spinosa* fruit extract makes the plant and, particularly, the fruits further interesting and worthy of attention suggesting a potential anti-inflammatory property to be tested and (eventually) quantified. In fact, polyphenols have already been described to exert an anti-inflammatory activity. For example, Angel-Morales, Noratto, and Mertens-Talcott (2012a) observed a reduction of mRNA expression of some LPS-induced inflammatory markers (NFkB; ICAM-1, VCAM-1 and PECAM) in human colon-derived CCD-18Co myofibroblast cells which - according to the authors - was mediated, at least in part, by the induction of miR-126, a molecule that plays an important role in the inflammation process since it is responsible for regulating cell adhesion molecules (ICAM-1 and VCAM-1). In another case study, grape tendril extract (40 μg/mL) was able to prevent the LPS stimulus in monocyte (U937) and endothelial (HUVEC) cells (Fraternale et al., 2016), probably by the same mechanism hypothesized by Angel-Morales et al. (2012a).

In addition, many authors (Cosmulescu, Trandafir, & Nour, 2017; Fraternale et al., 2009; Ganhao, Estevez, Kylli, Heinonen, & Morcuende, 2010; Radovanović et al., 2013; Varga et al., 2017; Veličković, Ilić, Mitić, Mitić, & Kostić, 2016; Veličković et al., 2014) have demonstrated a powerful antioxidant activity of *P. spinosa* fruit juice/extract by DPPH (2,2-diphenyl-1-picrylhydrazyl) test. These results strongly suggest that *P. spinosa* fruits show a very high potential. In fact, it is widely known that the consumption of fruits with a high capacity of radical scavenging is associated with a lower occurrence of degenerative diseases such as inflammation and arthritis (Egea, Sanchez-Bel, Romojaro, & Pretel, 2010).

Given all these considerations, it clearly emerges that *P. spinosa* has notably aroused the interest of the scientific community for its potential and partially already proven biological properties. Within this scenario, since some years ago, our attention has focused on the characterization of *P. spinosa* fruits from our country (the Marches, Central Italy) with the aim to promote its adoption as new food beneficial for consumers or as a supplementary source of additive elements (i.e. natural pigments or antioxidants) for food or pharmaceutical industries. In particular, in a former study including chemical composition and biological activities of *P. spinosa* fruit juice from Italy, Fraternale et al. (2009) reported that the juice shows high antioxidant properties which are likely due to particularly abundant anthocyanins. To further investigate on this item, present study was carried out with the purpose of assessing the properties of *P. spinosa* fruit ethanol extract by evaluating its antioxidant, anti-inflammatory and antimicrobial activities against a panel of isolates of five bacterial and two fungi strains for: (i) a potential use as new food or supplementary source of functional additives; or (ii) providing additional data for further development of research on antimicrobial products of natural origin. Moreover, the phenolic profile of the ethanol extract was also investigated and results were compared with available data on *P. spinosa* fruit methanol/ethanol extract from other (i.e. out of Italy) Countries.

2. Materials and methods

2.1. Chemicals and reagents

Chromatographic solvents (water, acetonitrile and formic acid) were HPLC grade, purchased from Merck (Italy). HPLC-grade Standards of cyanidin 3-glucoside (≥97%), was purchased from Sigma-Aldrich (Italy); cyanidin chloride (≥96%) was purchased from Extrasynthese (Genay, France).

2.2. Preparation of P. spinosa extract

Plant species was identified by Prof. D. Fraternale (University of Urbino). Voucher samples were deposited in the herbarium of Urbino University Botanical garden: code "*Pp*125". Ripe fruits were collected in November 2017 at "La Caputa" Urbania (PU, Marche, Italy), GPS coordinates: N43°40'46.512'' E12°31'42.291'' (350 m above sea level) and, immediately after harvesting, frozen and stored at −20 °C until use. *P. spinosa* fruit extract was prepared as in Albertini et al. (2019). In particular, 50 g of ripe fruit pulp of *P. spinosa* were homogenized in Osterizer for 3 min in 50 mL of 70% aqueous ethanol solution (70 mL ethanol/30 mL distilled H_2O). The homogenate was subsequently filtered with a Buchner filter under vacuum and the filtrate was centrifuged at 10000*g* for 15 min. The supernatant was collected while the pellets and the residue of the first extraction were re-extracted under the same initial conditions. Subsequently, the two surnatants were combined and concentrated under vacuum up to a volume of 50 mL in a Büchi rotavapor at 37 °C. In this way, 1 mL of concentrated extract corresponds to 1 g of *P. spinosa* fruit pulp. The extract was aliquoted in eppendorf tubes, dried under vacuum using a Savant concentrator and stored at −20 °C until analysis.

2.3. Determination of phenolic compounds by HPLC-DAD and HPLC/MS analysis

The separation, identification and quantification of flavanols, hydroxycinnamic acids and benzoic acids in prune extracts was performed by High Performance Liquid Chromatography-Diode Array Detection (HPLC-DAD) in an Agilent 1200 chromatographic system, equipped with quaternary pump, UV–VIS diode-array detector, automatic injector, and ChemStation software (Agilent Technologies, Palo Alto, USA). Prior direct injection, the samples were filtered through a 0.45 μm Nylon filter (E0034, Análisis Vínicos, Spain). Phenolic compounds were separated using a Zorbax C18 column (250 × 4.6 mm, 5 μm particle size) maintained at 40 °C following the method described in Gordillo et al. (2014). Acetonitrile/formic acid/water (3:10:87) was used as solvent A and acetonitrile/formic acid/water (50:10:40) was used as solvent B. The elution profile was 0–10 min with 6% B; 10–15 min with 11% B; 15–20 min with 20% B; 20–25 min with 23% B; 25–30 min with 26% B; 30–35 min with 40% B; 35–38 min with 50% B; 38–46 min with 60% B; and 46–47 min with 6% B. The flow rate was 0.63 mL/min, and the injection volume was 50 μL. All UV–Vis spectra were recorded from 200 to 800 nm with a bandwidth of 2.0 nm. The wavelengths of detection were 280 nm (flavanols and benzoic acids), 320 nm (hydroxycinnamic acids) and 525 nm (anthocyanins). The identification was achieved by comparison of the retention times and spectra characteristics of individual compounds with those of the available pure standards and our data library. The external calibration method was used for quantification, by comparing the areas with commercial standards of gallic acid, caffeic acid and catechin.

The determination of anthocyanin compounds in prune extract was performed by HPLC-PDA-ESI-MS. Chromatographic analysis was carried out with a Waters system equipped with an automatic injector, Alliance HT 2795 separation module, column heater, and Waters 2996 Photo Diode Array (PDA). The column used was a Merk Purospher Star RP-18 endcapped (4.0 mm × 250 mm, 5 μm particle size),

thermostated at 25 °C. The solvents used were (A) aqueous 0.1% formic acid in double distilled water and (B) Acetonitrile. The elution profile was as follows: 0–10 min, 94% A; 10–15 min, 83% A; 15–25 min, 78% A; 25–35 min, 76% A; 35–40 min, 74% A; 40–45 min, 68% A. The flow rate was 0.7 mL/min, and the injection volume was 50 μL (10 mg/mL of extract, dissolved in EtOH/H_2O 70:30 v/v). UV–Vis spectra were recorded from 220 to 800 nm with a bandwidth of 1.2 nm. Before direct injection, the samples were filtered through a 0.45 μm nylon filter. For the anthocyanin identification, the mass spectrometer was connected to the HPLC system via the PDA cell outlet. MS detection was carried out at 525 nm and performed with a Waters micromass ZQ MS system, single quadrupole, equipped with an Electrospray Ionization (ESI) interface. The instrument was operated in positive (ESI +) ion mode with a scan range from *m/z* 200–700. Capillary voltage was set at 3 kV, source temperature at 100 °C and desolvation temperature at 300 °C. The cone and desolvation nitrogen gas flows were 50 and 500 L/h, respectively. Data were processed using MassLynx 4.1 (Waters, Milford, USA). The quantification of anthocyanins was carried out by external calibration from the areas of the chromatographic peaks at 525 nm using a calibration curve of cyanidin-3-glucoside standard.

All analyses were performed in triplicate and the results were expressed as mg/100 g DW (dry weight). Total flavanols, hydroxycinnamic acids, benzoic acids and anthocyanins were estimated by summing the content of each member quantified.

2.4. Test organisms and inocula preparation

The *in vitro* activity quantification of *P. spinosa* crude extract was performed according to CLSI standard methods (CLSI, 1999, 2008; NCCLS, 2002).

Five bacterial and two fungal reference strains were used: *Enterococcus faecalis* ATCC 29212, *Escherichia coli* ATCC 25922, *Pseudomonas aeruginosa* ATCC 9027, *Salmonella enteriditis* ATCC 13076, *Staphylococcus aureus* ATCC 6538, *Candida albicans* ATCC 10231 and *Aspergillus niger* ATCC 9642.

Starting from cultures in Tryptic Soy Agar (TSA, Liofilchem, Roseto degli Abruzzi, Italy), bacteria were grown overnight at 36 ± 1 °C in Mueller Hinton Broth (MHB, Sigma-Aldrich, Milan, Italy); each culture broth was used to obtain a standard inoculum. *C. albicans* (yeast) was grown on Sabouraud Dextrose Agar (SDA, Liofilchem) at 36 ± 1 °C for 24 h and *A. niger* (mold) on Potato Dextrose Agar (PDA, Liofilchem) at 25 °C for 7 days. The colonies were then used to prepare the fungal inoculum in sterile saline.

The microorganism suspensions were standardized to 0.5 McFarland scale (10^8 CFU/mL) using spectrophotometric measurement (600 nm for bacteria, 530 nm for yeast), and plate count method (for mold). Then the suspensions of each strains were diluted with standard culture media: MHB to obtain 10^6 CFU/mL of bacteria, RPMI 1640 (Sigma-Aldrich) to obtain 10^3 CFU/mL of yeast and 10^4 CFU/mL of mold.

2.5. Antimicrobial activity

The standard antimicrobial susceptibility test based on the determination of microorganism growth as a function of decreasing concentrations of the test product was performed by using 96-well microtiter plates. Serial doubling dilutions of *P. spinosa* extract (over the range of 69.75–0.07 mg/mL) were prepared in the standard culture media (100 μL in each well). Afterwards, extract dilutions were inoculated with the test strains (100 μL in each well); positive control (culture medium + test strains, without extract) to test viability, and negative control (only culture medium) to test sterility conditions were also added. Bacteria and yeast were incubated for 24–48 h at 36 ± 1 °C, mold for 72 h at 25 °C. Macroscopic observation of turbidity allowed the qualitative assessment of microbial growth which was, on the other hand, quantitatively determined and expressed as OD (Optical Density) units by absorbance at 600 nm (bacteria) and 530 nm (yeast) using the universal microplate reader Multiskan EX (Thermo Electron Corporation). Growth of the filamentous fungus *A. niger* was evaluated only by plate count. Minimal inhibitory concentration (MIC) was defined as the lowest concentration of *P. spinosa* fruit ethanol extract at which microorganisms showed no visible growth. Data were reported as mg/mL of crude extract and μg/mL of total phenolic content.

In order to further evaluate the effect of the extract on microbial growth, a broth microdilution method was carried out by a series of sterile tubes containing aliquots of 5 mL of culture medium (TSB Tryptic Soy Broth, Sigma-Aldrich), different concentrations of *P. spinosa* extract (over the range of 69.75–0.07 mg/mL) and suspensions of each strain. Experimental conditions were the same as those described above.

After MIC determination, aliquots (20 μL) taken from each well showing complete growth inhibition (100% inhibition or an optically clear well), from the last positive well (showing growth similar to that of positive control well), and from the positive control well (containing extract-free medium) were subcultured on agar plates of TSA for bacteria, SDA for yeast and PDA for mold. The plates were then incubated at the specific temperature of the microbial strains. The lack of growth (i.e. the absence of colonies on the surface of the agar plates) determines the Minimum Bactericidal Concentration or Minimum Fungicidal Concentration (MBC/MFC) which is defined as the lowest concentration of the extract required to kill 99.9% of the initial inoculum (Balouiri et al., 2016; Espinel-Ingroff, Fothergill, Peter, Rinaldi, & Walsh, 2002). Every series of tests was performed in triplicate.

2.6. Quantitative real time PCR (RT-qPCR) of mature microRNAs and mRNA

The total RNA isolation kit (Norgen Biotek, Thorold, Canada) was used to isolate total RNA (including both microRNA and larger RNA species) from 1×10^6 U937 cells, following the manufacturer's recommended protocol; RNA was stored at −80 °C until use. Human miR-126, miR-146a and human RNU44 (reference miRNA) expressions were quantified using the TaqMan MicroRNA assay (Applied Biosystems, Foster City, CA, USA), as previously described (Olivieri et al., 2013).

Isolated RNA was used to synthesise cDNA using a reverse transcription kit (Applied Biosystems, Foster City, CA, USA) according to the manufacturer's protocol. Quantitative polymerase chain reaction real time (RT-qPCR) was performed with the SYBR Green PCR master mix (Applied Biosystems, Foster City, CA, USA) on an ABI Prism 7500 Real Time PCR System (Applied Biosystems, Foster City, CA, USA). The primers (ICAM-1: Forward TGGCCCTCCATAGACATGTGT and Reverse TGGCATCCGTCAGGAAGTG; VCAM-1: Forward ACAGAAGAAGTGGCC CTCCAT and Reverse TGGCATCCGTCAGGAAGTG; IL-6: Forward AGG GCTCTTCGGCAAATGTA and Reverse GAAGGAATGCCCATTAACAA CAA; IRAK-1: Forward CAGACAGGGAAGGGAAACATTTT and Reverse CATGAAACCTGACTTGCTTCTGAA) we used were the ones designed by Angel-Morales, Noratto, and Mertens-Talcott (2012b). TATA binding protein (TBP; Forward TGCACAGGAGCCAAGAGTGAA and Reverse CACATCACAGCTCCCCACCA) was used as an endogenous control to determine relative mRNA expression. The pairs of forward and reverse primers were purchased from Sigma-Aldrich. Product specificity was examined by dissociation curve analysis. Results were calculated using the 2-ΔΔCt method and are expressed in the figures as fold change related to untreated control (CTRL) (Fraternale et al., 2016).

2.7. Monocyte-endothelial cell adhesion

HUVECs (3×10^5) were grown on coverslips (Sigma-Aldrich) placed into a six-well plate to reach semiconfluence. HUVECs were treated with *P. spinosa* ethanol extract during LPS (1 μg/mL) stimulation (Fraternale et al., 2016). U937 cells (1×10^6) were added to each well and incubated for 1 h. U937 non-adherent cells were removed by

three PBS washes and coverslips were placed on glass microscope slides (Sigma-Aldrich). Images were captured under an optical microscope (using a BX-51 Olympus microscope with a 40 × objective) and adherent cells were counted (three random fields) and expressed as the number of adhered cells per field related to the number of HUVECs (i.e. U937/HUVEC per field).

2.8. DPPH radical assay

The DPPH (DiPhenylPicrylHydrazyl) radical-scavenging method was used to evaluate the anti-oxidant capacity of *Prunus spinosa* following experimental protocol described in Fraternale et al. (2016). Briefly, the reaction solution (400 µL final volume) was mixed with 80 µL of 0.5 mM DPPH (Sigma-Aldrich) ethanol solution and 40 µL of *P. spinosa* ethanol extract at different final concentrations (ranging from 10 to 600 µg/mL). After shaking, mixtures were left for 1 h in the dark. Absorbance was measured at 517 nm using ethanol as blank. The negative control was prepared with only DPPH (80 µL of 0.5 mM) diluted in ethanol (400 µL final volume). Lower absorbance indicates high free radical scavenging ability. DPPH inhibition (I, expressed in %) was used to evaluate the antioxidant activity by the following equation:

$$I(\%) = [(A_0 - A_s)/A_0] \times 100$$

where A_0 is the absorbance of the negative control and A_s is the absorbance of the tested sample.

All analyses were performed in triplicate. L-ascorbic acid (Sigma-Aldrich) was used as standard control at a concentration of 0.040 mg/mL.

2.9. Statistical analysis

Growth curve analysis was used to analyze microbial OD in function of extract concentrations. A non-linear regression fitting of 4 parameter logistic growth curve was performed: $N_x = N_0 + \frac{N_{max}}{(1 + e^{-1/b(x-c)})}$

where × is the *P. spinosa* extract concentration, N_x is the microbial OD at concentration ×, N_{max} is the maximal microbial OD expected, c is the point of inflection, and b is inversely related to the tangent slope (m) in flex point. The × value has been transformed using x* = Log (100x + 1), in order to obtain an arithmetic progression from a geometric progression. The inflection point coordinates (*Flex*) were calculated as follows: $Flex = \left(c; \frac{N_{max}}{2} + N_0\right)$ and the tangent slope (m) in flex point was estimated as: $m = \frac{N_{max}}{4b}$.

Non-linear regression (Bates & Watts, 2007), was performed using Levenberg-Marquardt algorithm on SPSS 22.0 software. Multivariate analysis of variance (MANOVA) was performed in order to compare the groups. The significance level was set at $\alpha = 0.05$.

The two-tailed paired Student's *t*-test was used for the anti-inflammatory (miR-126, ICAM-1, VCAM-1, miR-146a, IRAK-1, IL-6 and cell adhesion count) analyses. The results were considered significant at the level of $p < 0.05$.

Linear regression analysis was used to evaluate the DPPH scavenging activity of *P. spinosa* extract.

3. Results and discussion

3.1. Phenolic composition and antioxidant effect of P. spinosa extract

The phenolic profile of *P. spinosa* crude extract is shown in Fig. 1. Different classes of colourless phenolics were identified and quantified by HPLC (Fig. 1a) including hydroxycinnamic acids (caffeic, coumaric, chlorogenic acids and derivatives), hydroxybenzoic acids (gallic acid and derivatives of syringic and vainillic acids), and flavanols ((+)-catechin). Most of these compounds have already been described in fresh prune fruits (Madrau, Sanguinetti, Del Caro, Fadda, & Piga, 2010). However, the most common hydroxycinammic acid (neochlorogenic acid) was not found in *P. spinosa* extract, probably due to genetic differences between cultivars (Miletic et al., 2013). Regarding anthocyanin pigments, the chromatogram registered at 525 nm shows the presence of the two main anthocyanins (Fig. 1b). Both compounds were identified as cyanidin derivatives according to the HPLC-PDA-MS analysis (Fig. 1c and 1d). Table 1 shows the concentrations (mg/100 g DW ± SD, n = 3) of the different phenolic families described. The most abundant phenolic compounds in *P. spinosa* extract were anthocyanins (58%) and hydroxycinnamic acids (22%). Similar proportions (40–45%) of anthocyanins have been reported in literature for fresh prune fruits (Stacewicz-Sapuntzakis, Bowen, Hussain, Damayanti-Wood, & Farnsworth, 2001). Nevertheless, other studies found much higher proportions (50–70%) of hydroxycinnamic acids (Madrau et al., 2010; Piga, Del Caro, & Corda, 2003). Although in lower amounts, hydroxybenzoic acids (12%) and flavanols (8%) were also present in the extract. Amongst anthocyanins, cyanidin 3-rutinoside and cyanidin 3-glucoside have been indicated as the main ones present in prunes, especially the wild and dark varieties, being responsible for the red, or violet to black colours (Madrau et al., 2010; Mikulic-Petkovsek, Stampar, Veberic, & Sircelj, 2016). In our case, in *P. spinosa* ethanol extract, the major anthocyanin corresponded - according to its mass molecular ion ($[M]^+ = 287$) and UV–visible spectra features (Fig. 1d) - with the aglycon cyanidin (85.95 ± 1.94 mg/100 g DW). A possible explanation that could be offered for such a discrepancy with precedent findings respect to the presence of cyanidin 3-rutinoside is that, typically, the production of crude extracts with several contaminants submitted to concentration procedures can result in the hydrolysis of labile linkages of anthocyanins such as sugar residues (Rodriguez-Saona & Wrolstad, 2001) which could explain the presence of the aglycon cyanidin. Its glycoside analogue cyanidin 3-glucoside ($[M]^+ = 449$), was also detected, but in lower amount respect to what reported by Mikulic-Petkovsek et al., 2016 (about 2 mg/Kg FW vs about 1286 mg/kg FW), but - on the other hand - higher (about 13.33 mg/100 g DW vs 19.83 µg/100 g DW) than what reported by Guimarães et al. (2013). Other minor anthocyanins were also detected but their absorption or mass spectra were insufficient to allow speculation about their identity. Notably, an aspect that should not be underestimated and that perhaps could, at least, in part justify the strong discrepancy between the values observed in our study and those previously reported for *P. spinosa*, is probably related with: (i) different "environmental conditions" (i.e. fruit ripening level, temperature, insolation, pH and rainfall precipitations); (ii) different extraction techniques (i.e. methanol: water; BHT: formic acid: methanol; ethanol: water) and (iii) different concentrations of the solvent (Guimarães et al., 2013; Mikulic-Petkovsek et al., 2016), given that the conditions of each methodology may interfere with the results.

P. spinosa extract showed a concentration-dependent antioxidant activity (Fig. 2) when analysed by DPPH assay ($R^2 = 0.955$). The phenolic compounds (see Table 1) may be responsible for the antioxidant activity observed, as hypothesized in other studies (Radovanović et al., 2013).

3.2. Antimicrobial effect of P. spinosa ethanol extract on target microorganisms

The antimicrobial effects of *P. spinosa* extract against target microorganisms, as determined by evaluating the Minimum Inhibitory Concentration (MIC) and Minimum Bactericidal/Fungicidal Concentration (MBC/MFC) values (in mg/mL) of *P. spinosa* extract, are shown in Table 2. In particular, the extract appeared to exert a wide antibacterial activity and yeast inhibition, with the exception of *A. niger* (MIC 34.78 mg/mL). No specific inhibitory action was observed against the tested Gram-negative or Gram-positive bacteria, as suggested by comparable MIC values ranging from 4.36 to 8.72 mg/mL. *P. spinosa* extract concentration necessary to kill bacteria or fungi (MBC/MFC) mostly resulted to be nearly twofold the observed correspondent MIC

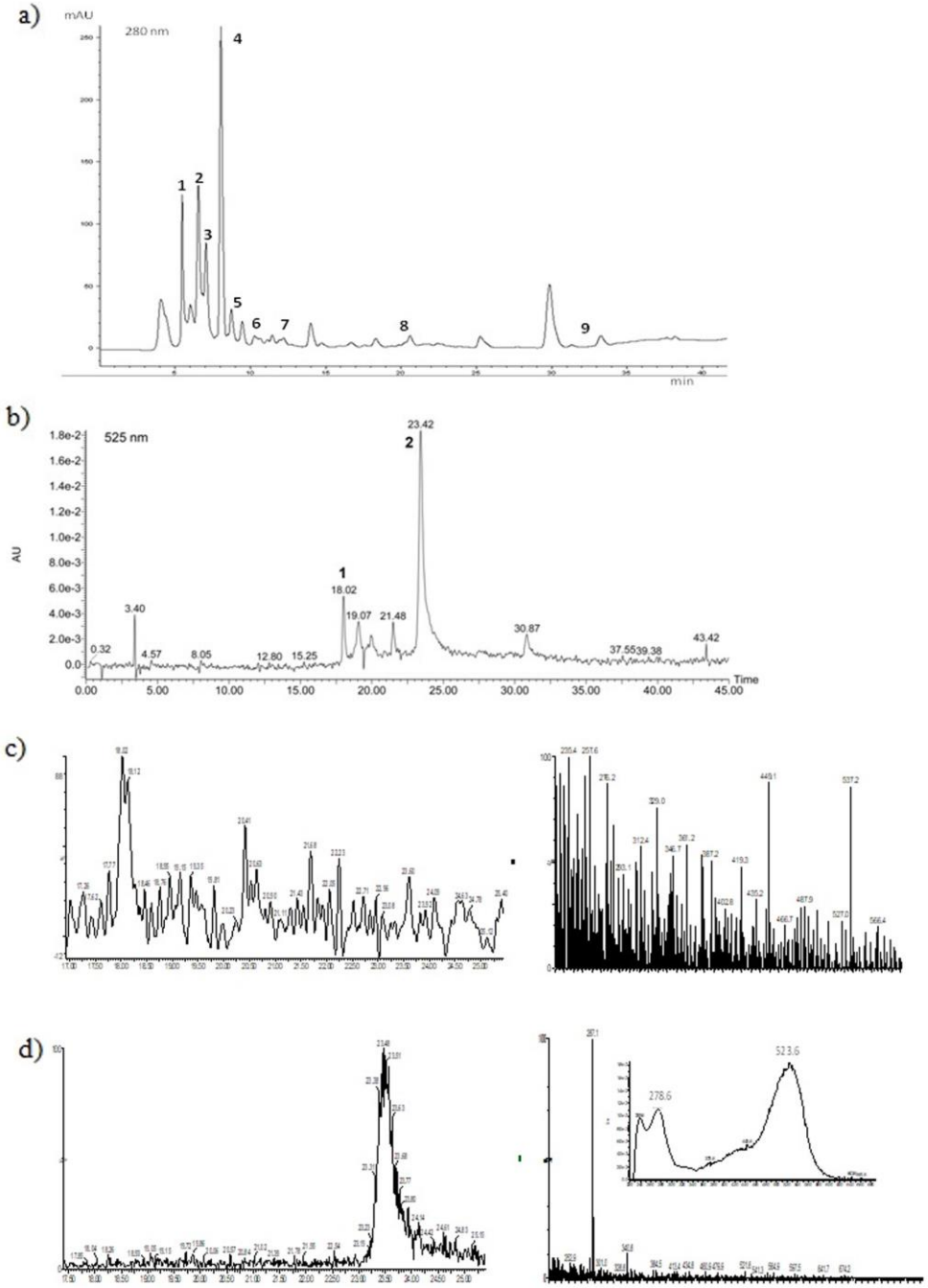

Fig. 1. (a) HPLC chromatogram of *P. spinosa* extract recorded at 280 nm, peaks: 1, Gallic acid; 2, m-coumaric derivative; 3, Vainillic acid derivative 1; 4, (+)-catechin; 5, Syringic acid derivative; 6, Vanillic acid derivative 2; 7, Caffeic acid; 8, *p*-coumaric acid; 9, Chlorogenic acid; (b) HPLC chromatogram recorded at 525 nm (0.00–45.00 min) showing the two major anthocyanins peaks: 1, cyanidin 3-glucoside; 2, cyanidin; (c) Expanded ion chromatogram at *m/z* value of 449 (TIC scan ES + 449.1 0PPM) and Mass spectra (ES^+) on peak 1 (r.t. 18.02 min); (d) Expanded ion chromatogram at *m/z* value of 287 (TIC scan ES + 287.1 0PPM) and UV–Vis and Mass spectra (ES^+) on peak 2 (r.t. 23.42 min).

Table 1
Phenolic content (mg/100 g DW ± SD) of different phenolic families in *P. spinosa* ethanol extract.

Phenolic compounds	Concentration (mg/100 g DW ± SD)
Sum of anthocyanins (525 nm)	150.11 ± 2.08
Sum of flavanols (280 nm)	30.10 ± 0.35
Sum of hydroxycinnamic acids (320 nm)	56.50 ± 1.26
Sum of benzoic acids (280 nm)	21.66 ± 0.38

value. Also in this case, no differences in antibacterial activity were evidenced between Gram-negative or Gram-positive strains.

Our findings are in accordance with other studies; for example, Veličković et al. (2014) reported the antimicrobial effect of *P. spinosa* with extract concentration ranging from 10 to 30 mg/mL; and Coccia et al. (2012) examined the antimicrobial effect of *Prunus cerasus* L. extract on different microbial strains, obtaining MICs in the range of 2.0–6.6 mg/mL. Moreover, comparing our results with available data, it was observed that MIC of *P. aeruginosa* was similar (4.36 vs 4.4 mg/mL) to that found in the study of Coccia et al. (2012). Notably, when comparing MIC values, expressed as total phenolic content, MIC for *P. spinosa* (10.50 μg/mL, present study) is lower than that of *P. cerasus* (108.24 μg/mL of GAE, Coccia et al., 2012). Taking into account that *P. spinosa* extract shows a total content of anthocyanins higher than that reported in various studies on different *Prunus* species (Coman et al., 2018), it seems reasonable to hypothesize that the greater efficacy in the antimicrobial activity demonstrated by *P. spinosa* ethanol extract may be due to anthocyanins, even if, at the moment, the hypothesis of a possible combined action of bioactive compounds cannot be ruled out.

For fungal strains, the anti-proliferative action was obtained on *C. albicans* at high concentrations, while growth of *A. niger* was inhibited only at the maximum concentration tested (69.75 mg/mL), thus confirming that the extract is not particularly active against fungi, as pharmacologically active molecules act in the microgram per millilitre (μg/mL) range, which is substantially lower than values here reported (see also Coccia et al., 2012).

In order to evaluate more accurately the minimum inhibitory concentrations (MICs), we employed a non-linear regression analysis to create microbial growth curves with OD 600 nm values vs different extract concentrations (Chorianopoulos et al., 2006). As indicated in Fig. 3, the microbial growth curves show that the antimicrobial effect of *P. spinosa* extract ranges from 2.18 mg/mL to 17.44 mg/mL.

Table 2
Minimum Inhibitory Concentration (MIC) and Minimum Bactericidal/Fungicidal Concentration (MBC/MFC) values (mg/mL) of *P. spinosa* extract related to crude extract (mg/mL) and total phenolic content (μg/mL).

	MIC		MBC/MFC	
Target microorganisms	mg/ml	μg/ml	mg/ml	μg/ml
E. coli ATCC 25922	8.72	20.90	17.44	41.80
S. aureus ATCC 6538	8.72	20.90	17.44	41.80
P. aeruginosa ATCC 9027	4.36	10.50	8.72	20.90
E. faecalis ATCC 29212	4.36	10.50	8.72	20.90
S. enteriditis ATCC 13076	4.36	10.50	8.72	20.90
C. albicans ATCC 10231	8.72	20.90	17.44	41.80
A. niger ATCC 9642	34.87	83.70	69.75	167.40

Moreover, to compare MIC values calculated with this method to the previous MIC identified, we considered further data obtained by non-linear regression analysis indicated in Table 3. The xflex corresponds to the extract concentration (x values) where growth curve changes and microbial growth decreases. This value can be considered as the MIC value, with associated R^2 values representing the goodness of fitting. As indicated by xflex, the MIC values in the non-linear regression analysis (Table 3) were consistent to the values previously obtained (see Table 2).

Regarding the OD values (Fig. 3) and CFU mL^{-1} (data not shown), in order to evaluate the trend of microbial growth, it was observed that concentrations lower than MIC caused an increase in OD compared with untreated control (which was confirmed by CFU count), thus indicating a "paradox" effect of stimulation of both bacterial and fungal growth (Table 4).

For *E. coli, S. aureus, P. aeruginosa, S. enteriditis* and *C. albicans* these concentrations were lower than 1 mg/mL (0.07 to 0.55 mg/mL). *E. faecalis* showed the highest growth at 1.1 mg/mL. This is in line with previous results by Silva et al. (2016) who observed that on *Acinetobacter baumannii, Proteus mirabilis* and two *Pseudomonas* strains the blueberry extract did not act as an antimicrobial compound, but rather promoted microbial growth. In addition, Coccia et al. (2012) verified

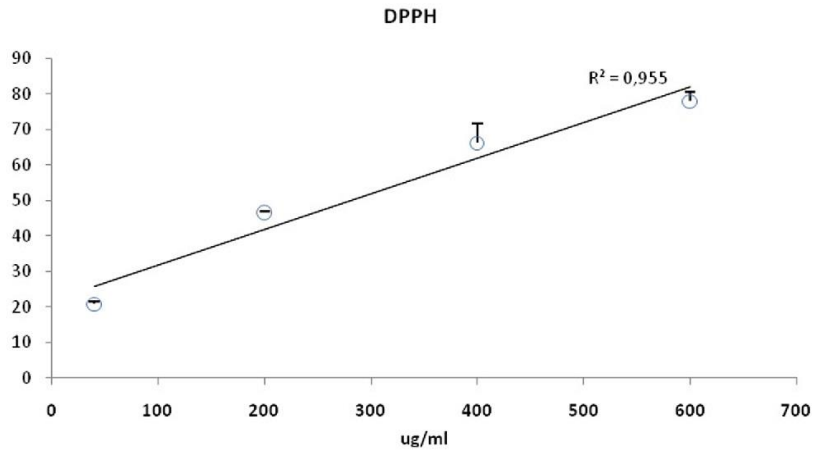

Fig. 2. DPPH analysis of *P. spinosa* extract antioxidant activity was carried out at different concentrations (from 20 μg/ml to 600 μg/ml). R^2 = 0.955 shows a concentration-dependent effect.

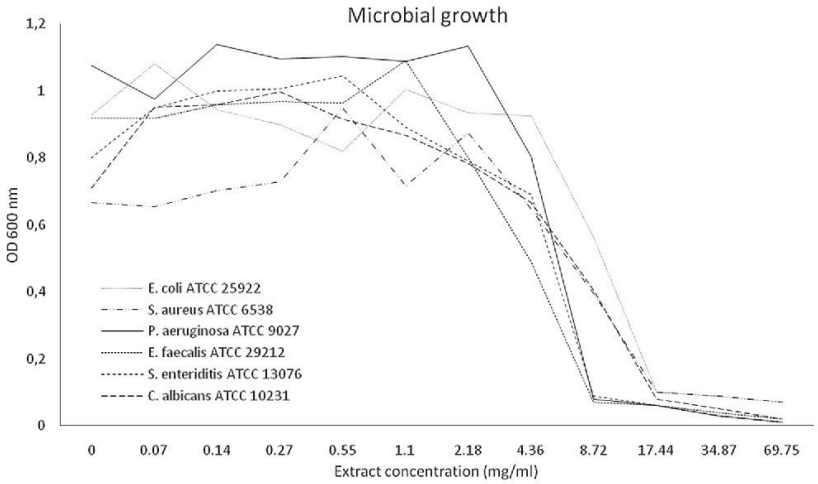

Fig. 3. Growth curve non-linear regression analysis 24 h after treatment at different extract concentrations (mg/mL). *Escherichia coli*; *Staphylococcus aureus*; *Pseudomonas aeruginosa*; *Enterococcus faecalis*; *Salmonella enteritidis*; *Candida albicans*.

Table 3
Growth parameters obtained from non-linear regression analysis.

	E. coli ATCC 25922	*S. aureus ATCC 6538*	*P. aeruginosa ATCC 9027*	*E. faecalis ATCC 29212*	*S. enteriditis ATCC 13076*	*C. albicans ATCC 10231*
y0	0.078	0.071	0.035	0.029	0.024	−0.003
ymax	0.866	0.682	1.052	0.935	0.907	0.903
xflex	9.130	8.264	5.146	4.158	5.352	7.338
yflex	0.511	0.412	0.561	0.496	0.478	0.448
mflex	−2.716	−1.364	−3.748	−1.749	−2.278	−1.037
R^2	0.975	0.925	0.993	0.986	0.971	0.962

Table 4
P. spinosa extract concentration exerting the highest microbial growth (highest OD values) obtained from non-linear regression analysis.

	P. spinosa concentration (mg/mL)	OD	MIC (mg/mL)
E. coli ATCC 25922	0.07	1.081	9.130
S. aureus ATCC 6538	0.55	0.95	8.264
P. aeruginosa ATCC 9027	0.14	1.138	5.146
E. faecalis ATCC 29212	1.1	1.09	4.158
S. enteriditis ATCC 13076	0.27	1.006	5.352
C. albicans ATCC 10231	0.27	0.997	7.338

that the sour cherry crude extract exerted a prebiotic-like effect at low concentrations against nine bacterial species and two yeast species.

3.3. Anti-inflammatory effect of P. spinosa ethanol extract

To investigate whether *P. spinosa* ethanol extract could have an anti-inflammatory activity, we first analyzed the expression of miR-126 and its cell adhesion molecules targets (ICAM-1 and VCAM-1). When miR-126 is down-regulated during pro-inflammatory stimulation, the expression of its targets is enhanced; while in our experimental conditions, during an acute pro-inflammatory challenge by LPS, treatment with *P. spinosa* (P. spinosa + LPS) increased miR-126 and decreased ICAM-1 and VCAM-1 expression levels (Fig. 4).

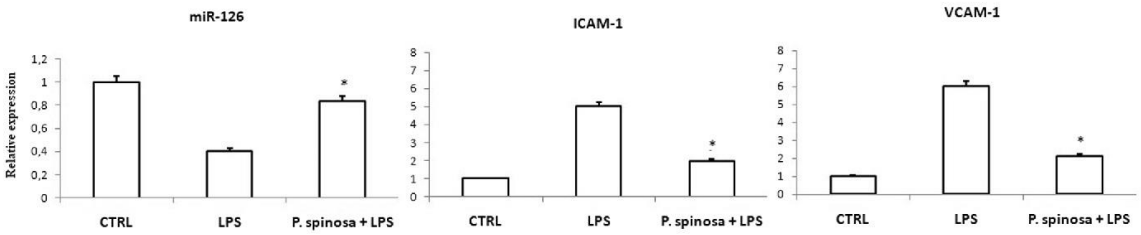

Fig. 4. Effect of *P. spinosa* extract on miR-126 and its cell adhesion molecules targets (ICAM-1 and VCAM-1) expression in LPS (lipopolysaccharide) stimulated cells. In U937, the LPS down-regulation of miR-126 (LPS) was restored during *P. spinosa* extract treatment (P. spinosa + LPS). *P. spinosa* extract treatment caused a decreased expression of both miR-126 targets, ICAM-1 (intercellular adhesion molecule 1) and VCAM-1 (vascular cell adhesion protein 1). RT-qPCR values are reported as fold induction related to CTRL. Two-tailed paired Student's *t*-test: * = $p < 0.05$ LPS vs P. spinosa + LPS.

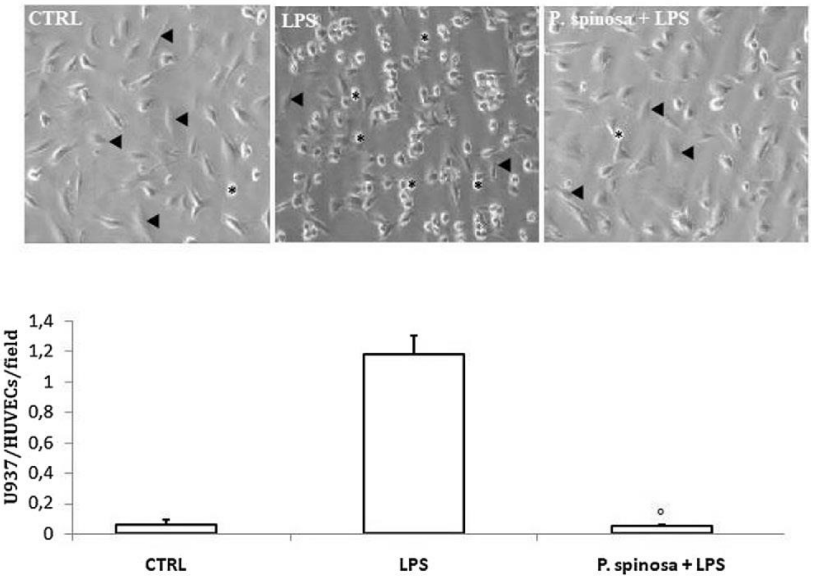

Fig. 5. U937 endothelial adhesion was evaluated adding untreated U937 cells to LPS-stimulated HUVECs without/with *P. spinosa* ethanol extract (LPS /P. spinosa + LPS, respectively). Images captured on a BX-51 Olympus microscope with a 40 × objective of U937 adherent to HUVECs were used to evaluate the number of adherent U937 (*) cells related to HUVECs (◀) present in each field analysed (3 fields for each treatment conditions). The number of adhered cells per field related to the number of HUVECs (U937/HUVECs/field) are reported in the bar graph, * = $p < 0.05$.

To confirm our results, the adherence of untreated U937 to HUVEC treated (at the same previously described experimental conditions) cells was determined. Our results identified a marked reduction of adherent U937 cells when LPS stimulated HUVECs were treated with *P. spinosa* ethanol extract, as demonstrated by both microscope images (Fig. 5) and adherent U937 cell count.

We further investigated *P. spinosa* ethanol extract anti-inflammatory activity by analyzing the TLR4 signalling through miR-146a, IRAK-1 and IL-6 expressions. As indicated in Fig. 6, when miR-146a is down-regulated during a pro-inflammatory challenge, the expression of its targets, IRAK-1 and IL-6, is enhanced. On the other hand, during an acute pro-inflammatory stimulus induced by LPS, treatment with *P. spinosa* ethanol extract (P. spinosa + LPS) increased miR-146a and decreased IRAK-1 and IL-6 expression levels.

Although the real nature of molecular interactions between TLR4 and *P. spinosa* ethanol extract are still to be investigated, our findings confirm that *P. spinosa* ethanol extract can up-regulate intracellular miR-126 and miR-146a expression levels with a consequent down-regulation of the TLR-NF-κB-mediated inflammatory response. In particular (see Fig. 7), treatment with *P. spinosa* ethanol extract can prevent the LPS stimulation by inhibiting TLR4 signalling and reducing cytokines (IL-6 and TNFα) production and cell adhesion molecules (ICAM-1 and VCAM-1).

4. Conclusions

This is the first report on the study of antimicrobial, anti-inflammatory and antioxidant properties of *P. spinosa* (from Central Italy, the Marche region) fruit ethanol extract along with its phytochemical (mostly phenolic) profile. The results are indicative of an intense anthocyanin accumulation which could explain the antioxidant activity and may be crucial for promoting consumption of *P. spinosa* fruit juice or extract. In fact, besides in case of diseases related to oxidative stress or inflammation, anthocyanins have been found to have also beneficial effects for people with obesity and metabolic syndrome (Shi, Mathai, Xu, McAinch, & Su, 2019) and, moreover, represent a source of natural pigments and antioxidants for food or pharmaceutical industries. Therefore *P. spinosa* fruits show a high potential and could be used as new food or food additives which could be considered beneficial for consumers.

As shown, the extract exhibited an interesting antimicrobial activity (higher than other *Prunus* species) against a range of bacteria and yeast, with the exception of the mold *A. niger*. As not all strains tested in the present study are pathogenic, and to assure whether there is any variability in the spectrum of the antimicrobial activity against a larger panel of pathogenic isolates, further studies in animal models and clinical trials would be essential to fill these gaps of knowledge and determine the *in vivo* benefits. Nevertheless, our findings attest that *P.*

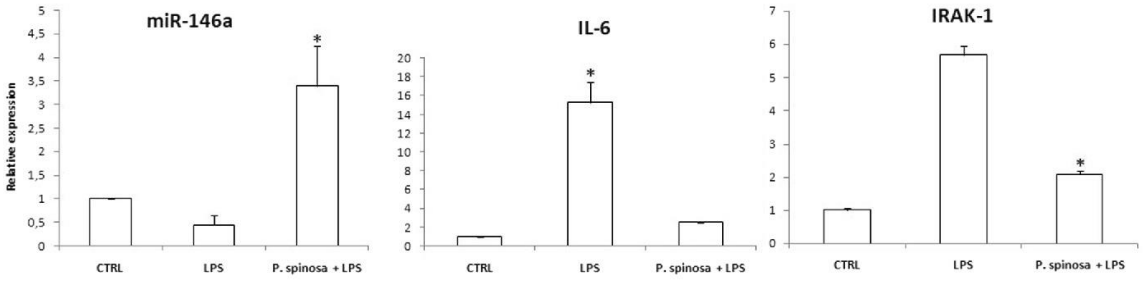

Fig. 6. Effect of *P. spinosa* extract on miR-146a, its cell IRAK-1 target and IL-6 expressions in LPS (lipopolysaccharide) stimulated cells. In U937, the LPS down-regulation of miR-146a (LPS) was increased during *P. spinosa* extract treatment (P. spinosa + LPS). *P. spinosa* extract treatment caused a decreased expression of both IRAK-1 and IL-6. RT-qPCR values are reported as fold induction related to CTRL. Two-tailed paired Student's *t*-test: * = $p < 0.05$ LPS vs P. spinosa + LPS.

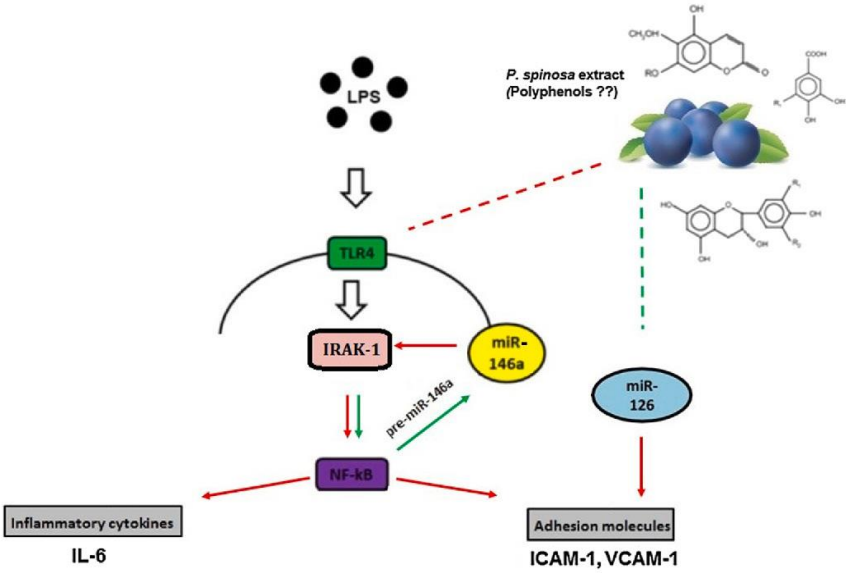

Fig. 7. Schematic representation of the possible *P. spinosa* extract action mechanism. TLR4 signalling has been analyzed to evaluate the anti-inflammatory effect of *P. spinosa* extract. During a pro-inflammatory stimulus (LPS) TLR4 and IRAK-1 activate NFkB transcription factor to express miR-146a, IL-6 and cell adhesion molecules (ICAM-1, VCAM-1). When cells are treated with *P. spinosa* extract, TLR4 signalling can be blocked by a negative feedback loop mechanism where miR-146a targets IRAK-1 (down-regulation) leading to a decreased expression of IL-6 and cell adhesion molecules (ICAM-1, VCAM-1). Furthermore, miR-126 up-regulation may also participate to decrease its cell adhesion molecules (ICAM-1, VCAM-1) targets expression. Legend: Red-dotted line: hypothesized negative interaction; Green-dotted line: hypothesized positive interaction; Red arrow: negative interaction; Green arrow: positive interaction. (For interpretation of the references to colour in this figure legend, the reader is referred to the web version of this article.)

spinosa extract is a promising candidate for the prevention of several bacterial infections, although the responsible mechanisms behind the beneficial effects require further investigation.

Finally, preliminary data seems to suggest a very interesting anti-inflammatory activity of the extract. In fact, treatment with *P. spinosa* fruit ethanol extract prevented U937 cells stimulation by LPS, inhibiting TLR4 signalling, along with pro-inflammatory cytokine production and cell adhesion. In particular, according to our experimental results the action mechanism tentatively suggested is as follows: polyphenols, (as proposed by Fraternale et al., 2016) would be capable of influencing the activation of the intracellular NF-kB signaling pathway which (along with MAPK and JAK-STAT) is responsible for the production of various inflammatory mediators. NF-kB activation increases miR-146a expression, which in turn inhibits IRAK-1 (one of the key mediators of the Toll-like receptor 4 pathway, along with TRAF-6 and MYD88) expression as a negative feedback loop. Such a process reduces NF-kB translocation into the nucleus causing a down-regulation of the transcription of target genes, including IL-6, ICAM-1 and VCAM-1. Moreover, polyphenols would increase miR-126 expression with a further down-regulation of ICAM-1 and VCAM-1. Although at the moment the molecular basis of the anti-inflammatory properties of *P. spinosa* extract needs further studies, present findings seem, however, to corroborate this hypothesis. Nevertheless, the action mechanism tentatively proposed in this report will be certainly explored in the next future to better clarify this item.

Author contributions

M.C. designed the study, wrote the main manuscript and revised the ms.; L.S. designed and performed the microbial experimental trials; D.F. prepared *P. spinosus* ethanol extract and revised the ms.; M.C.A. performed quantitative Real Time PCR, monocyte-endothelial cell adhesion and DPPH radical assays and revised the ms.; M.B.L.R. and D.S. performed the data analyses;.B.D.G., M.M. and B.G. performed HPLC-DAD and HPLC/MS analyses; All authors reviewed the ms.

Authors' declaration

The manuscript contains original unpublished work and is not being submitted for publication elsewhere at the same time.

Ethics statements

The study comprised two main items including: (i) chemical analyses by HPLC-DAD and HPLC/MS to determine the phenolic compounds; and (ii) *in vitro* experiments to assess the antioxidant, anti-inflammatory and antimicrobial properties of *P. spinosa* fruit ethanol crude extract. Neither animals nor human subjects were involved therefore no institutional or national ethical committee approval was needed.

Author contribution

M.C.: Conceptualization, Writing - original draft, Writing - review & editing; L.S.: Investigation (microbial experimental trials); D.F.: Methodology (P. spinosus ethanol extract preparation), review & editing; M.C.A.: Investigation (quantitative Real Time PCR, monocyte-endothelial cell adhesion and DPPH radical assays), review & editing; M.B.L.R. and D.S.: Data curation (statistical analysis);.B.D.G., M.M. and B.G.: Investigation (HPLC-DAD and HPLC/MS analyses); All authors reviewed the ms.

Declaration of Competing Interest

The authors declare that they have no known competing financial interests or personal relationships that could have appeared to influence the work reported in this paper.

Acknowledgements

The authors are grateful to Prof. Anna Pianetti for her support and Dr. Raffaella Campana for her assistance on microbial growth analysis.

References

Albertini, M. C., Fraternale, D., Semprucci, F., Cecchini, S., Colomba, M., Rocchi, M. B. L., ... Guidi, L. (2019). Bioeffects of *Prunus spinosa* L. fruit ethanol extract on reproduction and phenotypic plasticity of *Trycoplax adhaerens* Schulze, 1883 (Placozoa). *PeerJ*. https://doi.org/10.7717/peerj.6789.

Aleksic, V., & Knezevic, P. (2014). Antimicrobial and antioxidative activity of extracts and essential oils of *Myrtus communis* L. *Microbiological Research, 169*(4), 240–254.

Angel-Morales, G., Noratto, G., & Mertens-Talcott, S. (2012a). Red wine polyphenolics

reduce the expression of inflammation markers in human colon-derived CCD-18Co myofibroblast cells: Potential role of microRNA-126. *Food & Function, 3*(7), 745–752.
Angel-Morales, G., Noratto, G., & Mertens-Talcott, S. (2012b). Standardized curcuminoid extract (*Curcuma longa* L.) decreases gene expression related to inflammation and interacts with associated microRNAs in human umbilical vein endothelial cells (HUVEC). *Food & Function, 3*(12), 1286–1293.
Balouiri, M., Sadiki, M., & Ibnsouda, S. K. (2016). Methods for *in vitro* evaluating antimicrobial activity: A review. *Journal of Pharmaceutical Analysis, 6*(2), 71–79.
Bates, D. M., & Watts, D. G. (2007). *Nonlinear regression analysis and its applications.* Hoboken, New Jersey: John Wiley & Sons32–52.
Bernardini, S., Tiezzi, A., Larghezza Masci, V., & Ovidi, E. (2018). Natural products for human health: An historical overview of the drug discovery approaches. *Natural Product Research, 32*(16), 1926–1950.
Chorianopoulos, N. G., Lambert, R. J. W., Skandamis, P. N., Evergetis, E. T., Haroutounian, S. A., & Nychas, G. J. E. (2006). A newly developed assay to study the minimum inhibitory concentration of *Satureja spinosa* essential oil. *Journal of Applied Microbiology, 100*(4), 778–786.
Cisowska, A., Wojnicz, D., & Hendrich, A. B. (2011). Anthocyanins as antimicrobial agents of natural plant origin. *Natural Products Communications, 6*(1), 149–156.
CLSI. (1999). Methods for Determining Bactericidal Activity of Antimicrobial Agents; Approved Guideline. CLSI document M26-A. Clinical and Laboratory Standards Institute, 950 West Valley Road Suite 2500,Wayne, Pennsylvania 19087, USA. https://clsi.org/media/1462/m26a_sample.pdf.
CLSI. (2008). Reference Method for Broth Dilution Antifungal Susceptibility Testing of Filamentous Fungi, Approved Standard-second edition. NCCLS document M38-A2, 950 West Valley Road, Suite 2500, Wayne, Pennsylvania 19087, USA. https://clsi.org/media/1455/m38a2_sample.pdf.
Coccia, A., Carraturo, A., Mosca, L., Masci, A., Bellini, A., Campagnaro, M., & Lendaro, E. (2012). Effects of methanolic extract of sour cherry (*Prunus cerasus* L.) on microbial growth. *International Journal of Food Science and Technology, 47*(8), 1620–1629.
Coman, M. M., Oancea, A. M., Verdenelli, M. C., Cecchini, C., Bahrim, G. E., Orpianesi, C., ... Silvi, S. (2018). Polyphenol content and *in vitro* evaluation of antioxidant, antimicrobial and prebiotic properties of red fruit extracts. *European Food Research and Technology, 244*(4), 735–745.
Cosmulescu, S., Trandafir, I., & Nour, V. (2017). Phenolic acids and flavonoids profiles of extracts from edible wild fruits and their antioxidant properties. *International Journal of Food Properties, 20*(12), 3124–3134.
Egea, I., Sanchez-Bel, P., Romojaro, F., & Pretel, M. T. (2010). Six edible wild fruits as potential antioxidant additives or nutritional supplements. *Plant Foods for Human Nutrition, 65*(2), 121–129.
Espinel-Ingroff, A., Fothergill, A., Peter, J., Rinaldi, M. G., & Walsh, T. J. (2002). Testing conditions for determination of minimum fungicidal concentrations of new and established antifungal agents for *Aspergillus* spp.: NCCLS Collaborative Study. *Journal of Clinical Microbiology, 40*(9), 3204–3208.
Fraternale, D., Giamperi, L., Bucchini, A., Sestili, P., Paolillo, M., & Ricci, D. (2009). *Prunus spinosa* fresh fruit juice: Antioxidant activity in cell-free and cellular systems. *Natural Product Communications, 4*(12), 1665–1670.
Fraternale, D., Rudov, A., Prattichizzo, F., Olivieri, F., Ricci, D., Giacomini, E., ... Albertini, M. C. (2016). Chemical composition and *in vitro* anti-inflammatory activity of *Vitis vinifera* L. (var. Sangiovese) tendrils extract. *Journal of Functional Foods, 20*, 291–302.
Ganhao, R., Estevez, M., Kylli, P., Heinonen, M., & Morcuende, D. (2010). Characterization of selected wild Mediterranean fruits and comparative efficacy as inhibitors of oxidative reactions in emulsified raw pork burger patties. *Journal of Agricultural and Food Chemistry, 58*(15), 8854–8861.
Georgiev, M. I. (2014). Natural products utilization. *Phytochemistry Reviews, 13*(2), 339–341.
Gordillo, B., Cejiudo-Bastante, M. J., Rodriguez-Pulido, F. J., Jara-Palacios, M. J., Ramirez-Perez, P., Gonzalez-Miret, M. L., & Heredia, F. J. (2014). Impact of adding white pomace to red grapes on the phenolic composition and color stability of syrah wines from a warm climate. *Journal of Agricultural and Food Chemistry, 62*(12), 2663–2671.
Govardhan Singha, R. S., Negib, P. S., & Radhaa, C. (2013). Phenolic composition, antioxidant and antimicrobial activities of free and bound phenolic extracts of *Moringa oleifera* seed flour. *Journal of Functional Foods, 5*, 1883–1891.
Guimarães, R., Barros, L., Duenas, M., Carvalho, A. M., Queiroz, M. J. R. P., Santos-Buelga, C., & Ferreira, I. C. (2013). Characterisation of phenolic compounds in wild fruits from Northeastern Portugal. *Food Chemistry, 141*(4), 3721–3730.
Hayek, S. A., Gyawali, R., & Ibrahim, S. A. (2013). Antimicrobial Natural Products. In A. Méndez-Vilas (Ed.). *Microbial pathogens and strategies for combating them: science, technology and education* (pp. 910–921). Barcelona, Spain: Formatex Research Center.
Kubacey, T. M., Haggag, E. G., El-Toumy, S. A., Amany, A. A., El-Ashmawy, I. M., & Youns, M. M. (2012). Biological activity and flavonoids from *Centaurea alexanderina* leaf extract. *Journal of Pharmacy Research, 5*(6), 3352–3361.
Madrau, M. A., Sanguinetti, A. M., Del Caro, A., Fadda, C., & Piga, A. (2010). Contribution of melanoidins to the antioxidant activity of *Prunus*. *Journal of Food Quality, 33*(s1), 155–170.
Mikulic-Petkovsek, M., Stampar, F., Veberic, R., & Sircelj, H. (2016). Wild *Prunus* fruit species as a rich source of bioactive compounds. *Journal of Food Science, 81*(8), C1928–1937.
Miletic, N., Mitrovic, O., Popovic, B., Nedovic, V., Zlatkovic, B., & Kandic, M. (2013). Polyphenolic content and antioxidant capacity in fruits of plum (*Prunus domestica* L.) cultivars "Valjevka" and "Mildora" as influenced by air drying. *Journal of Food Quality, 36*(4), 229–237.
Mostafa, A. A., Al-Askar, A. A., Almaary, K. S., Dawoud, T. M., Sholkamy, E. N., & Bakri, M. M. (2018). Antimicrobial activity of some plant extract against bacterial strains causing food poisoning diseases. *Saudi Journal of Biological Sciences, 25*(2), 161–166.
NCCLS. (2002). Reference Method for Broth Dilution Antifungal Susceptibility Testing of Yeasts; Approved Standard-Second Edition. NCCLS document M27-A2 (ISBN 1-56238-469-4). NCCLS, 940 West Valley Road, Suite 1400, Wayne, Pennsylvania 19087-1898 USA. https://webstore.ansi.org/standards/clsi/m27a2.
Olivieri, F., Lazzarini, R., Babini, L., Prattichizzo, F., Rippo, M. R., Tiano, L., ... Procopio, A. D. (2013). Anti-inflammatory effect of ubiquinol-10 on young and senescent endothelial cells via miR-146a modulation. *Free Radical Biology and Medicine, 63*, 410–420.
Piga, A., Del Caro, A., & Corda, G. (2003). From plums to prunes: Influence of drying parameters on polyphenols and antioxidant activity. *Journal of Agricultural and Food Chemistry, 51*(12), 3675–3681.
Pinacho, R., Cavero, R. Y., Astiasaran, I., Ansorena, D., & Calvo, M. I. (2015). Phenolic compounds of blackthorn (*Prunus spinosa* L.) and influence of *in vitro* digestion on their antioxidant capacity. *Journal of Functional Foods, 19*, 49–62.
Radovanović, B. C., Milenković Andelković, A. S., Radovanović, A. B., & Andelković, M. Z. (2013). Antioxidant and antimicrobial activity of polyphenol extracts from wild berry fruits grown in southeast Serbia. *Tropical Journal of Pharmaceutical Research, 12*(5), 813–819.
Rodriguez-Saona, L. E., & Wrolstad, R. E. (2001). Extraction, isolation and purification of anthocyanins. *Current Protocols in Food Analytical Chemistry*. https://doi.org/10.1002/0471142913.faf0101s00.
Shi, M., Mathai, M. L., Xu, G., McAinch, A. J., & Su, X. Q. (2019). The effects of supplementation with Blueberry, cyaniding-3-O-β-glucoside, yoghurt and its peptides on obesity and related comorbidities in a diet-induced obese mouse model. *Journal of Functional Foods, 56*, 92–101.
Sikora, E., Bieniek, M. I., & Borczak, B. (2013). Composition and antioxidant properties of fresh and frozen stored blackthorn fruits (*Prunus spinosa* L.). *Acta Scientiarum Polonorum Technologia Alimentaria, 12*(4), 365–372.
Silva, S., Costa, E. M., Mendes, M., Morais, R. M., Calhau, C., & Pintado, M. M. (2016). Antimicrobial, antiadhesive and antibiofilm activity of an ethanolic, anthocyanin-rich blueberry extract purified by solid phase extraction. *Journal of Applied Microbiology, 121*(3), 693–703.
Stacewicz-Sapuntzakis, M., Bowen, P. E., Hussain, E. A., Damayanti-Wood, B. I., & Farnsworth, N. R. (2001). Chemical composition and potential health effects of prunes: A functional food? *Critical reviews in food science and nutrition, 41*(4), 251–286.
Varga, E., Dornokos, E., Fogarasi, E., Steanesu, R., Fulop, I., Croitoru, M. D., & Laczko-Zold, E. (2017). Polyphenolic compounds analysis and antioxidant activity in fruits of *Prunus spinosa* L. *Acta pharmaceutica Hungarica, 87*(1), 19–25.
Veličković, J. M., Ilić, S., Mitić, S. S., Mitić, M. N., & Kostić, D. A. (2016). Comparative analysis of phenolic and mineral composition of hawthorn and blackthorn from southeast Serbia. *Oxidation Communications, 39*(3), 2280–2290.
Veličković, J. M., Kostić, D. A., Stojanović, G. S., Mitić, S. S., Randelović, S. S., & Dordević, A. S. (2014). Phenolic composition, antioxidant and antimicrobial activity of the extracts from *Prunus spinosa* L. fruit. *Hemijska Industrija, 68*(3), 297–303.

nanomaterials

MDPI

Article

Prunus spinosa Extract Loaded in Biomimetic Nanoparticles Evokes In Vitro Anti-Inflammatory and Wound Healing Activities

Mattia Tiboni [1,†], Sofia Coppari [1,†], Luca Casettari [1], Michele Guescini [1], Mariastella Colomba [1], Daniele Fraternale [1], Andrea Gorassini [2], Giancarlo Verardo [3], Seeram Ramakrishna [4], Loretta Guidi [1], Barbara Di Giacomo [1], Michele Mari [1], Roberto Molinaro [1,5,*] and Maria Cristina Albertini [1,*]

1 Department of Biomolecular Sciences, University of Urbino Carlo Bo, 61029 Urbino (PU), Italy; mattia.tiboni@uniurb.it (M.T.); s.coppari3@campus.uniurb.it (S.C.); luca.casettari@uniurb.it (L.C.); michele.guescini@uniurb.it (M.G.); mariastella.colomba@uniurb.it (M.C.); daniele.fraternale@uniurb.it (D.F.); loretta.guidi@uniurb.it (L.G.); barbara.digiacomo@uniurb.it (B.D.G.); michele.mari@uniurb.it (M.M.)

2 Department of Humanities and Cultural Heritage, University of Udine, 33100 Udine, Italy; andrea.gorassini@uniud.it

3 Department of Agricultural, Food, Environmental and Animal Sciences, University of Udine, 33100 Udine, Italy; giancarlo.verardo@uniud.it

4 Center for Nanofibers and Nanotechnology, National University of Singapore, Singapore 119077, Singapore; mpesr@nus.edu.sg

5 IRCCS Ospedale San Raffaele srl, 20132 Milan, Italy

* Correspondence: molinaro.roberto@hsr.it (R.M.); maria.albertini@uniurb.it (M.C.A.); Tel.: +39-0226434987 (R.M.); +39-0722305260 (M.C.A.)

† These authors contributed equally to this work.

Abstract: *Prunus spinosa* fruits (PSF) contain different phenolic compounds showing antioxidant and anti-inflammatory activities. Innovative drug delivery systems such as biomimetic nanoparticles could improve the activity of PSF extract by promoting (i) the protection of payload into the lipidic bilayer, (ii) increased accumulation to the diseased tissue due to specific targeting properties, (iii) improved biocompatibility, (iv) low toxicity and increased bioavailability. Using membrane proteins extracted from human monocyte cell line THP-1 cells and a mixture of phospholipids, we formulated two types of PSF-extract-loaded biomimetic vesicles differing from each other for the presence of either 1,2-dioleoyl-sn-glycero-3-phosphocholine (DOPC) or 1,2-dioleoyl-sn-glycero-3-phospho-(1′-rac-glycerol) (DOPG). The biological activity of free extract (PSF), compared to both types of extract-loaded vesicles (PSF-DOPCs and PSF-DOPGs) and empty vesicles (DOPCs and DOPGs), was evaluated in vitro on HUVEC cells. PSF-DOPCs showed preferential incorporation of the extract. When enriched into the nanovesicles, the extract showed a significantly increased anti-inflammatory activity, and a pronounced wound-healing effect (with PSF-DOPCs more efficient than PSF-DOPGs) compared to free PSF. This innovative drug delivery system, combining nutraceutical active ingredients into a biomimetic formulation, represents a possible adjuvant therapy for the treatment of wound healing. This nanoplatform could be useful for the encapsulation/enrichment of other nutraceutical products with short stability and low bioavailability.

Keywords: biomimicry; lipid nanoparticles; drug delivery systems; phenolic compounds; scratch assay; micro-RNA; leukosome

Citation: Tiboni, M.; Coppari, S.; Casettari, L.; Guescini, M.; Colomba, M.; Fraternale, D.; Gorassini, A.; Verardo, G.; Ramakrishna, S.; Guidi, L.; Di Giacomo, B.; et al. *Prunus spinosa* Extract Loaded in Biomimetic Nanoparticles Evokes In Vitro Anti-Inflammatory and Wound Healing Activities. *Nanomaterials* **2021**, *11*, 36. https://dx.doi.org/10.3390/nano11010036

Received: 5 December 2020
Accepted: 22 December 2020
Published: 25 December 2020

1. Introduction

The wound-healing process involves different phases: hemostasis, inflammation, tissue proliferation, and tissue remodeling [1]. Tissue injury causes the immediate onset of the acute inflammatory response, which is essential to provide growth factor and chemokines signals that orchestrate cell movements and tissue remodeling necessary for

repair. Successful repair after tissue injury requires inflammatory resolution that starts with the production of anti-inflammatory cytokines and downregulation of proinflammatory mediators (Figure 1). An excessive or prolonged inflammatory phase results in increased tissue injury and poor healing. The process depends on the persistence of inflammatory cells, the consequent generation of proinflammatory cytokines (Interleukin 1 and 6, tumor necrosis factor α), and on the increase of reactive oxygen species (ROS), which can lead to direct damage of cells or extracellular matrix molecules [2].

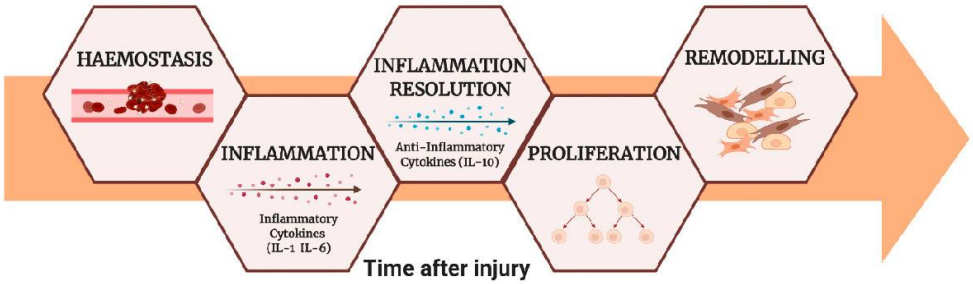

Figure 1. The wound-healing phases.

Bioactive phytochemical constituents such as phenolic compounds can promote beneficial effects on wound healing through anti-inflammatory and antioxidant activities. Moreover, they can modulate one or more phases of the wound-healing process [3]. They assist in wound healing, mainly with inhibitory effects on the production and activity of inflammatory mediators.

Among plant products, *Prunus spinosa* Linnaeus (*P. spinosa*) fruits have been extensively described for their biological properties and beneficial effects [4,5]. It is a perennial deciduous plant growing as a shrub in wild, uncultivated areas of Europe, temperate regions of Asia, and Mediterranean countries. In particular, chemical composition, antioxidant and anti-inflammatory properties of *P. spinosa* fruit ethanol extract have been recently reported [6]. The most representative molecules in the extract are phenolic compounds such as anthocyanins, which represent the most abundant antioxidants in the diet. This high content of active molecules and the resulting nutraceutical potential could prevent chronic diseases, including chronic complications in wound closure [7,8].

Polyphenol-rich plant extracts can interfere with the production of cytokines and, therefore, can offer an important alternative for the treatment of inflammatory diseases [9]. The main disadvantage of using natural extracts is their low bioavailability. Effective concentrations of these substances are unlikely to be found in the bloodstream and therefore hardly exert anti-inflammatory activity in their site of action.

Nanomedicine arose as an innovative tool to overcome these drawbacks [10]. Indeed, drug delivery systems (DDS), such as lipid vesicles [11,12] and polymeric nanoparticles [13], showed several advantages in enhancing the pharmacokinetic properties of their payload by promoting, for example, its protection from enzymatic or chemical degradation [14], preferential targeting towards specific cells or tissues [15], improved biocompatibility, low toxicity and increased bioavailability [16].

Among the different nanomedicine approaches, recently, biomimetic nanoparticles were developed as the last generation DDS endowed with unexpected biological properties [17–20]. Biomimetic approaches include mimicking leukocytes [21], red blood cells [22], platelets [23], and cancer cells [24]. These approaches provided unique functionalities by incorporating cellular coating, synthesizing cell-derived nanovesicles, or mimicking the physical properties of cells to create novel nanoparticles. Biomimetic carriers showed innate biological features and intrinsic functionalities typical of the donor cell source [18]. Among them, leukosomes, i.e., leukocyte-like nanovesicles, showed prolonged circulation and preferential targeting of inflamed vasculature [20,25–27].

Here, we enriched biomimetic vesicles with *P. spinosa* fruit ethanolic extract (hereafter-termed PSF) and evaluated whether its "encapsulation" provided improved biological properties in an in vitro setting, recapitulating the wound-healing process. From a pharmaceutical standpoint, PSF has been incorporated in two different biomimetic nanovesicles formulations, termed leukosomes, differing from each other for the presence of either 1,2-dioleoyl-*sn*-glycero-3-phosphocholine (DOPC), a neutral phospholipid, or 1,2-dioleoyl-*sn*-glycero-3-phospho-(1′-*rac*-glycerol) (DOPG), an anionic phospholipid, in the lipid mixture (hereafter reported as DOPCs and DOPGs, respectively).

The object of the present work is to evaluate and characterize the effective incorporation of the active molecules present in PSF from both a qualitative and a quantitative standpoint and to evaluate the ability of the formulations to reduce the inflammation process and improve the wound-healing repair.

2. Materials and Methods

2.1. Chemicals and Materials

1,2-dioleoyl-*sn*-glycero-3-phosphocholine (DOPC), 1,2-dioleoyl-*sn*-glycero-3-phospho-(1′-*rac*-glycerol) (DOPG), 1,2-distearoyl-*sn*-glycero-3-phosphocholine (DSPC), 1,2-Dipalmitoyl-*sn*-glycero-3-phosphocholine (DPPC), and cholesterol (CHOL) were purchased from Avanti Polar Lipids (Alabaster, AL, USA). Chloroform ($CHCl_3$), methanol (MeOH), pure ethanol (EtOH), and formic acid (HCOOH) for High Performance Liquid Cromatography coupled with mass spectrometry (HPLC-MS), chlorogenic acid, phloridzin, gallic acid, cyanidin chloride, uranyl acetate were purchased from Sigma-Aldrich (Milan, Italy). Quercetin-3-O-galactoside was obtained from ExtraSynthese (Lyon, France). Quercetin-3-O-arabinoside and quercetin-3-O-rhamnoside were purchased from Carbosynth (Berkshire, UK). Milli-Q® grade water was produced by the Elgastat UHQ-PS system (ELGA, High Wycombe Bucks, UK). Solid phase extraction (SPE) columns ISOLUTE C18, 1 g, 6 mL were from Biotage (Milan, Italy).

2.2. Fruits Collection and P. spinosa Extract Preparation

P. spinosa L. (Also known as blackthorn, Rosaceae family) was identified by Prof. D. Fraternale (University of Urbino). Voucher samples were deposited in the herbarium of Urbino University Botanical garden: code "Pp125". Ripe fruits were collected in November 2019 from plants around Urbino (PU, Marche, Italy), GPS coordinates N43°40′46.512" E12°31′42.291" (350 m above sea level) and, immediately after harvesting, frozen and stored at −20 °C until use. For the extraction, 50 g of fruit pulp were homogenized in an Osterizer for 3 min in 50 mL of 70% acidified aqueous ethanol solution (70 mL ethanol/29.9 mL distilled H_2O/0.1 mL HCl 36%). The homogenized solution was filtered with a Buchner filter, and the filtrate was centrifuged at 10,000 g for 15 min. The supernatant obtained was collected, while the pellet and the residues of the first extraction were subjected again to the initial extraction conditions. Both supernatants were combined and concentrated under vacuum at 37 °C using a rotary evaporator. In the end, the final product was aliquoted in centrifuge tubes and dried using a Savant concentrator (Thermo Scientific, San Jose, CA, USA). The dried samples were stored at −20 °C until use.

2.3. Formulation of Biomimetic Nanovesicles

Biomimetic vesicles were manufactured as previously reported [21,28]. Briefly, two different mixtures of phosphocholine-based phospholipids and cholesterol: DPPC:DOPC:DSPC:CHOL (named DOPCs) or DPPC:DOPG:DSPC:CHOL (named DOPGs) at a molar ratio of 5:3:1:1, were dissolved in chloroform into a round-bottomed flask and then, the solvent was evaporated using a rotary evaporator (Laborota 4000, Heidolph, Germany) to form a lipidic film according to the well-established thin layer evaporation method. A precise amount of freeze-dried PSF ethanolic extract was added to the lipid phase (1:6.67 weight ratio) to prepare PSF extract-loaded nanoparticles (named as PSF-DOPCs and PSF-DOPGs). Films were then hydrated with a water dispersion of human monocyte (THP-1, ATCC) membrane proteins (1:300 protein-to-lipid ratio) to assemble the biomimetic

vesicles. The lipidic suspensions obtained were extruded ten times through 200 nm pore-size cellulose acetate membranes (Avanti Polar Lipid, Alabama, AL, USA) at 45 °C to obtain smaller and more homogeneous vesicles.

2.4. Physicochemical Characterization of Biomimetic Nanovesicles

The prepared vesicles were characterized with a Nanosizer ZS (Malvern Instrument, Worcestershire, UK) using the dynamic light scattering (DLS) technique to measure the average particle size (Z-average) and their dimensional homogeneity, i.e., polydispersity index (PDI). Moreover, the Z-potential was measured to determine the surface charge of the plain (empty) and loaded biomimetic vesicles.

Both the formulated biomimetic suspensions were then ultracentrifuged at 100,000 g for 1 h and freeze-dried (Lio5P, 5Pascal, Milano, Italy) to characterize the incorporated PSF active molecules by HPLC-DAD-ESI-MS^n (see Supplementary Materials).

2.5. Cell Culture

Human umbilical vein endothelial cells (HUVECs) used in this study are derived from multiple donors, purchased from Life Technologies Corporation (Gibco™ C01510C, 1×10^6 cells). The HUVECs were cultured in the growth medium of Gibco™ Medium 200 (Life Technologies Corporation, Grand Island, NY, USA). This basal medium requires the addition of Gibco™ low serum growth supplement kit (LSGS Kit) (Life Technologies Corporation, Grand Island, NY, USA), and the final concentrations of the components in the integrated medium are: fetal bovine serum (2% *v/v*), hydrocortisone (1 µg/mL), growth factor human epidermal (10 ng/mL), basic fibroblast growth factor (3 ng/mL) and heparin (10 µg/mL). Cultures were passaged on, reaching 80% confluence, using trypsin–EDTA solution (Sigma-Aldrich, St. Louis, MO, USA). The experiments were performed in the third culture passage (P3).

2.6. In Vitro Wound Healing Assay

HUVECs were seeded in T25 tissue culture flasks, incubated at 37 °C and 5% CO_2 and allowed to grow to confluence as a monolayer. The cell monolayer was subjected to a mechanical scratch wound, horizontal along the flask, using the tip of a sterile pipette. Subsequently, the medium of each flask was removed, and the cells were washed with PBS solution. Diluting with fresh medium, the cells (200,000/mL) were treated with 80 µg/mL of free PSF, empty vesicles (DOPCs and DOPGs), and 80 µg/mL PSF-loaded vesicles (PSF-DOPCs and PSF-DOPGs). The untreated cells were used as a control and the incubation time was 48 h for all conditions. After the treatment, to evaluate cell viability, the cells were detached from the flask, and the cell suspension was mixed with trypan blue. Then, the cells that took up (dead cells) or excluded (vital cells) the dye were evaluated [29]. The images were obtained from the same lesion area immediately after scratching (t_0) and then after 24 and 48 h using a phase-contrast microscope (Olympus Ix51 10X objective). To evaluate wound closure, images were analyzed through the ImageJ software to select the total area of the wound region. The percentage of wound closure was calculated using Equation (1).

$$[(\text{wound area } t_0 - \text{wound area t})/\text{wound area } t_0] \times 100 \quad (1)$$

The experiments were conducted in triplicate.

2.7. RT–qPCR Analysis

The analysis was performed on the HUVECs used for the wound-healing assay. The RT–qPCR protocol includes total RNA isolation, which was performed through the Total RNA isolation kit (Norgen Biotek, Thorold, ON, USA) following the manufacturer's instructions. The concentration and purity of the RNA were determined using a NanoDrop ND 1000 spectrophotometer (Thermo Scientific, San Jose, CA, USA). RNA was stored at −80 °C until use.

The cDNA was synthesized from the isolated RNA using the High-Capacity cDNA reverse transcription kit (Applied Biosystems, Foster City, CA, USA). RT–qPCR was performed with the SYBR Green PCR master mix (Applied Biosystems, Foster City, CA, USA) on ABI Prism 7500 real-time PCR system (Applied Biosystems, Foster City, CA, USA). TATA-binding protein (TBP) has been used as an endogenous control to determine relative mRNA expression. Primer sequences used were as follow:

VCAM-1 (F: ACAGAAGAAGTGGCCCTCCAT-R: TGGCATCCGTCAGGAAGTG); IL-6 (F: AGGGCTCTTCGGCAAATGTA-R: GAAGGAATGCCCATTAACAACAA); IRAK-1 (F: CAGACAGGGAAGGGAAACATTTT-R: CATGAAACCTGACTTGCTTCTGAA); TBP (F: TGCACAGGAGCCAAGAGTGA-R: CACATCACAGCTCCCCACCA).

For miRNA analysis, human miR-126 and human miR-146a were quantified by RT–qPCR using TaqMan MicroRNA assay (Applied Biosystems, Foster City, CA, USA) according to the manufacturer's guidelines. The RT–qPCR data were standardized to RNU44 (reference miRNA).

Product specificity was examined by dissociation curve analysis. Results were calculated using the delta-delta Ct method ($2^{-\Delta\Delta Ct}$) and were expressed as fold change related to untreated control (CTRL).

2.8. Statistical Analysis

The two-tailed paired Student's *t*-test was used for the miR-126, VCAM-1, miR-146a, IRAK-1, IL-6 analyses. The results were considered significant at the level of $p < 0.05$. All the experiments were conducted in triplicate. Linear regression analysis was used to evaluate the wound-healing dose-dependent capacity, where R-squared (R^2) measures how close the data are to the fitted regression line (the higher the R^2 to 100%, the better the model fits the data).

3. Results

3.1. Physicochemical Characterization of Empty and Extract-Loaded Vesicles

We undertook to characterize the contribution of two different lipid mixtures having the DPPC:DSPC:CHOL as lipid backbone by adding either DOPC or DOPG to obtain an almost neutral (DOPCs) or negatively charged formulation (DOPGs).

Empty and loaded DOPCs and DOPGs, assembled with the technique developed by Molinaro et al. [21], were characterized from a physicochemical standpoint by measuring their average size (PDI, and surface charge (Z-potential) (Figure 2).

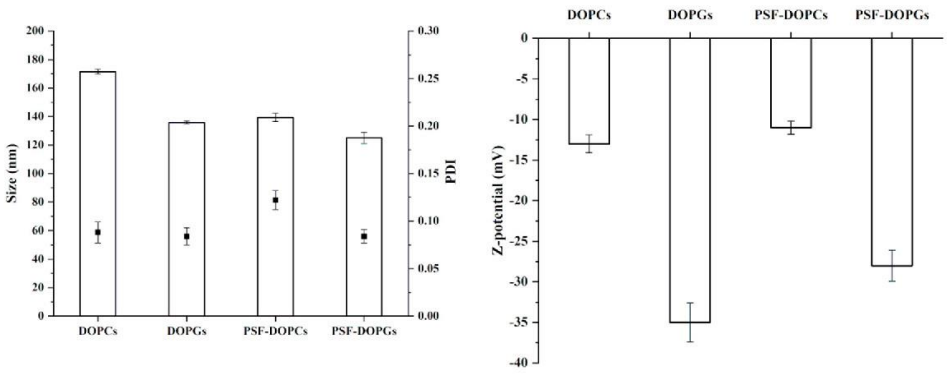

Figure 2. Characterization of formulated vesicles by Z-average size, polydispersity index (PDI), and Z-potential.

DOPCs and DOPGs revealed an average size of 171 nm and 135 nm, respectively, a narrow size distribution (PDI below 0.13) and a surface charge of −13 mV and −35 mV, respectively. PSF incorporation did not significantly affect size distribution, while we could observe some differences regarding the average diameter and surface charge (Figure 1).

PSF incorporation induced a significant reduction of vesicle size for the DOPCs (171 vs. 140 nm before and after PSF-loading, respectively), while the effect was only minimal for the DOPGs (135 vs. 125 nm before and after PSF-loading, respectively). On the contrary, DOPGs showed a significant reduction of the surface charge after PSF incorporation (−35 vs. −28 mV before and after PSF-loading, respectively), while a very slight difference could be observed for the DOPCs (−13 vs. −11 mV before and after PSF-loading, respectively).

Taken together, these findings reveal a different effect of PSF incorporation in the two formulations, which was predictable considering both the heterogeneity of PSF composition and the net difference between DOPC and DOPG, which confer distinct physicochemical properties to the vesicles.

HPLC chromatograms acquired at 280 nm of purified samples of free PSF, PSF-DOPCs and PSF-DOPGs are reported in Supplementary Figure S1, and the characterization of the main phenolic compounds is reported in Table S1 in the Supplementary Material.

As reported in Table 1, the dominant classes of phenolic compounds present in PSF are hydroxycinnamic acid derivatives (44.4%), anthocyanins (32.7%), and flavonoid derivatives (21.1%), which is in accordance with literature data [30–32].

Table 1. The total concentration of phenolic compounds in *P. spinosa* fruit ethanolic extract (free PSF) and in extract-loaded vesicles (PSF-DOPCs and PSF-DOPGs).

Peak No	Compound	Free PSF (μg/g)	PSF-DOPCs (μg/g)	PSF-DOPGs (μg/g)
1	3-O-caffeoylquinic acid	2112.0 ± 23.3	418.4 ± 13.0	94.0 ± 1.3
2	3-O-p-cumaroylquinic acid	70.0 ± 3.9	9.6 ± 0.1	3.5 ± 0.2
3	Chlorogenic acid dehydrodimer	75.8 ± 0.8	11.2 ± 0.1	2.7 ± 0.3
4	3-O-feruloylquinic acid	218.4 ± 1.4	37.2 ± 0.3	9.3 ± 0.3
5	4-O-caffeoylquinic acid	187.3 ± 3.9	41.2 ± 0.3	8.7 ± 0.1
7	Chlorogenic acid dehydrodimer	184.5 ± 2.3	24.8 ± 0.1	6.9 ± 0.2
	Total hydroxycinnamic acid derivatives	**2847.9 ± 23.5**	**542.3 ± 12.5**	**125.1 ± 1.5**
8	Cyanidin 3-O-glucoside	490.5 ± 6.3	26.4 ± 0.1	13.3 ± 0.1
10	Cyanidin 3-O-rutinoside	638.9 ± 1.9	11.2 ± 0.1	29.4 ± 0.2
11	Peonidin 3-O-glucoside	315.0 ± 4.4	4.6 ± 0.1	3.9 ± 0.2
12	Peonidin 3-O-rutinoside	650.3 ± 0.8	7.4 ± 0.1	7.2 ± 0.1
	Total anthocyanins	**2094.8 ± 11.8**	**49.7 ± 0.1**	**53.8 ± 0.1**
15	Ellagic acid derivative	40.6 ± 1.5	19.7 ± 0.2	10.1 ± 0.1
16	4-(vanilloyloxy)-2,6,6-trimethylcyclohexene-1-carboxylic acid	74.6 ± 2.2	40.6 ± 0.7	40.6 ± 0.2
	Total hydroxybenzoic acid derivatives	**115.1 ± 0.7**	**60.3 ± 2.3**	**50.7 ± 0.3**
6	Apigenin pentoside	27.4 ± 0.1	9.9 ± 0.1	3.9 ± 0.1
9	Apigenin pentoside isomer	28.1 ± 1.6	6.3 ± 0.1	4.3 ± 0.1
17	Quercetin hexoside	240.7 ± 6.4	64.6 ± 0.1	54.5 ± 0.1
18	Quercetin 3-O-hexoside-O-pentoside	145.3 ± 1.7	78.0 ± 0.1	24.6 ± 0.2
19	Rutin	168.9 ± 1.2	75.8 ± 0.2	23.9 ± 0.1
20	Quercetin galactoside	366.8 ± 4.8	215.7 ± 0.1	73.7 ± 0.2
21	Quercetin xyloside	29.5 ± 0.4	29.0 ± 0.1	4.1 ± 0.1
22	Quercetin arabinoside	107.7 ± 0.4	78.9 ± 0.2	22.5 ± 0.1
23	Quercetin pentoside	193.1 ± 1.1	108.0 ± 0.1	23.2 ± 0.1
24	Quercetin 3-O-rhamnoside	43.6 ± 0.3	20.8 ± 0.1	n.d.
	Total flavonoid derivatives	**1351.0 ± 8.4**	**687.1 ± 13.0**	**234.7 ± 0.1**
	Total phenolic compounds	**6408.9 ± 4.1**	**1339.4 ± 13.1**	**464.3 ± 1.1**

We observed preferential incorporation within PSF-DOPCs than PSF-DOPGs for hydroxycinnamic acid derivatives (542 vs. 125 μg/g, respectively), hydroxybenzoic acid derivatives (60 vs. 51 μg/g, respectively), and flavonoid derivatives (687 vs. 235 μg/g, respectively) (Table 1). Overall, the amount of total phenolic compounds detected in PSF-DOPCs was about three times higher than the amount found in PSF-DOPGs (1339 μg/g vs. 464 μg/g, respectively).

As mentioned above, phenolic compounds are biologically relevant molecules with an active role in the control of oxidative stress and consequently of the inflammatory response [33,34]. Among the most abundant polyphenols present in *P. spinosa* extract, HPLC–DAD/ESI–MS^n detected 3-O-caffeoylquinic acid (2112 μg/g), peonidin 3-O-rutinoside (650 μg/g), cyanidin 3-O-rutinoside (639 μg/g), cyanidin 3-O-glucoside (490 μg/g), quercetin galactoside (367 μg/g), peonidin 3-O-glucoside (315 μg/g), quercetin hexoside (240 μg/g), and 3-O-feruloylquinic acid (218 μg/g).

Furthermore, quercetin xyloside was mostly loaded by PSF-DOPCs than by PSF-DOPGs (29 vs. 4 μg/g, respectively), as well as quercetin 3-O-rhamnoside, which was undetected in PSF-DOPGs.

3.2. Wound Healing Repair Activity of PSF-Loaded Vesicles

We investigated the wound-healing properties of *P. spinosa* fruit extract at different concentrations (20 to 80 μg/mL) on HUVECs up to 48 h of incubation (Figure 3).

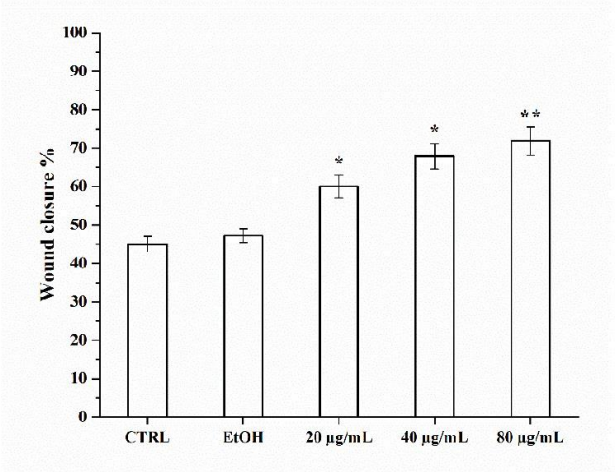

Figure 3. Wound-healing repair after *P. spinosa* extract (20–80 μg/mL) and its vehicle alone (EtOH) treatment. The graph shows the percentage of wound closure compared to the untreated control (CTRL) after 48 h. The values reported are the mean ± SD of three independent experiments. * $p < 0.05$, ** $p < 0.001$ vs. CTRL (Student's *t*-test).

We found that the percentage of wound closure after free PSF treatment showed a concentration-dependent effect. Linear regression analysis showed $R^2 = 84\%$ considering 20–80 μg/mL of free PSF, and $R^2 = 98\%$ considering 20–40 μg/mL of free PSF. On this basis, we deduced that the wound-healing capacity of the extract is saturated at 80 μg/mL.

We further evaluated whether incorporated PSF had similar activity. To this end, wound-healing assay was performed to the monolayer of HUVECs in different experimental conditions using: the free extract at the most effective concentration (80 μg/mL); the extract-loaded vesicles (PSF-DOPCs and PSF-DOPGs) and the plain vesicles (DOPCs and DOPGs). 80 μg/mL PSF-loaded nanovesicles were employed. After the treatment, no cytotoxicity was noticed for any formulation with the trypan blue exclusion assay. The free PSF and PSF-DOPCs groups showed a significant wound-healing repair activity compared to the control (Figure 4). More specifically, PSF-DOPCs showed increased wound-healing repair even related to free PSF alone.

3.3. Anti-Inflammatory Activity of PSF-Loaded Vesicles

To dissect the biological mechanisms at the basis of the wound-healing activity above reported, we evaluated the anti-inflammatory ability of the free PSF, either free or incorporated. To this end, we measured the expression of the inflammation markers miR-146a, IRAK-1, and IL-6 after 48 h of treatment.

As indicated in Figure 5, the relative expression of the proinflammatory cytokine IL-6 is significantly lower in the groups treated with free PSF and PSF-DOPCs than the control. Interestingly, both empty DOPCs and DOPGs revealed an intrinsic anti-inflammatory activity, thus confirming previous reports [28], while we could not observe any significant effect for loaded PSF-DOPGs. Furthermore, we observed a decreased IRAK-1 and increased

miR-146a expressions for free PSF and PSF-DOPCs groups, with the latter having a more pronounced effect.

To support previous results, the expression of miR-126 and its target VCAM-1 were analyzed for all the experimental conditions (Figure 6). Furthermore, in this case, in free PSF and PSF-DOPCs groups, decreased VCAM-1 and increased miR-126 expression levels were observed. Treatment with empty DOPCs lowered the expression of VCAM-1, thus confirming the intrinsic anti-inflammatory properties observed for these biomimetic nanovesicles.

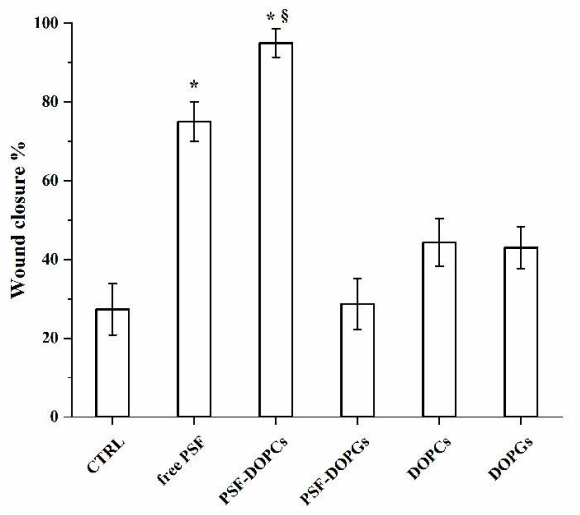

Figure 4. Wound-healing repair after free *P. spinosa* fruit extract (free PSF), extract-loaded vesicles (PSF-DOPCs and PSF-DOPGs) and empty vesicles (DOPCs and DOPGs) treatment. The graph shows the percentage of wound closure compared to untreated control (CTRL) after 48 h. The values reported are the mean ± SD of three independent experiments. * $p < 0.05$ vs. CTRL (Student's *t*-test). § $p < 0.05$ vs. *P. spinosa* extract.

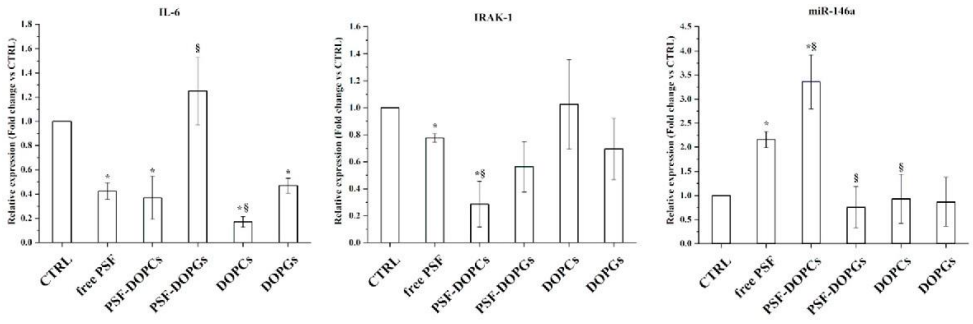

Figure 5. Effect of free *P. spinosa* fruit extract (free PSF), incorporated extract (PSF-DOPCs and PSF-DOPGs), and empty vesicles (DOPCs and DOPGs) on the IL-6, IRAK-1, and miR-146a expressions. RT–qPCR values are reported as fold induction related to CTRL. The values reported are the mean ± SD of three independent experiments. * $p < 0.05$ vs. CTRL (Student's *t*-test). § $p < 0.05$ vs. *P. spinosa* extract.

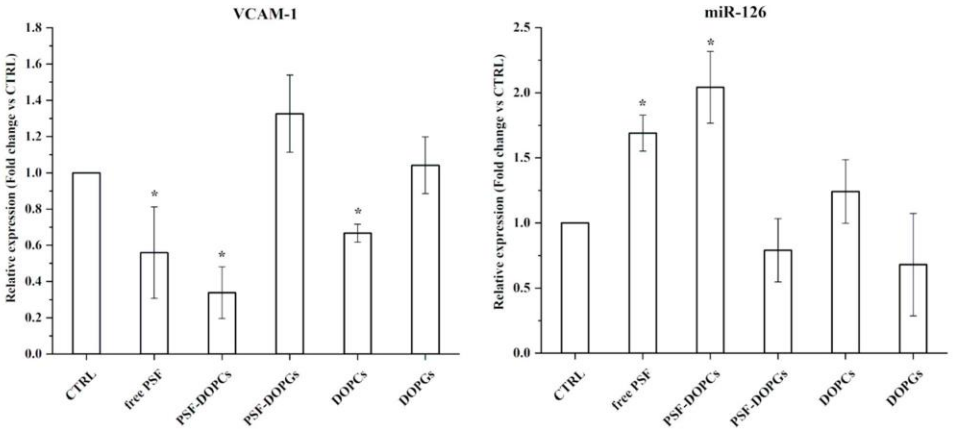

Figure 6. Effect of free *P. spinosa* fruit extract (free PSF), incorporated extract (PSF-DOPCs and PSF-DOPGs) and empty vesicles (DOPCs and DOPGs) on the VCAM-1 and miR-126 (cell adhesion molecules target). RT–qPCR values are reported as fold induction related to CTRL. Two-tailed paired Student's *t*-test: * = $p < 0.05$.

4. Discussion

In this work, we have demonstrated how biomimetic nanoparticles can improve the nutraceutical anti-inflammatory properties of *P. spinosa* extract, derived from a wild fruit widely present in the Mediterranean area. Phenolic compounds contained in the PSF extract demonstrated different nutraceutical effects such as antioxidant and anti-inflammatory activities [35] that can be enhanced when paired with the active targeting to inflamed endothelium, as carefully characterized in previous works [21,36].

Taking advantage of the well-established thin layer evaporation method, purified membrane proteins extracted from human monocyte cell line THP-1 were assembled with synthetic choline-based phospholipids to mimic the physiologic composition of the plasmalemma [21,37]. This manufacturing process allowed for the production of biomimetic vesicles that combine the high surface complexity typical of cell-derived nanoparticles with the pharmaceutical versatility typical of liposomes, such as the ability to carry, transport, and release different kinds of payloads, an elevated and standardized yield of the manufacturing process and a stable, biocompatible and non-immunogenic final product. Moreover, this manufacturing protocol does not require chemical synthesis or complex purification steps to reach the final biomimetic product.

The prepared vesicles presented an optimal dimension and narrow size distribution with effective incorporation of the *P. spinosa* extract. In particular, PSF-DOPCs presented a number of phenolic compounds three times higher than PSF-DOPGs. We observed the same trend for hydroxycinnamic acid and flavonoid derivatives (four and three times higher for PSF-DOPCs compared to PSF-DOPGs). More specifically, PSF-DOPCs preferentially incorporated quercetin xyloside (present in free extract), unlike PSF-DOPGs. These differences could be attributed to electronic interactions between the active compounds present in the extract and the utilized phospholipids. Our findings reveal that the neutral DOPC allowed for higher incorporation of those compounds compared to the DOPG, which has a net negative charge that most likely hindered their loading.

As this kind of biomimetic vesicles presented an effective active targeting to inflamed endothelium as reported already in literature [28], the prepared nanovesicle formulations were studied on in vitro inflammatory conditions evaluating the wound-healing properties on endothelial HUVEC cells. Analyzing the percentage of wound closure, treatment with PSF-DOPCs showed a significantly higher wound-healing activity compared to all other experimental conditions (Figure 7).

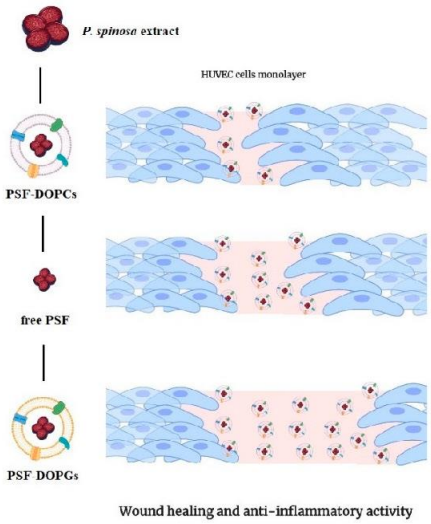

Figure 7. Free *P. spinosa* extract (free PSF) and loaded biomimetic formulations (PSF-DOPCs and PSF-DOPGs) acting on wound healing. As shown, PSF-DOPCs are the most efficient in wound closure, followed by free PSF and, finally, PSF-DOPGs, which are the least performing.

In the wound-healing process, immediately after the wound, an acute inflammation mediated by cytokines and growth factors (e.g., IL-1, IL-6, TNF-α) occurs [2]. Among these, interleukin 6 (IL-6) plays an important role in wound healing. Indeed, the progression towards complete wound healing involves the downregulation of proinflammatory cytokines, essential for correct repair. TLR4 is an important regulator of inflammation [38]. The TLR4 signaling pathway, through the IRAK-1 mediator, promotes the activation of the NF-κB transcriptional complex, which is responsible for the production of proinflammatory cytokines, including IL-6. The miR-146a also regulates TLR4 pathway activation through a negative feedback loop. Hence, during a proinflammatory condition, miR-146a is downregulated and allows the expression of IRAK-1 and, consequently, IL-6.

We evaluated the expression of markers directly related to the inflammation and wound-healing processes such as IL-6, miR-146a, IRAK-1, miR-126, and VCAM-1. MicroRNA-126 is also responsible for regulating cell adhesion molecule VCAM-1 during inflammation [6].

The expression level of IL-6 was significantly decreased during free *P. spinosa* extract and PSF-DOPCs treatment. Moreover, in the same experimental groups, the limited expression of IRAK-1 and the high expression of miR-146a demonstrate the activation of the negative miR-146a-mediated feedback loop mechanism that modulates the TLR4 signaling pathway and the consequent inflammatory profile, thus confirming a significant anti-inflammatory activity of the active compounds of the extract. In line with recent experimental evidence showing that miR-126 is upregulated during wound healing, thus promoting cell migration and proliferation [39], while the expression of VCAM-1 is decreased [40], our findings showed that PSF-DOPCs significantly increased the expression level of miR-126 and decreased expression of its target VCAM-1. Authors speculate that PSF-DOPCs increased the intracellular bioavailability of some components of PSF extract, thus modulating the expression of proinflammatory markers, also through the antioxidant activity.

On the other hand, PSF-DOPGs did not significantly modulate the molecules associated with the TLR4 pathway, as for the empty DOPCs and DOPGs. However, the latter lowered the level of IL-6 associated with inflammation, probably due to the intrinsic anti-inflammatory capacity of the biomimetic nanovesicles [19]. The wound-healing effect of PSF-DOPGs was considerably lower compared to the free PSF extract and PSF-DOPCs probably due, as we report below, to (i) less efficient incorporation; and (ii) differences in

active molecules incorporated (as shown by HPLC). In particular, PSF-DOPCs contained a higher amount of hydroxycinnamic acids (Table 1—Peaks no. 1–5, 7) and flavonoids including quercetin derivatives (Table 1—Peaks no. 6, 9, 17–24) that are known as wound-healing modulators [41]. Furthermore, molecules highly loaded into PSF-DOPCs such as caffeic acid and quercetin derivatives (quercetin xyloside) have already been explored in the literature showing an antioxidant [42] and anti-inflammatory effect through downregulation of the TLR-4 signaling pathway [43,44]. On this basis, our findings seem to confirm that these are the components of the PSF extract most directly involved in determining the observed experimental results.

As for the mechanism of action, the authors hypothesize that the improved anti-inflammatory activity of PSF extract results from their enhanced delivery by biomimetic nanovesicles. We have previously reported how leukosomes show a preferential targeting towards inflamed HUVEC [21], which results in an increased intracellular release of their payload, thus modulating the inflammatory cascade resulting in anti-inflammatory activity. Since there are no data on how long the vesicles remain loaded before emptying yet, the experiments have always been performed with the vesicles freshly loaded in order to reasonably exclude that part of the payload was released into the culture medium before vesicles engaged HUVECs. Obviously, further in-depth analyses are needed to better clarify this point. In addition, a possible synergistic effect between the anti-inflammatory action of some components of the extract and the intrinsic anti-inflammatory capacity of the nanovesicles should not be ruled out.

Authors speculate that the incorporation of PSF within DOPGs (negatively charged) induced a perturbation of the system, probably destabilizing the correct incorporation of membrane proteins inside the lipid bilayer. This effect is most likely a consequence of the electrostatic interactions occurring between the DOPG and the compounds present in the ethanolic extract, in particular the anthocyanins, which are positively charged and the acidic components, in their negatively ionized form, could be responsible for destabilizing the membrane of PSF-DOPG through electrostatic repulsive forces. This validates the incorporation efficiency findings reported in Table 1, where DOPCs showed increased loading properties compared to the DOPGs. Further physicochemical analyses will be performed to understand the dynamics of these interactions, as well as their effect on membrane proteins incorporation.

5. Conclusions

In this work, we demonstrated that PSF-DOPCs were more efficient than free *P. spinosa* fruit extract in promoting the wound-healing process through an anti-inflammatory activity, indicating an additive effect between the properties of the natural molecules and the drug delivery potential of the biomimetic nanovesicles (Figure 7). In addition, we highlighted how the chemical properties of the payload must be considered in view of a possible perturbation of the system with a consequent loss of activity of the complex biomimetic surface of leukosomes. This innovative biomimetic nanosystem, which combines nutraceutical active ingredients, purified membrane proteins, and fully biocompatible synthetic lipids, represents a possible effective adjuvant therapy for the treatment of wound healing. Biomimetic nanovesicles platform could be useful for the encapsulation/incorporation of other nutraceutical products, whose pharmacological properties in vivo are hindered by their poor chemical stability and low bioavailability.

Supplementary Materials: The following are available online at https://www.mdpi.com/2079-4991/11/1/36/s1, Figure S1: Chromatograms of purified samples of *P. spinosa* ethanolic extract (free PSF) (A), PSF-DOPCs (B) and PSF-DOPGs (C) detected at 280 nm. Peak numbers correspond to those reported in Table S1. Table S1: Characterization of the main phenolic compounds from samples of *P. spinosa* ethanolic extract by HPLC–DAD/ESI–MSn in positive or negative mode.

Author Contributions: M.T. and S.C.: Investigation, data curation, formal analysis, methodology, visualization, and writing—original draft; M.G., A.G., G.V., M.C., S.R., and D.F.: formal analysis, investigation, methodology, writing—review and editing; B.D.G., M.M., and L.G.: formal analysis, visualization and writing—review and editing; L.C.: funding acquisition, resources, data curation, writing—review and editing; R.M. and M.C.A.: conceptualization, experimental design, supervision, data curation, writing—review and editing and funding acquisition (M.C.A.). All authors have read and agreed to the published version of the manuscript.

Funding: This work was supported by University of Urbino Carlo Bo, Urbino (PU), Italy (DISB_Albertini_Progetti_valorizzazione_2018; DISB_Casettari_Progetti_valorizzazione_2018).

Data Availability Statement: The data presented in this study are available on request from the corresponding author.

Acknowledgments: The graphical abstract, Figures 1 and 7, were created with BioRender.com. The authors truly acknowledge the Ph.D. School of Biomolecular and Health Sciences (BHS) of the University of Urbino Carlo Bo (Urbino, Italy). We are grateful to Marco Bruno Luigi Rocchi (Department of Biomolecular Sciences, University of Urbino Carlo Bo, Urbino, Italy) for his general support and Laura Teodori (Laboratory of Diagnostics and Metrology, Division of Health Physical Sciences (FSN-TECFIS-DIM), ENEA, C.R. Frascati, Rome, Italy) for her assistance in study design.

Conflicts of Interest: The authors declare no conflict of interest.

References

1. Rodrigues, M.; Kosaric, N.; Bonham, C.A.; Gurtner, G.C. Wound healing: A cellular perspective. *Physiol. Rev.* **2019**, *99*, 665–706. [CrossRef] [PubMed]
2. Eming, S.A.; Krieg, T.; Davidson, J.M. Inflammation in Wound Repair: Molecular and Cellular Mechanisms. *J. Invest. Dermatol.* **2007**, *127*, 514–525. [CrossRef]
3. Ibrahim, N.; Wong, S.; Mohamed, I.; Mohamed, N.; Chin, K.-Y.; Ima-Nirwana, S.; Shuid, A. Wound Healing Properties of Selected Natural Products. *Int. J. Environ. Res. Public Health* **2018**, *15*, 2360. [CrossRef] [PubMed]
4. Fraternale, D.; Giamperi, L.; Bucchini, A.; Sestili, P.; Paolillo, M.; Ricci, D. *Prunus spinosa* fresh fruit juice: Antioxidant activity in cell-free and cellular systems. *Nat. Prod. Commun.* **2009**, *4*, 1665–1670. [CrossRef]
5. Pinacho, R.; Cavero, R.Y.; Astiasarán, I.; Ansorena, D.; Calvo, M.I. Phenolic compounds of blackthorn (*Prunus spinosa* L.) and influence of in vitro digestion on their antioxidant capacity. *J. Funct. Foods* **2015**, *19*, 49–62. [CrossRef]
6. Sabatini, L.; Fraternale, D.; Di Giacomo, B.; Mari, M.; Albertini, M.C.; Gordillo, B.; Rocchi, M.B.L.; Sisti, D.; Coppari, S.; Semprucci, F.; et al. Chemical composition, antioxidant, antimicrobial and anti-inflammatory activity of *Prunus spinosa* L. fruit ethanol extract. *J. Funct. Foods* **2020**, *67*, 103885. [CrossRef]
7. Blesso, C.N. Dietary Anthocyanins and Human Health. *Nutrients* **2019**, *11*, 2107. [CrossRef] [PubMed]
8. Yan, H.; Peng, K.J.; Wang, Q.L.; Gu, Z.Y.; Lu, Y.Q.; Zhao, J.; Xu, F.; Liu, Y.L.; Tang, Y.; Deng, F.M.; et al. Effect of pomegranate peel polyphenol gel on cutaneous wound healing in alloxan-induced diabetic rats. *Chin. Med. J.* **2013**, *126*, 1700–1706. [CrossRef]
9. Georgescu, M.; Marinas, O.; Popa, M.; Stan, T.; Lazar, V.; Bertesteanu, S.V.; Chifiriuc, M.C. Natural Compounds for Wound Healing. In *Worldwide Wound Healing-Innovation in Natural and Conventional Methods*; InTech: London, UK, 2016.
10. Blanco, E.; Shen, H.; Ferrari, M. Principles of nanoparticle design for overcoming biological barriers to drug delivery. *Nat. Biotechnol.* **2015**, *33*, 941–951. [CrossRef]
11. Wolfram, J.; Suri, K.; Huang, Y.; Molinaro, R.; Borsoi, C.; Scott, B.; Boom, K.; Paolino, D.; Fresta, M.; Wang, J.; et al. Evaluation of anticancer activity of celastrol liposomes in prostate cancer cells. *J. Microencapsul.* **2014**, *31*, 501–507. [CrossRef]
12. Kirui, D.K.; Celia, C.; Molinaro, R.; Bansal, S.S.; Cosco, D.; Fresta, M.; Shen, H.; Ferrari, M. Mild Hyperthermia Enhances Transport of Liposomal Gemcitabine and Improves In Vivo Therapeutic Response. *Adv. Healthc. Mater.* **2015**, *4*, 1092–1103. [CrossRef]
13. Cosco, D.; Molinaro, R.; Morittu, V.M.; Cilurzo, F.; Costa, N.; Fresta, M. Anticancer activity of 9-cis-retinoic acid encapsulated in PEG-coated PLGA-nanoparticles. *J. Drug Deliv. Sci. Technol.* **2011**, *21*, 395–400. [CrossRef]
14. Cosco, D.; Federico, C.; Maiuolo, J.; Bulotta, S.; Molinaro, R.; Paolino, D.; Tassone, P.; Fresta, M. Physicochemical features and transfection properties of chitosan/poloxamer 188/poly(D,L-lactide-co-glycolide) nanoplexes. *Int. J. Nanomedicine* **2014**, *9*, 2359–2372. [CrossRef]
15. Paolino, D.; Cosco, D.; Molinaro, R.; Celia, C.; Fresta, M. Supramolecular devices to improve the treatment of brain diseases. *Drug Discov. Today* **2011**, *16*, 311–324. [CrossRef]
16. Carter, A.M.; Tan, C.; Pozo, K.; Telange, R.; Molinaro, R.; Guo, A.; De Rosa, E.; Martinez, J.O.; Zhang, S.; Kumar, N.; et al. Phosphoprotein-based biomarkers as predictors for cancer therapy. *Proc. Natl. Acad. Sci. USA* **2020**, *117*, 18401–18411. [CrossRef]
17. Mohammadi, M.R.; Corbo, C.; Molinaro, R.; Lakey, J.R.T. Biohybrid Nanoparticles to Negotiate with Biological Barriers. *Small* **2019**, *15*, e1902333. [CrossRef]

18. Parodi, A.; Molinaro, R.; Sushnitha, M.; Evangelopoulos, M.; Martinez, J.O.; Arrighetti, N.; Corbo, C.; Tasciotti, E. Bio-inspired engineering of cell- and virus-like nanoparticles for drug delivery. *Biomaterials* **2017**, *147*, 155–168. [CrossRef]
19. Corbo, C.; Cromer, W.E.; Molinaro, R.; Toledano Furman, N.E.; Hartman, K.A.; De Rosa, E.; Boada, C.; Wang, X.; Zawieja, D.C.; Agostini, M.; et al. Engineered biomimetic nanovesicles show intrinsic anti-inflammatory properties for the treatment of inflammatory bowel diseases. *Nanoscale* **2017**, *9*, 14581–14591. [CrossRef]
20. Molinaro, R.; Pastò, A.; Corbo, C.; Taraballi, F.; Giordano, F.; Martinez, J.O.; Zhao, P.; Wang, X.; Zinger, A.; Boada, C.; et al. Macrophage-derived nanovesicles exert intrinsic anti-inflammatory properties and prolong survival in sepsis through a direct interaction with macrophages. *Nanoscale* **2019**, *11*, 13576–13586. [CrossRef]
21. Molinaro, R.; Corbo, C.; Martinez, J.O.; Taraballi, F.; Evangelopoulos, M.; Minardi, S.; Yazdi, I.K.; Zhao, P.; De Rosa, E.; Sherman, M.B.; et al. Biomimetic proteolipid vesicles for targeting inflamed tissues. *Nat. Mater.* **2016**, *15*, 1037–1046. [CrossRef]
22. Hu, C.M.J.; Fang, R.H.; Zhang, L. Erythrocyte-inspired delivery systems. *Adv. Healthc. Mater.* **2012**, *1*, 537–547. [CrossRef] [PubMed]
23. Wei, X.; Gao, J.; Fang, R.H.; Luk, B.T.; Kroll, A.V.; Dehaini, D.; Zhou, J.; Kim, H.W.; Gao, W.; Lu, W.; et al. Nanoparticles camouflaged in platelet membrane coating as an antibody decoy for the treatment of immune thrombocytopenia. *Biomaterials* **2016**, *111*, 116–123. [CrossRef] [PubMed]
24. Li, S.-Y.; Cheng, H.; Xie, B.-R.; Qiu, W.-X.; Zeng, J.-Y.; Li, C.-X.; Wan, S.-S.; Zhang, L.; Liu, W.-L.; Zhang, X.-Z. Cancer Cell Membrane Camouflaged Cascade Bioreactor for Cancer Targeted Starvation and Photodynamic Therapy. *ACS Nano* **2017**, *11*, 7006–7018. [CrossRef] [PubMed]
25. Molinaro, R.; Evangelopoulos, M.; Hoffman, J.R.; Corbo, C.; Taraballi, F.; Martinez, J.O.; Hartman, K.A.; Cosco, D.; Costa, G.; Romeo, I.; et al. Design and Development of Biomimetic Nanovesicles Using a Microfluidic Approach. *Adv. Mater.* **2018**, *30*, 1702749. [CrossRef]
26. Molinaro, R.; Martinez, J.O.; Zinger, A.; De Vita, A.; Storci, G.; Arrighetti, N.; De Rosa, E.; Hartman, K.A.; Basu, N.; Taghipour, N.; et al. Leukocyte-mimicking nanovesicles for effective doxorubicin delivery to treat breast cancer and melanoma. *Biomater. Sci.* **2020**, *8*, 333–341. [CrossRef]
27. Boada, C.; Zinger, A.; Tsao, C.; Zhao, P.; Martinez, J.O.; Hartman, K.; Naoi, T.; Sukhoveshin, R.; Sushnitha, M.; Molinaro, R.; et al. Rapamycin-Loaded Biomimetic Nanoparticles Reverse Vascular Inflammation. *Circ. Res.* **2020**, *126*, 25–37. [CrossRef]
28. Martinez, J.O.; Molinaro, R.; Hartman, K.A.; Boada, C.; Sukhovershin, R.; De Rosa, E.; Kirui, D.; Zhang, S.; Evangelopoulos, M.; Carter, A.M.; et al. Biomimetic nanoparticles with enhanced affinity towards activated endothelium as versatile tools for theranostic drug delivery. *Theranostics* **2018**, *8*, 1131–1145. [CrossRef]
29. Strober, W. Trypan Blue Exclusion Test of Cell Viability. *Curr. Protoc. Immunol.* **2015**, *111*, A3.B.1–A3.B.3. [CrossRef]
30. Popović, B.M.; Blagojević, B.; Ždero Pavlović, R.; Mićić, N.; Bijelić, S.; Bogdanović, B.; Mišan, A.; Duarte, C.M.M.; Serra, A.T. Comparison between polyphenol profile and bioactive response in blackthorn (*Prunus spinosa* L.) genotypes from north Serbia-from raw data to PCA analysis. *Food Chem.* **2020**, *302*. [CrossRef]
31. Gironés-Vilaplana, A.; Villaño, D.; Moreno, D.A.; García-Viguera, C. New isotonic drinks with antioxidant and biological capacities from berries (maqui, açaí and blackthorn) and lemon juice. *Int. J. Food Sci. Nutr.* **2013**, *64*, 897–906. [CrossRef]
32. Guimarães, R.; Barros, L.; Dueñas, M.; Carvalho, A.M.; Queiroz, M.J.R.P.; Santos-Buelga, C.; Ferreira, I.C.F.R. Characterisation of phenolic compounds in wild fruits from Northeastern Portugal. *Food Chem.* **2013**, *141*, 3721–3730. [CrossRef] [PubMed]
33. Biesalski, H.K. Polyphenols and inflammation: Basic interactions. *Curr. Opin. Clin. Nutr. Metab. Care* **2007**, *10*, 724–728. [CrossRef]
34. Natsume, M. Polyphenols: Inflammation. *Curr. Pharm. Des.* **2018**, *24*, 191–202. [CrossRef]
35. Albertini, M.C.; Fraternale, D.; Semprucci, F.; Cecchini, S.; Colomba, M.; Rocchi, M.B.L.; Sisti, D.; Di Giacomo, B.; Mari, M.; Sabatini, L.; et al. Bioeffects of *Prunus spinosa* L. Fruit ethanol extract on reproduction and phenotypic plasticity of *Trichoplax adhaerens* Schulze, 1883 (Placozoa). *PeerJ* **2019**, *7*. [CrossRef]
36. Corbo, C.; Molinaro, R.; Taraballi, F.; Toledano Furman, N.E.; Hartman, K.A.; Sherman, M.B.; De Rosa, E.; Kirui, D.K.; Salvatore, F.; Tasciotti, E. Unveiling the in Vivo Protein Corona of Circulating Leukocyte-like Carriers. *ACS Nano* **2017**, *11*, 3262–3273. [CrossRef] [PubMed]
37. Millán, C.G.; Marinero, M.L.S.; Castañeda, A.Z.; Lanao, J.M. Drug, enzyme and peptide delivery using erythrocytes as carriers. *J. Control. Release* **2004**, *95*, 27–49. [CrossRef] [PubMed]
38. Chen, L.; Dipietro, L.A. Toll-like receptor function in acute wounds. *Adv. Wound Care* **2017**, *6*, 344–355. [CrossRef] [PubMed]
39. Chang, L.; Liang, J.; Xia, X.; Chen, X. miRNA-126 enhances viability, colony formation, and migration of keratinocytes HaCaT cells by regulating PI3 K/AKT signaling pathway. *Cell Biol. Int.* **2019**, *43*, 182–191. [CrossRef]
40. Fei, J.; Ling, Y.M.; Zeng, M.J.; Zhang, K.W. Shixiang plaster, a traditional Chinese medicine, promotes healing in a rat model of diabetic ulcer through the receptor for advanced glycation end products (RAGE)/Nuclear Factor kappa B (NF-kB) and Vascular Endothelial Growth Factor (VEGF)/Vascular Cell Adhesion Molecule-1 (VCAM-1)/Endothelial Nitric Oxide Synthase (eNOS) signaling pathways. *Med. Sci. Monit.* **2019**, *25*, 9446–9457. [CrossRef]
41. Shahzad Aslam, M.; Syarhabil Ahmad, M.; Riaz, H.; Atif Raza, S.; Hussain, S.; Salman Qureshi, O.; Maria, P.; Hamzah, Z.; Javed, O. Role of Flavonoids as Wound Healing Agent. *Intech* **2016**. [CrossRef]

42. Elmowafy, E.; El-Derany, M.O.; Biondo, F.; Tiboni, M.; Casettari, L.; Soliman, M.E. Quercetin loaded monolaurate sugar esters-based niosomes: Sustained release and mutual antioxidant—hepatoprotective interplay. *Pharmaceutics* **2020**, *12*, 143. [CrossRef] [PubMed]
43. Lee, E.S.; Park, S.H.; Kim, M.S.; Han, S.Y.; Kim, H.S.; Kang, Y.H. Caffeic acid disturbs monocyte adhesion onto cultured endothelial cells stimulated by adipokine resistin. *J. Agric. Food Chem.* **2012**, *60*, 2730–2739. [CrossRef] [PubMed]
44. Azam, S.; Jakaria, M.; Kim, I.S.; Kim, J.; Ezazul Haque, M.; Choi, D.K. Regulation of toll-like receptor (TLR) signaling pathway by polyphenols in the treatment of age-linked neurodegenerative diseases: Focus on TLR4 signaling. *Front. Immunol.* **2019**, *10*, 1000. [CrossRef] [PubMed]

antioxidants

Article

Antioxidant and Anti-Inflammaging Ability of Prune (*Prunus Spinosa* L.) Extract Result in Improved Wound Healing Efficacy

Sofia Coppari [1,†], Mariastella Colomba [1,†], Daniele Fraternale [1], Vanessa Brinkmann [2], Margherita Romeo [2], Marco Bruno Luigi Rocchi [1], Barbara Di Giacomo [1], Michele Mari [1], Loretta Guidi [1], Seeram Ramakrishna [3], Natascia Ventura [2,‡] and Maria Cristina Albertini [1,*,‡]

[1] Department of Biomolecular Sciences, University of Urbino Carlo Bo, 61029 Urbino, Italy; s.coppari3@campus.uniurb.it (S.C.); mariastella.colomba@uniurb.it (M.C.); daniele.fraternale@uniurb.it (D.F.); marco.rocchi@uniurb.it (M.B.L.R.); barbara.digiacomo@uniurb.it (B.D.G.); michele.mari@uniurb.it (M.M.); loretta.guidi@uniurb.it (L.G.)

[2] Medical Faculty, Institute of Clinical Chemistry and Laboratory Diagnostic, Heinrich Heine University and the IUF- Leibniz Research Institute for Environmental Medicine Auf'm Hennekamp 50, 40225 Düsseldorf, Germany; Vanessa.Brinkmann@uni-duesseldorf.de (V.B.); Margherita.Romeo@iuf-duesseldorf.de (M.R.); natascia.ventura@uni-duesseldorf.de (N.V.)

[3] Center for Nanofibers and Nanotechnology, National University of Singapore, Singapore 119077, Singapore; seeram@nus.edu.sg

* Correspondence: maria.albertini@uniurb.it; Tel.: +39-0722-305260

† equally contributed.

‡ equally contributed.

Abstract: *Prunus spinosa L.* fruit (PSF) ethanol extract, showing a peculiar content of biologically active molecules (polyphenols), was investigated for its wound healing capacity, a typical feature that declines during aging and is negatively affected by the persistence of inflammation and oxidative stress. To this aim, first, PSF anti-inflammatory properties were tested on young and senescent LPS-treated human umbilical vein endothelial cells (HUVECs). As a result, PSF treatment increased miR-146a and decreased IRAK-1 and IL-6 expression levels. In addition, the PSF antioxidant effect was validated in vitro with DPPH assay and confirmed by in vivo treatments in *C. elegans*. Our findings showed beneficial effects on worms' lifespan and healthspan with positive outcomes on longevity markers (i.e., miR-124 upregulation and miR-39 downregulation) as well. The PSF effect on wound healing was tested using the same cells and experimental conditions employed to investigate PSF antioxidant and anti-inflammaging ability. PSF treatment resulted in a significant improvement of wound healing closure (ca. 70%), through cell migration, both in young and older cells, associated to a downregulation of inflammation markers. In conclusion, PSF extract antioxidant and anti-inflammaging abilities result in improved wound healing capacity, thus suggesting that PSF might be helpful to improve the quality of life for its beneficial health effects.

Keywords: polyphenols; MicroRNA; HUVEC; lifespan; *C. elegans*; tissue regeneration; cell migration; aging phenotype; biological aging

check for updates

Citation: Coppari, S.; Colomba, M.; Fraternale, D.; Brinkmann, V.; Romeo, M.; Rocchi, M.B.L.; Di Giacomo, B.; Mari, M.; Guidi, L.; Ramakrishna, S.; et al. Antioxidant and Anti-Inflammaging Ability of Prune (*Prunus Spinosa* L.) Extract Result in Improved Wound Healing Efficacy. *Antioxidants* **2021**, *10*, 374. https://doi.org/10.3390/antiox10030374

Academic Editor: Dorothy Klimis-Zacas

Received: 5 February 2021
Accepted: 23 February 2021
Published: 2 March 2021

1. Introduction

The wound healing process consists of different phases including hemostasis, inflammation, tissue proliferation, and tissue remodeling. Tissue injury activates the acute inflammatory response, which is necessary to provide tissue remodeling for repair. Successful repair requires the production of anti-inflammatory cytokines and downregulation of proinflammatory mediators. An excessive or prolonged inflammatory phase result in increased tissue injury and poor healing. The process depends on the persistence of inflammatory and oxidative stress conditions, which increase reactive oxygen species (ROS) formation leading to direct damage of cells [1].

Inflammaging, meaning that the aging process shows a chronic progressive proinflammatory phenotype [2], plays an increasingly important role in age-related diseases. In particular, inflammaging along with oxidative stress are among the main causes of chronic wound healing delay. Research in this area has attracted attention of academics in different fields of study revealing that several physiological and pathological mechanisms are supported by small non-coding RNAs, particularly microRNAs (miRNAs, post-transcriptional regulators of gene expression), which regulate inflammaging, as they are associated with many physiological processes correlated with aging, including cellular senescence. It has been previously demonstrated that miR-146a is associated with the human umbilical vein endothelial cell (HUVEC) senescent phenotype since it is highly downregulated in senescent cells [3]. Moreover, miR-146a is deeply involved in inflammatory responses as a very important actor in modulating the inflammation cascade since it can negatively regulate IRAK-1 expression [4].

Aiming at detecting novel agents to treat inflammatory diseases, several natural compounds or herbs have been tested to evaluate their anti-inflammatory potential. One of this is *Prunus spinosa* L. (also known as blackthorn, order Rosales, Rosaceae family, genus *Prunus,* species *P. spinosa*), a thorny shrub growing wild in uncultivated areas of Europe, West Asia, and the Mediterranean. The plant, used in phytotherapy for the treatment of cough but also as a diuretic, laxative, antispasmodic, and anti-inflammatory has, since a few decades, notably aroused the interest of the scientific community for its potential biological properties, and has been subject to extensive investigations [5–10]. For example, some of these authors have demonstrated a powerful antioxidant activity of *P. spinosa* fruit juice or extract (likely due to the presence of high levels of polyphenolic compounds) by DPPH (2,2-diphenyl-1-picrylhydrazyl) test. *P. spinosa* fruit (PSF) extract was also analyzed for bioactive effects in vivo on *Trichoplax adhaerens* (Placozoa) cultures and for antioxidant, antimicrobial, and anti-inflammatory activities in vitro with the aim to promote its adoption as new food beneficial for consumers or as a supplementary source of additive elements (i.e., natural pigments or antioxidants) for food or pharmaceutical industries.

In this study, our attention focused on a further characterization of PSF ethanol extract from our country (the Marche, Central Italy) in order to test its wound healing efficacy, after evaluating its antioxidant, anti-inflammatory, and antiaging properties, which are necessary for a good and effective wound healing activity. Wound healing is a primary therapeutic target for regenerative interventions, which aim to facilitate restoration of normal tissue architecture and function. Wound repair is a highly complex, multifaceted response, which is temporally and spatially coordinated across multiple stages through cooperative actions of diverse cell types, extracellular matrix molecules, cytokines, and growth factors [11]. Therefore, given increasing interest in identifying biologically active plant constituents for wound care, screening PSF ethanol extract for wound healing seemed particularly interesting and potentially a prelude to new and future applications.

The work hypothesis was that *Prunus* extract could exert a positive effect on wound healing as its bioactive polyphenols exhibit antioxidant, anti-inflammatory, and antimicrobial properties [12,13], which makes the extract ideal to play such a role in tissue repair.

Hence, after assessing the chemical composition of the extract, the study was organized considering either in vitro and in vivo experimental conditions in order to verify the beneficial properties of PSF, antioxidant (in vitro and in vivo), anti-inflammatory (in vitro), and antiaging (in vitro and in vivo) capacities. All these aspects were necessary to proceed the in vitro analysis of the PSF wound healing efficacy. Furthermore, in order to be able to correlate the wound healing activity with the anti-inflammaging property, after assessing the wound closure, the exact same PSF-treated cells were detached and used to evaluate the expression levels of markers associated to inflammation.

2. Materials and Methods

2.1. Chemicals and Reagents

Chromatographic solvents (water, acetonitrile, and formic acid) were HPLC grade, purchased from Merck (MERCK S.P.A., Milano, Italy).

2.2. Plant Material and Extract Preparation

P. spinosa L. ripe fruits were collected in November 2017 at "La Caputa" Urbania (PU, Marche, Italy), GPS coordinates: N43°40′46.512″ E12°31′42.291″ (350 m above sea level) and immediately frozen and stored at −20 °C until use. Voucher samples were deposited in the herbarium of Botanical Garden of Urbino University Carlo Bo: code "Pp125". As for the extraction preparation, we followed the protocol previously described [13], except for one modification. In particular, we employed an acidified aqueous ethanol homogenizing solution (70 mL ethanol/29.9 mL distilled H_2O/0.1 mL HCl 36%). In the end, the total amount of dried PSF extract obtained from 50 g of fruit and peel was 11.6 g.

2.3. Determination of Phenolic Compounds in Prunus Extract by HPLC/MS Analysis

The identification of phenolic compounds was achieved by comparison of the retention times and the spectra characteristics with those in data library [14] phenol express, and/or in literature, following a previously reported method [13]. Briefly, 10 mg of dried *Prunus* extract were dissolved in 1 mL of 70:30 *v/v* EtOH/H_2O solution, and analyzed by HPLC-PDA/ESI-MS. The volume for injection was set at 50 µL. Before (direct) injection, all samples were cleared through a 0.45 µm nylon filter. Chromatographic analyses were performed using a MerkPurospher Star RP-18 endcapped column (4.0 mm × 250 mm, 5 µm particle size), thermostated at 25 °C, setting the elution flow rate at 0.7 mL/min. A system of two mobile phases was used for the elution: (A) aqueous 0.1% formic acid in double distilled water and (B) acetonitrile. The elution profile was as follows: 0–10 min, 94% A; 10–15 min, 83% A; 15–25 min, 78% A; 25–35 min, 76%A; 35–40 min, 74%A; and 40–45 min, 68%A.

The HPLC Waters system utilized for the analysis was equipped with an automatic injector, Alliance HT2795 separation module, column heater, Waters 2996 Photo Diode Array (PDA) connected to the mass spectrometer, Waters micromass ZQ MS system, and single quadrupole equipped with an electrospray ionization (ESI) interface. The instrument was operated in positive (ES+) and negative (ES-) ion mode with a scan range *m/z* 200–700. Capillary voltage was set at 3.50–3.51 kV (ES+) and 2.75–3.51 kV (ES-), source temperature at 100 °C and desolvation temperature at 300 °C. The cone and desolvation nitrogen gas flows were 50 and 500 L/h, respectively. UV–Vis spectra were recorded from 220 to 800 nm, with a bandwidth of 1.2 nm.

2.4. Cell Culture and Treatments

Human umbilical vein endothelial cells (HUVECs) derived from multiple donors were purchased from Life Technologies Corporation (Gibco™ C01510C, 1 × 10^6 cells). Cells were seeded at a density of 5000/cm^2 in T25 flasks (Corning Costar, Sigma Aldrich, St. Louis, MO, USA). HUVECs were cultured in the growth medium of Gibco ™ Medium 200 (Life Technologies Corporation, Grand Island, NY). The medium required the addition of the Gibco™ Low Serum Growth Supplement Kit (LSGS Kit) (Life Technologies Corporation, Grand Island, NY). The final concentrations of the components in the medium are fetal bovine serum (2% *v/v*), hydrocortisone (1 µg/mL), growth factor human epidermal (10 ng/mL), basic fibroblast growth factor (3 ng/mL), and heparin (10 µg/mL). Cells were incubated at 37 °C and 5% CO_2 and allowed to grow to confluence as a monolayer. When cells reached 80% confluence, they were passaged with Trypsin-EDTA Solution (Sigma-Aldrich, St. Louis, MO, USA). All the experiments were performed using cells obtained from passage 3 (P3) to passage 15 (P5). HUVECs were treated with *P. spinosa* fruit (PSF) ethanol extract during a 6 h LPS (1 µg/mL) stimulation, while for replicative senescence and (P2–P15) wound healing, as specified in figure legends. PSF extract has been used at

different concentrations (20/40/80 µg/mL): during 6 h for LPS stimulated HUVECs; 48 h for wound healing repair (as indicated below) and during P2-P15 replicative senescence.

2.5. In Vitro Wound Healing Assay

HUVEC cells were seeded in T25 tissue culture flasks, the cell monolayer was subjected to a mechanical scratch wound, horizontal along the flask, using the tip of a sterile pipette. HUVECs were treated with 20/40/80 µg/mL of ethanolic *P. spinosa* extract for 48 h. The untreated cells were used as a control and the vehicle condition was added too (ETOH). The images were acquired from the same lesion area immediately after scratching (t0) and after 48 h using a phase contrast microscope (Olympus Ix51 10× objective). We used ImageJ software to evaluate the total migration area during wound closure. The percentage of wound closure was calculated using the following formula:

$$[(\text{Wound area t0} - \text{Wound area t}) / \text{Wound area t0}] \times 100. \quad (1)$$

The experiments were conducted in triplicate.

2.6. HUVEC Replicative Senescence Analysis

Each time that cells reached confluence, they were passaged through trypsinization, counted (using a Neubauer chamber) and replated. Replicative senescence was induced by culturing cells up to the 15th passage (160 days). The sum of all PD (population doubling) changes was used to calculate the cumulative population doubling level (CPDL).

SA-β-Gal analysis has been performed using the senescence cells histochemical staining kit (Sigma-Aldrich, St. Louis, MO, USA) where senescent cells positive for SA-β-Gal activity (colored in blue) were counted as a percentage related to the total cell number.

Cells were considered young when SA-β-Gal < 5%, and senescent when SA-β-Gal > 50%. SA-β-Gal activity was assessed as described previously [15].

2.7. Quantitative Real Time PCR (RT-qPCR) of Mature MicroRNAs and mRNA

The total RNA isolation kit (NorgenBiotek, Thorold, Canada) was used to isolate total RNA (including both microRNA and larger RNA species) from HUVEC cells, following the manufacturer's recommended protocol; RNA was stored at −80 °C until use. Human miR-146a and human RNU44 (reference miRNA) expressions were quantified using the TaqMan MicroRNA assay (Applied Biosystems, Foster City, CA, USA), as previously described [4].

The same total RNA isolation kit (NorgenBiotek, Thorold, ON, Canada) was used to isolate total RNA from *C. elegans*. Total RNA was extracted from 1000 worms/condition after growing them for 3 days (from embryo) on plates with or without *Prunus* extract supplementation to the nematode growth media (NGM). *C. elegans* miR-124, miR-39, and U6 (reference miRNA) expressions were quantified using the same TaqMan MicroRNA assay mentioned before (Applied Biosystems, Foster City, CA, USA).

Isolated RNA was used to synthesize cDNA using a reverse transcription kit (Applied Biosystems, Foster City, CA, USA) according to the manufacturer's protocol. Quantitative polymerase chain reaction real time (RT-qPCR) was performed with the SYBR Green PCR master mix (Applied Biosystems, Foster City, CA, USA) on an ABI Prism 7500 Real Time PCR System (Applied Biosystems, Foster City, CA, USA). The primers (IL-6: Forward AGGGCTCTTCGGCAAATGTA and Reverse GAAGGAATGCCCATTAACAACAA; IRAK-1: Forward CAGACAGGGAAGGGAAACATTTT and Reverse CATGAAACCTGACTTGCTTCTGAA) we used were the ones designed by Angel-Morales et al. [16]. TATA binding protein (TBP; Forward TGCACAGGAGCCAAGAGTGAA and Reverse CACATCACAGCTCCCCACCA) was used as an endogenous control to determine relative mRNA expression. The pairs of forward and reverse primers were purchased from (Sigma-Aldrich, St. Louis, MO, USA).

Product specificity was examined by the dissociation curve analysis. Results were calculated using the $2^{-\Delta\Delta Ct}$ method and are expressed as the fold change related to untreated control (CTRL).

2.8. DPPH Radical Assay

The antioxidant capacity of *Prunus spinosa* extract was evaluated by DPPH (diphenylpicrylhydrazyl) radical-scavenging method as in Fraternale et al. [17]. Of the reaction solution 280 µL was mixed with 80 µL of 0.5 mM DPPH (Sigma-Aldrich) ethanol solution and 40 µL of *P. spinosa* ethanol extract at different concentrations (from 12.5 to 100 µg/mL). Absorbance (A) was measured at 517 nm using ethanol as a blank. Of 0.5 mM DPPH 80 µL added to 320 µL of ethanol was used as negative control. DPPH inhibition (I, expressed in %) was calculated to evaluate the antioxidant activity by the following equation:

$$I\,(\%) = [(A_0 - As)/\,A_0] \times 100 \quad (2)$$

where A_0 corresponds to the negative control absorbance and As corresponds to the tested sample absorbance. The higher the inhibition the higher the free radical scavenging ability. All analyses were performed in triplicate. L-ascorbic acid (Sigma-Aldrich, St. Louis, MO, USA) was used as a standard control at a concentration of 0.040 mg/mL.

The equation obtained by linear regression analysis was used to calculate the EC50 (considering y = 50).

2.9. C. elegans Cultivation

Wildtype (N2) nematodes were kept at 20 °C on NGM plates supplemented with 0.01% of ampicillin and 0.0005% of tetracycline *E. coli* HT115 (L4440) that was used as a food source.

2.10. E. coli Strains and Growth

HT115 (L4440) was obtained from Ahringer *C. elegans* RNAi feeding library [18]. It was grown in LB medium supplemented with 0.01% of ampicillin and 0.0005% of tetracycline at 37 °C overnight.

2.11. Prunus Extract Treatment in C. elegans

The *Prunus* extract was dissolved in 50% EtOH in a concentration 50 times higher than the desired final concentration. The extract was then spread on the NGM plates seeded with *E. coli HT115* (L4440). Of the stock solution 140 µL was spread on 7 mL NGM plates, while 360 µL was spread on 18 mL NGM plates.

2.12. Life and Healthspan

For lifespan and healthspan assays, age-synchronous populations were obtained by egg-lay on NGM plates containing the desired concentrations of *Prunus* extract. The treatment with *Prunus* extract was continued for the entire lifespan. Starting from adulthood, the worms were transferred to fresh NGM plates daily and the numbers of dead, alive, and censored animals were scored. For the healthspan analysis animals not moving, moving, and censored were scored. After the fertile phase, worms were transferred and scored every alternate day. Animals with internal hatching, an exploded vulva, or which died desiccated on the wall were censored. Survival analysis of pooled populations was performed in OASIS 2 [19,20].

2.13. Pharyngeal Pumping Rate and Body Bends Assay

Age-synchronized N2 nematodes were obtained by a worm bleaching protocol [21]. Eggs were then left to hatch during the night with a slight rocking. The day after, L1 larvae were spotted onto fresh NGM plates seeded with HT115 (L4440) and containing 400 µg/mL of *Prunus* extract or 1% ethanol (EtOH).

For the behavioral tests, nematodes (L4 larval stage) were collected and washed twice with M9 buffer to eliminate bacteria [22,23]. Worms were then incubated 2 h with 1 mM H_2O_2 (Sigma-Aldrich, St. Louis, MO, USA) in M9 buffer, on orbital shaking in dark conditions (100 worms/100 µL). Control worms were incubated with M9 buffer (vehicle)

alone (100 worms/100 µL). After incubation, worms were transferred onto fresh NGM plates seeded with HT115 (L4440) and containing 400 µg/mL of *Prunus* extract or 1% ethanol. The body bends and the pharyngeal pumping rate were scored 20 h later [23,24]. Locomotor defects have been scored by measuring the number of body bends in liquid over a 1-min interval (body bends/min).

2.14. Statistical Analysis

All experiments were performed in triplicate if not differently specified. Statistical significance of *C. elegans* in vivo treatments was evaluated using the log-rank test. The *p*-values were corrected for multiple comparisons using the Bonferroni method. For the behavioral test, data were analyzed using GraphPad Prism 8.0 software (GraphPad Software, San Diego, CA, USA) two-way analysis of variance, and Bonferroni's post hoc test. DPPH results are reported as linear regression analysis. For all the other experiments, statistical significance was determined at $p < 0.05/0.01$ using the Student's *t*-test.

3. Results

3.1. Chemical Characterization

Chemical characterization of *Prunus spinosa* ethanolic extract was improved with respect to that previously described for a similar *Prunus* extract [13]. In particular, as reported in Table 1, the most abundant compounds among phenolic components (detected by HPLC–PDA/ESI–MS analysis) are the following: one isomer of caffeoylquinic acid, cyanidine-3-*O*-rutinoside, and peonidine-3-*O*-rutinoside (both showing anthocyanins typical UV absorption bands around 520 and 280 nm). The presence of a variety of quercetine derivatives, with higher retention time than the previous compounds, was also detected. In particular, based on retention time, typical flavonol UV absorption bands (around 260 and 350 nm), positive and negative molecular peaks, quercetine base peak 303 as a positive ion fragment, and the phenol express database (or references reported in Table 1), we tentatively identified the following derivatives: quercetine-3-O-rutinoside, quercetine-3-*O*-esoside-*O*-pentoside; quercetine-3-*O*-glucoside or galactoside, two quercetine-3-*O*-pentosides and a quercetine-3-*O*-pentoside derivative, and quercetine-3-*O*-ramnoside. These findings are in part coherent with previously reported analysis [13]. Despite this similarity, we could not detect cyanidine-3-*O*-glucoside, indicated as the main anthocyanin derivative often found in wild *Prunus* species. This could be due to a lower concentration of the latter compound in this local cultivar, and/or to technical restriction of the HPLC Waters system utilized for the chromatographic separation.

Table 1. Characterization of the main phenolic compounds in samples of *Prunus spinosa* ethanolic extract by HPLC–PDA/ESI–MS in positive and/or negative mode.

Peak No	t_R (min)	λ_{max} (nm)	M^+ or $[M+Na]^+$ (*m/z*)	$[M-H]^-$ or $[M+Na]^-$ (*m/z*)	HPLC-ESI/MS^n *m/z* (% base Peak)	Tentative Assignment	Ref.
1	15.2	300sh, 325	355 [a]	353		O-Caffeoylquinic acid isomer	[1]
2	18.5	281, 514	595		MS^2[595]: 287 (100), 449 (65)	Cyanidin-3-O-rutinoside	[25–27]
3	19.4	282, 517	609		MS^2[609]: 301 (50), 463 (40)	Peonidin-3-O-rutinoside	[25–27]
4	25.9	260, 352	611 [a]	609	MS^2[611]: 303 (100), 465 (30)	Rutin (quercetin-3-O-rutinoside)	[1]
5	26.5	258,347	597 [a]	595	MS^2[597]: 303 (100), 465 [a](50)	Quercetin 3-O-hexoside-O-pentoside	[1]
6	27.4	258, 350	465 [a]	463	MS^2[463]: 301 20) MS^2[465]: 303 (100)	Quercetin glucoside or galactoside	[1]
7	29.0	275, 350	625 [a]	623 [a]	MS^2[623]: 433 (100), MS^2[625]: 303 (100), 435 [a] (20)	Quercetin xyloside or arabinoside derivative	[1]
8	29.8	260, 352	435 [a]	433	MS^2[435]: 303 (100)	Quercetin arabinoside or xyloside	[1]
9	30.6	278, 352		433	MS^2[435]: 303 (100)	Quercetin pentoside	[28]
10	31.4	278, 352		447	MS^2[449]: 303 (100)	Quercetin-3-O-rhamnoside	[1]

[a] Sodium adduct.

3.2. *In Vitro Analyses*

3.2.1. In Vitro Evaluation of Antioxidant Properties

The polyphenols identified are in line with the high phenolic content previously indicated and the high antioxidant activity demonstrated in vitro by the DPPH free radical assay [13]. DPPH is a well-known radical and a scavenger for other radicals. Generally, rate reduction of a chemical reaction upon addition of DPPH is used as an indicator of the radical nature of that reaction. DPPH radical has a deep violet color in solution, and it becomes colorless or pale yellow when neutralized. The greater DPPH inhibition (I %), the greater the antioxidant activity of the substance tested. Obtained results showed that the extract effectively acts as an antioxidant in a dose-dependent manner (Figure 1) with an EC50 corresponding to 64.2 µg/mL.

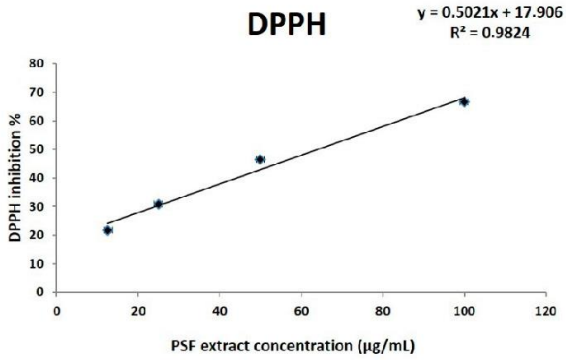

Figure 1. DPPH analysis of *P. spinosa* extract antioxidant activity was carried out at different *P. spinosa* extract (PSF) concentrations (from 12.5 to 100 µg/mL). DPPH inhibition (I, expressed in %) was used to evaluate PSF antioxidant activity. Linear regression analysis (R^2 = 0.982) shows an excellent concentration-dependent effect. *P. spinosa* exerts an antioxidant activity with an EC50 = 64.2 µg/mL (calculated (given y = 50) as: 50 = 0.502x + 17.906).

3.2.2. In Vitro Anti-inflammatory Activity

Considering the important role of oxidative stress and inflammation in the aging and wound healing processes, we first evaluated the anti-inflammatory effect of PSF in a classical cellular model, widely employed for aging and wound healing assays. In particular, young (P3) and senescent (P15) LPS-treated HUVECs, assayed separately, were employed. Senescent cells were identified based on the expression of senescence-associated biomarkers, including the senescence-associated secretory phenotype (SASP) (SA-β-Gal > 50%), (data not shown). In P3 cells, during an acute (6 h treatment) proinflammatory stimulus, PSF ethanol extract at different concentrations (20 µg/mL; 40 µg/mL; 80 µg/mL) increased miR-146a and decreased IRAK-1 and IL-6 expression levels (Figure 2). Although the real nature of molecular interactions between TLR4 and *P. spinosa* ethanol extract are still to be investigated, our findings showed, as observed in U937 cells under the same experimental conditions [13], that in HUVEC cells as well, *Prunus* extract can upregulate intracellular miR-146a, with a consequent downregulation of the TLR-NF-κB-mediated inflammatory response, particularly by inhibiting TLR4 signaling pathway and reducing cytokine (IL-6) production. We performed the same treatment on older cells. As shown in Figure 2, LPS stimulated P15 HUVECs showed upregulated miR-146a levels (LPS) that even increased with PSF extract treatment (20/40/80 µg + LPS). In addition, obtained results in both young and senescent HUVEC cells revealed that PSF was able to decrease IRAK-1 and IL-6 expressions, thus strongly suggesting an anti-inflammatory activity, which makes PSF extract a good candidate for wound healing.

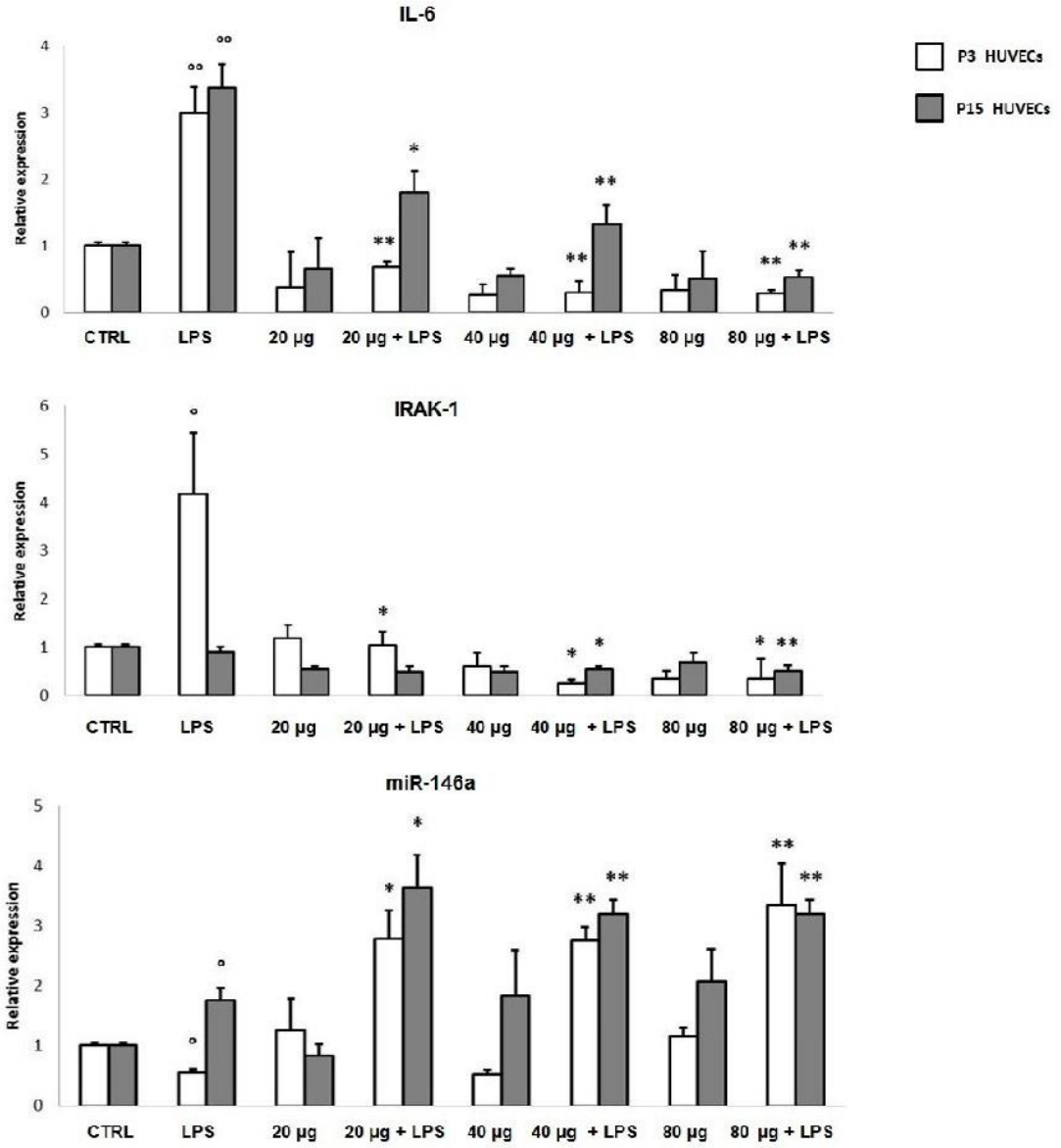

Figure 2. Anti-inflammatory effect of *P. spinosa* extract on IL-6, IRAK-1, and miR-146a expression levels in LPS (lipopolysaccharide, 1 µg/mL) stimulated young (P3) and older (P15) human umbilical vein endothelial cells (HUVECs) after 6 h of treatment. LPS stimulus downregulated miR-146a (LPS). When treated with *P. spinosa* extract during LPS stimulation (20/40/80 µg/mL *P. spinosa* + LPS), cells showed miR-146a upregulation with a decreased expression of both IRAK-1 and IL-6. Results are reported as fold change related to CTRL. Two-tailed paired Student's *t*-test: * $p < 0.05$ LPS vs. *P. spinosa* + LPS; ** $p < 0.01$ LPS vs. *P. spinosa* + LPS; ° $p < 0.05$ LPS vs. CTRL; °° $p < 0.05$ LPS vs. CTRL.

3.3. In Vivo Analyses

Taking into account that due to cost and duration, relatively little is known about whether dietary polyphenols are beneficial in whole animals, particularly with respect to aging, to test the potential bioeffects (i.e., antioxidant and antiaging activity) of PSF, in addition to the in vitro model, we also employed the nematode *Caenorhabditis elegans*, a powerful model organism widely used for aging and longevity studies, due to its short (2–

3-week) lifespan, rapid generation time, and experimental flexibility [29,30]. In particular, *C. elegans* is an excellent and useful model employed to analyze and understand organismal responses to different natural and synthetic compounds, including polyphenols, and their influence on aging and lifespan, as different biological processes and numerous aspects of aging are very similar in nematodes and mammals, including humans [31]. Significant changes in gene expression occur during *C. elegans* aging. In fact, the distinct age-dependent gene expression profiles that exist between genetically identical individuals are likely to be mediated through variations in gene regulatory networks and, once again, microRNAs represent likely candidates for mediating some of these variations even by modifying *C. elegans* lifespan. For example, overexpression of miR-124 causes the lifespan extension of *C. elegans* [32], whereas the loss of miR-124 increases ROS formation and accumulation of the aging markers, resulting in a reduction in lifespan [33]. Furthermore, miR-39 has been shown to be involved in strong age-specific changes [34].

3.3.1. Longevity Study

To strengthen the beneficial antiaging effects of PSF extract in vivo, we moved to a powerful model organism widely used for aging and longevity studies, the nematode *C. elegans*. Lifespan analysis was performed using wild-type worms exposed to different concentrations of the extract throughout the entire lifespan. When examining living organisms, the bioavailability has a key role while evaluating health effects. That is the reason why concentrations employed in in vivo assays are different and (often) higher that those tested in vitro. At the moment PSF bioavailability is unknown, therefore starting from a concentration (40 µg/mL) that had proved to be effective in vitro or in vivo experiments [12,13], we decided to test also a ten-fold lower (4 µg/mL) and a ten-fold higher one (400 µg/mL) on *C. elegans*.

Figure 3A shows the survival curves of treatment groups against the control group (ETOH) plotted by the Kaplan–Meier model. In particular, *C. elegans* treated with different concentrations (4, 40, and 400 µg/mL) of *Prunus* extract did not show any differences from each other and from CTRLs up to the first 10 days. While, worms treated with the highest concentration (400 µg/mL) showed a lifespan significantly extended (i.e., a right-shifted curve, Bonferroni *p*-value ETOH vs. 400 µg/mL 1.2×10^{-7}) compared with the other experimental conditions.

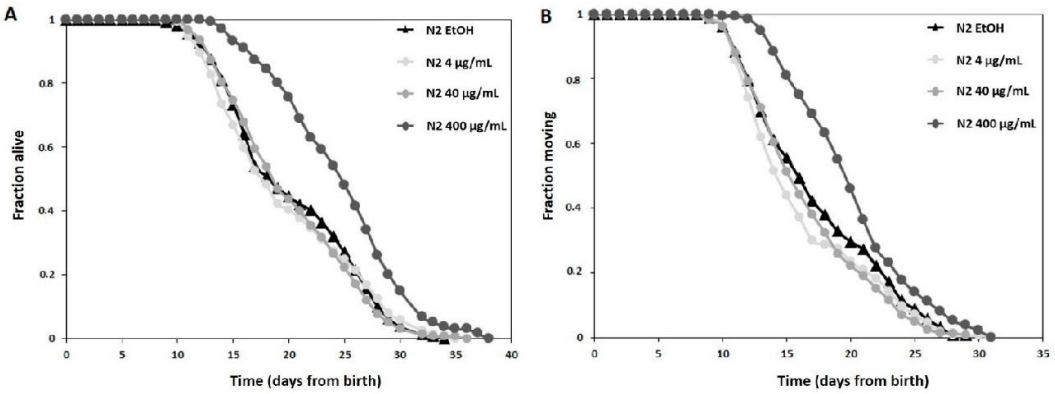

Figure 3. High concentrations (400 µg/mL) of *Prunus* extract extend lifespan and healthspan in *C. elegans*. (**A**) Kaplan–Meier survival curves of *C. elegans* treated with the indicated concentrations of *Prunus* extract showing extended lifespan at the highest concentration. (**B**) Kaplan–Meier survival curves of *C. elegans* treated with the indicated concentrations of *Prunus* extract showing extended healthspan at the highest concentration. For 3A and B panels, pooled data of 180 worms/condition in three independent replicates are shown. Bonferroni *p*-value ETOH vs. 400 µg/mL 1.2×10^{-7} in panel A. Bonferroni *p*-value ETOH vs. 400 µg/mL 0.0007 in panel B. Statistical test: Log Rank test.

The control group of nematodes without the *Prunus* extract had a mean lifespan of 20.26 ± 0.48 days under the proper survival conditions. Compared with the control, the highest concentration (400 µg/mL) group significantly extended the mean lifespan to 24.71 ± 0.48 days and the survival rate increased by 22%.

Moreover, healthspan, here defined as the time when the nematodes are still actively moving, was prolonged after treatment with PSF extract. As shown in Figure 3B, 400 µg/mL of *Prunus* extract significantly (Bonferroni *p*-value ETOH vs. 400 µg/mL 0.0007) increased the number of healthy worms with respect to the other experimental conditions. While the mean healthspan of control worms was 17.39 ± 0.41 days, worms treated with 400 µg/mL PSF had a healthspan of 20.18 ± 0.40 days, which is an increase of 16%.

3.3.2. In Vivo Evaluation of Antioxidant Properties

Taking into account that the antiaging effect of a given compound is often associated with the ability to increase stress resistance, to validate the antioxidant effects of PSF in vivo, we tested *C. elegans* resistance to H_2O_2 induced oxidative stress. To this aim, four-day old (L4) larvae of wild type (N2) nematodes were treated for 2 h with 1 mM H_2O_2 or M9 buffer (vehicle) and then moved back onto NGM plates containing 400 µg/mL *Prunus* extract or 1% EtOH. The behavioral tests were performed 20 h later. Wild type worms treated with the extract at the highest concentration (400 µg/mL) exhibited an enhanced resistance to H_2O_2 induced oxidative stress in comparison with untreated worms. Specifically, the detrimental effects on vital parameters (i.e., pharyngeal pumpings/min and body bends/min), induced by 2 h of treatment with peroxide, were significantly prevented in individuals fed with the *Prunus* extract compared to control vehicle (ETOH) fed animal (Figure 4A,B).

3.3.3. In Vivo MicroRNAs Modulation Associated to *Prunus* Antioxidant Activity

It has already been demonstrated that overexpression of miR-124 causes the lifespan extension of *C. elegans*, suggesting that miR-124 may be involved in regulation of longevity in *C. elegans* [32] and that the loss of miR-124 in *C. elegans* increases ROS formation and accumulation of the aging markers, resulting in a reduction in lifespan [33]. Furthermore, miR-39 has been shown to be involved in modulation of strong age-specific changes [34]. On this basis, we decided to analyze the expression of miR-124 and miR-39 in PSF treated *C. elegans*. As indicated in Figure 4C, miR-124 expression was increased after *P. spinosa* treatment, while miR-39 was decreased. Both results seem to suggest a potential positive effect of *Prunus* extract on *C. elegans* lifespan by the modulation of miR-124 and miR-39 expression levels. Hence, on the whole, our findings revealed that PSF extract may have potential antiaging and antioxidant effects in vivo through extending the lifespan, promoting the healthspan and, still, enhancing stress resistance of *C. elegans*.

3.4. PSF Extract Effect on Wound Healing

In order to better verify the correlation among PSF antioxidant, anti-inflammatory, and antiaging effects with wound healing capacity, once validated PSF beneficial effects either in vitro or in vivo, we moved to the principal goal of the study, which was to evaluate the activity of the extract on wound healing. In fact, the main hypothesis of the study was that a significant wound healing activity was to be expected based on PSF antioxidant and anti-inflammaging ability tested both in vitro and in vivo models, as herein previously reported. Noteworthy, our results showed that treatment with *P. spinosa* extract significantly improves wound healing closure both in P3 and P15 cells. In particular, concentrations of 40 and 80 µg/mL determined a significant increase in the percentage of wound healing compared to CTRL and ETOH groups. PSF treatment showed, albeit with some slight differences considering the concentrations used, a wound healing closure percentage around 70% both in younger and older cells, thus revealing an enhanced cell migration, which was unexpected in a relatively advanced phase of cellular aging (Figure 5A).

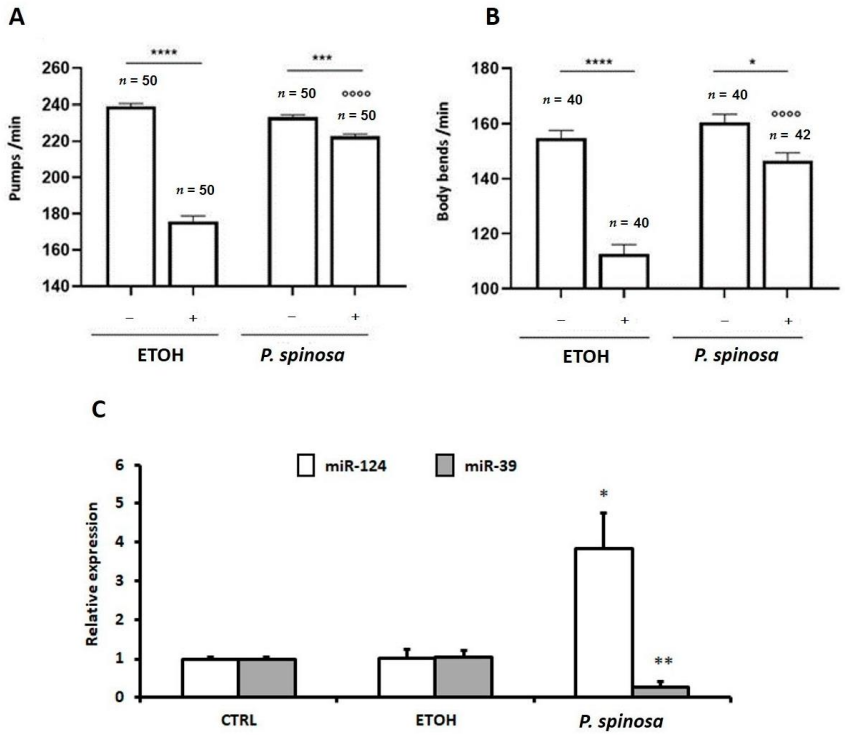

Figure 4. High concentrations of *Prunus* extract protect from H_2O_2-induced oxidative stress in *C. elegans*. (**A**) The pharyngeal pumping rate has been measured by counting the number of times the terminal bulb of the pharynx contracted over a 1-min interval (pump/min). Data are shown as mean pumps/min ± SE (n = 50 worms/assay, 3 assays). *** $p < 0.001$ and **** $p < 0.0001$, according to two-way ANOVA and Bonferroni's post hoc test. °°°° $p < 0.0001$ vs. H_2O_2-fed worms and grown on ETOH plates, according to two-way ANOVA and Bonferroni's post hoc test. Interaction < 0.0001. (**B**) The locomotor activity has been evaluated by measuring the number of body bends in liquid over a 1-min interval (body bends/min). Data are shown as mean pumps/min ± SE (n = 40 worms/assay, 3 assays). * $p < 0.05$, ****$p < 0.0001$, according to two-way ANOVA and Bonferroni's post hoc test. °°°° $p < 0.0001$ vs. H_2O_2-fed worms and grown on ETOH plates, according to two-way ANOVA and Bonferroni's post hoc test. Interaction < 0.0001. (**C**) MicroRNAs (miR-124 and miR-39) expression levels in *P. spinosa* treated *C. elegans* worms. Treatment of *C. elegans* from embryos with 400 µg/mL of PSF lead to miR-124 upregulation and miR-39 downregulation in the adults. Two-tailed paired Student's *t*-test: * $p < 0.05$ vs. CTRL; ** $p < 0.01$ vs. CTRL.

To better investigate a hypothetical mechanism of action, miR-146a along with IRAK-1 and IL-6 amounts, were analyzed in wound healing HUVECs as well. Young P3 cells treated with *Prunus* extract showed a significant increase in miR-146a expression level, with evident lowering of IL-6 and IRAK-1 amounts. Similar results were obtained treating senescent (P15) cells with PSF, indicating an anti-inflammatory activity during wound healing (Figure 5B–D). As concerns data illustrated in Figure 5B,C, showing that IL-6 and IRAK-1 were downregulated not only by PSF extract but also by EtOH alone (the vehicle), in our opinion this might be due to a technical bias (see discussion section).

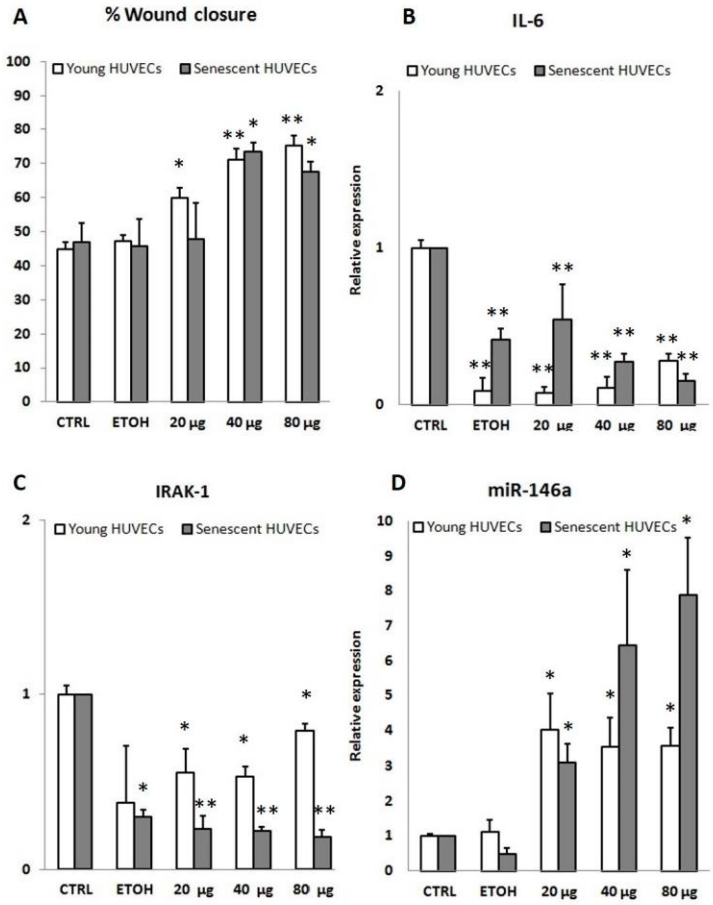

Figure 5. Wound healing (in % wound closure) in *P. spinosa* fruit extract (PSF) treated cells and expression levels of inflammation markers assessed in the same cells. Experimental conditions were the same as those employed for anti-inflammaging assays. (**A**) Percentage of wound healing closure related to CTRL in young (P3) and senescent (P15) HUVECs after 48 h of *P. spinosa* treatment. Our data showed, both in young and older cells, a significant improvement (up to 70%) of wound healing closure (expressed in percentage related to untreated cells) through cell migration. The same cells were detached and used for the evaluation of expression levels of anti-inflammatory markers, IL-6 (**B**), IRAK-1 (**C**), and miR-146a (**D**). MiR-146a upregulation was observed during PSF extract treatment (20/40/80 µg/mL *P. spinosa*). PSF extract treatment caused a decreased expression of both IRAK-1 and IL-6, thus revealing a downregulation of the inflammatory response. Results are reported as fold change related to CTRL. Two-tailed paired Student's *t*-test: $^{*}p < 0.05$ vs. CTRL; $^{**}p < 0.01$ vs. CTRL.

3.5. HUVEC Replicative Senescence Analysis and PSF Effect on Cell Biological Aging

HUVECs were also maintained in long-term cultures until growth arrest (XV passage) to mimic cellular aging, with cultures being supplemented with PSF ethanol extract at different concentrations (20, 40, and 80 µg/mL) for the entire period (160 days). Population doubling and senescence-associated β-galactosidase (SA-β-gal) staining, indicated a progressive acquisition of senescence status. A long-term treatment with PSF extract for nearly 160 days did not significantly increase HUVEC proliferation capability as indicated by the cumulative population doubling level (CPDL) (Figure 6A). Moreover, the extract did not delay the onset of aging phenotype shown by senescence-associated β-galactosidase (SA-β-gal), thus suggesting that PSF treatment does not seem to affect and/or change the

senescence process (Figure 6B). Noteworthy, however, *Prunus* extract appears to have an important "qualitative" effect on cell differentiation, at least at certain concentrations. In fact, while, on the one hand, older cells treated with the extract at 20 µg/mL did not differ from controls (and ETOH group) in morphology showing a typical cobblestone phenotype, interestingly, on the other hand, when treated with 40 or 80 µg/mL appeared as long cells with multiple protrusions connecting neighboring cell clusters (Figure 6C). These results lead us to think that the antioxidant and anti-inflammatory effects of PSF extract may allow older cells to behave as if they were younger, coping with the proinflammatory phenotype associated to cellular senescence. In fact, although the cells treated with the extract age at the same speed as the controls, they behave and act as if they were "biologically" younger.

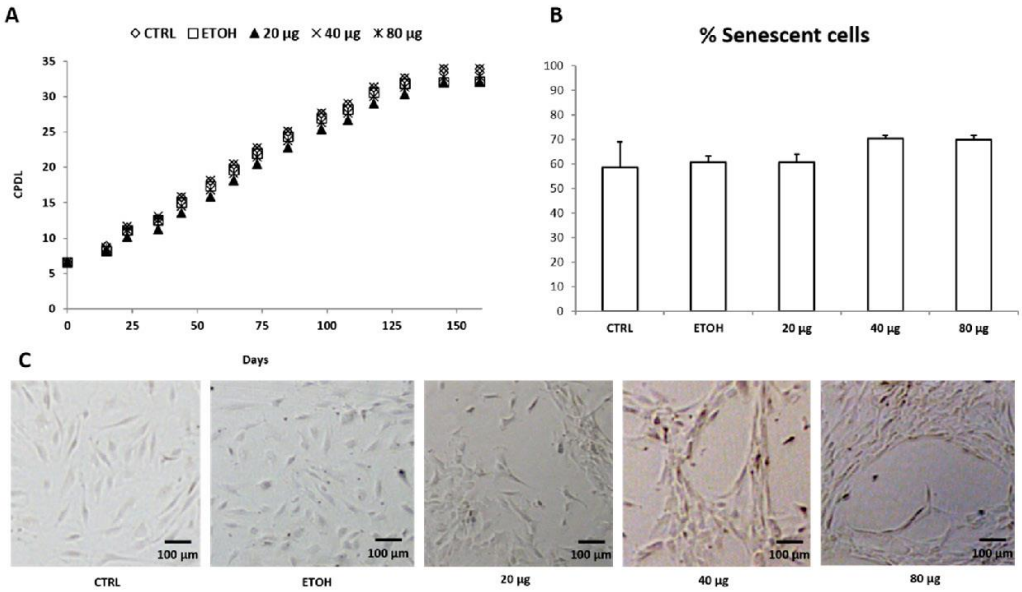

Figure 6. Senescence of HUVECs treated with *P. spinosa* at different concentrations (20, 40, and 80 µg/mL) during 160 days (P2-P15). (**A**) Growth curve showing the cumulative population doubling level (CPDL) during *P. spinosa* treatment (P2-P15). (**B**) Percentage of senescent HUVECs (P15) as a fraction of cells expressing SA-β-Gal. (**C**), Cellular morphology of P15 senescent HUVECs after 160-day *P. spinosa* treatment (Optical microscopy, 10x). The samples CTRL, ETOH and 20 µg/mL treated cells showed large cobblestone shaped cells, while cells treated with 40 µg/mL and 80 µg/mL *P. spinosa* extract showed long cells (spindle-shaped) with multiple protrusions (connecting neighboring cell clusters).

When examining the cellular senescence at the molecular level, in line with previous experimental data [4], older cells showed a proinflammatory, pro-oxidative senescence-associated phenotype (SASP), i.e., a proinflammatory condition characterized by high IRAK-1 and IL-6 amounts (see Figure 7, CTRLs). Notably, after PSF extract treatment, the modulation of miR-146a and IL-6 and IRAK-1 was comparable to what was observed in younger cells. More in detail, considering the effect of *P. spinosa* on HUVEC senescence without any additional triggers, although due to the current situation (i.e., COVID-19 emergency) our data were absolutely preliminary (one single experiment), the extract seemed to act as an anti-inflammatory agent, as shown by IL-6, IRAK-1, and miR-146a expression levels, evaluated in P2, P5, and P15 cells (Figure 7).

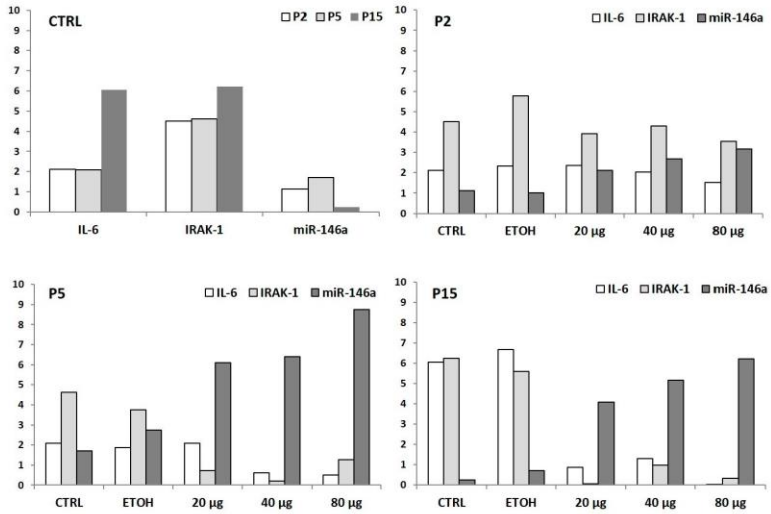

Figure 7. Anti-inflammatory effect of *P. spinosa* during HUVEC senescence (observed at P2, P5, and P15). Untreated (i.e., without any additional triggers) CTRL old cells showed increased IL-6/IRAK-1 expressions and miR-146a downregulation. Notably, in older cells, *P. spinosa* treatments (20/40/80 µg/mL) decreased IL-6/IRAK-1 expressions and upregulated miR-146a, showing a modulation of miR-146a expression level and IL-6 and IRAK-1 amounts comparable to what was observed in younger cells. The relative expression has been determined using the $2^{-\Delta Ct}$ method and is expressed as fold change related to the TATA binding protein (TBP) endogenous control.

4. Discussion

Cellular senescence is a persistent hyporeplicative state, first described by Hayflick [35], that can be induced by several types of internal or external (environmental) stress. At present, senescent cells are mostly identified by the combined presence of multiple traits, including senescence-associated protein expression and secretion, DNA damage and β-galactosidase activity. Senescent cells are known to adopt a secretory phenotype that comprises a large number of potent proinflammatory, angiogenic, and tissue-remodeling factors. This important trait, reported as the senescence-associated secretory phenotype (SASP), influences many biological processes such as tissue repair and regeneration, tumorigenesis, and the aging-associated proinflammatory state. At a biological level, senescence is a two-sided medal playing and important role in physiological and pathological processes: on the one hand it is beneficial for tissue remodeling, embryonic development, wound healing, and tumor suppression in young individuals [36–38], on the other hand, in old individuals, it promotes aging-associated declines and diseases including age-related chronic inflammation (i.e., neurodegeneration) [39,40] and cancer.

Oxidative stress and inflammation are the major mechanisms of endothelial dysfunction with advancing age and oxidative stress contributes to chronic inflammatory processes implicated in aging, referred to as "inflammaging". Plant polyphenolics have been shown to modify signal transduction pathways contributing to delaying or preventing inflammation [13,41,42]. In this study, the potential antioxidant, anti-inflammatory, and antiaging effects of *P. spinosa* L. fruit (PSF) ethanol extract (particularly rich in polyphenolics) were investigated in vitro and in vivo. Our results demonstrated that PSF extract exerted antioxidant activities, along with favorable anti-inflammatory and antiaging properties.

In line with available data reporting that plant polyphenols have anti-inflammatory effects via NF-kB-dependent mechanisms (i.e., by downregulating the NF-kB inflammatory cascade), at a molecular level, PSF extract exerts protective (anti-inflammatory) effects on HUVEC cells through modulation (i.e., upregulation) of miR-146a expression levels,

along with a consequent downregulation of IRAK-1 and inhibition of production of the proinflammatory cytokine IL-6.

Noteworthy, HUVEC cells senescence, besides high levels of β-galactosidase and low levels of telomerase expression, is associated with a SASP mainly characterized by high levels of IL-6 expression [4]. Moreover, aging-associated miRNAs are largely negative regulators of the immune innate response and target central nodes of aging-associated networks. In particular, miR-146a exerts its negative regulatory action on NF-κB, the downstream effector of TLR signals that leads to the induction of proinflammatory responses. While miR-146a expression levels in studies of cellular senescence are controversial [3,4] and interpreting such a controversy is beyond the scope of this study, it is very likely that high quantities of miR-146a reported in senescent cells might be explained by hypothesizing that miR-146a is also involved in alternative mechanisms.

C. elegans is a powerful model organism largely employed for aging studies. In this work, we identified PSF as a new polyphenolic compound with potent antioxidant and antiaging properties, two parameters that often strongly correlate in longevity studies. The in vivo beneficial effects of this dietary polyphenolic compound open the door for future studies aiming at addressing the impact on other important age-associated features and on the molecular mechanisms underlying its beneficial effects. To this extent, it is worth noting that besides their antioxidant activity, many substances, including polyphenols, exert their prolongevity effect through induction of autophagy, a key recycling process, which helps dampening damaged or old intracellular components [20,43]. While we have not tested this possibility yet, here we show that PSF may modify gene expression epigenetically by microRNAs modulation and, interestingly, miRNAs have been shown to modulate autophagy in different species, including *C. elegans* [44]. Specifically, we found that PSF modulated the expression of two important markers associated with aging and oxidative stress in *C. elegans*, i.e., miR-124 (upregulated) and miR-39 (downregulated), thus suggesting an interesting mode of action through which these dietary polyphenols could modulate aging and associated features [32,34].

Noteworthy, besides the antioxidant property, the activity of PSF polyphenolics in regulation of mechanisms that decrease the inflammation cascade resulted to promote wound healing (a complex molecular and cellular process made of several overlapping phases including inflammation) through cell migration, thus confirming our initial work hypothesis, which considered PSF as a good candidate for wound care and tissue regeneration. In particular, our results demonstrated that PSF extract enhanced endothelial wound closure (up to 70%) and cell migration, which are important properties of endothelial cells in order to be resilient to tissue injury [45]. Intriguingly, one unforeseen outcome was the high percentage of wound closure observed not only in young cells but also in older ones. Indeed, the results were almost overlapping in all cells, albeit with some small differences depending on the concentration of the extract. Moreover, in wound healing cells, expression levels of inflammation-associated biomarkers (miR-146a, IL-6, and IRAK-1) confirmed PSF anti-inflammaging ability, which, combined to its antioxidant capacity, is at the basis of the improved wound healing efficacy observed after PSF treatment. However, results observed in IL-6 and IRAK-1 expression levels may appear, in part, unexpected. In fact, as shown in the results section (Figure 5B-C), IL-6 and IRAK-1 were downregulated not only by PSF extract but also by EtOH alone (the vehicle). Given the proinflammatory effect of EtOH, one would have expected exactly the opposite (i.e., high levels of IL-6 and IRAK-1). However, considering that this apparent "anomaly" occurred only in PCR reactions performed on (messenger or micro) RNA extracted from HUVEC cells, a possible explanation is that it is a technical bias (i.e., in the case of real time PCR, ethanol acts as a reverse transcriptase inhibitor). This would be indirectly confirmed by the fact that no anomalies were noted in the experiments carried out directly on whole cells (treated with non-toxic EtOH concentrations). Finally, the fact that molecular amplifications on *C. elegans* did not show any bias could be due to the fact that in vivo the penetration of EtOH into the living tissues is considerably lower than that which occurs in an in vitro system, thus reducing

the risk of PCR inhibition. On the whole, although at present data are still preliminary and further investigation on this item will be necessarily needed, our findings suggest that *Prunus* extract can be considered among the products that, at appropriate doses, could be useful to prevent endothelial dysfunction, which is one of the major contributors to the development and progression of atherosclerosis and other cardiovascular (CVD) or neurodegenerative (i.e., Alzheimer's or Parkinson's) diseases.

When examining senescence of HUVECs treated with *Prunus* extract at different concentrations during 160 days (P2-P15), contrary to other reports [46], PSF extract did not delay the onset of the aging phenotype shown by senescence-associated β-galactosidase (SA-β-gal), but, rather, appeared to have an important "qualitative" effect on cell differentiation. In fact, P15 cells grown in a culture medium supplemented with PSF at 40 or 80 μg/mL showed (compared to the controls) a different phenotype characterized by long cells with multiple protrusions connecting neighboring cell clusters, revealing an unexpected differentiation capacity. Although this finding was certainly stimulating, the great difficulty of attending the laboratory with diligence, owing to the closure of the university facilities due to the COVID-19 emergency, created considerable problems in carrying out the first experimental test (which took 160 days) and made it absolutely impossible to repeat the entire experiment in triplicate. Unfortunately, the current situation is still very unstable and therefore we cannot provide more in-depth data at the moment. However, even if we are aware that this data could be omitted, the result itself appears so interesting that it convinced us to communicate it anyway, albeit in a preliminary way.

If confirmed, this outcome could be interpreted as related to the positive effect of polyphenols on microvascularization by enhancing cell migration [45]. Moreover, such an effect could be miR146a–mediated. In fact, it has been demonstrated that miR-146a upregulation promotes angiogenesis by inducing FGFBP1/FGF2 chemokine signaling events that are involved in the promotion of HUVEC proliferation, tube formation, and migration [45]. Furthermore, we suggest that the antioxidant and anti-inflammatory effects of PSF extract may allow older cells to behave as if they were younger, coping with the proinflammatory phenotype associated to cellular senescence. Indeed, although the cells treated with the extract age at the same speed as the controls, they behave, act, and react as if they were (biologically) younger. Therefore, it is as if the extract, while not changing the chronological age of the cells, can somehow act on their biological age by setting the functional clock back, probably due to the anti-inflammatory effect. This idea is also corroborated by the results obtained in the analysis of miR-146a, IL-6, and IRAK-1 expression levels in older cells (P15), which are much less inflamed than controls (i.e., levels of miR-146a are significantly higher and those of IL-6 and IRAK-1 lower). Briefly, CTRL and PSF-treated cells having the same chronological age end up not having the same biological age.

Biological aging (i.e., that aging occurs as you gradually accumulate damage to various cells and tissues in the body) is quite different from chronological age (the amount of time that has passed from your birth to the given date). Additionally, known as physiological or functional age, biological age differs from chronological age because it takes into consideration a number of factors other than just the day you were born. Chronological age will always be an easy-to-determine number, while biological age depends on a number of variables that can change on a continuing basis. Environmental factors may affect aging, thus making biological aging and chronological aging quite distinct concepts. Although more studies need to be done on factors for determining biological age, it has been suggested that there is a clear link between nutrition and biological age; therefore, being actively aware of what constitutes a healthy diet may help to improve biological age [47]. Speaking of which, we believe that PSF extract might be suggested in a healthy diet for healthy consumers (Figure 8).

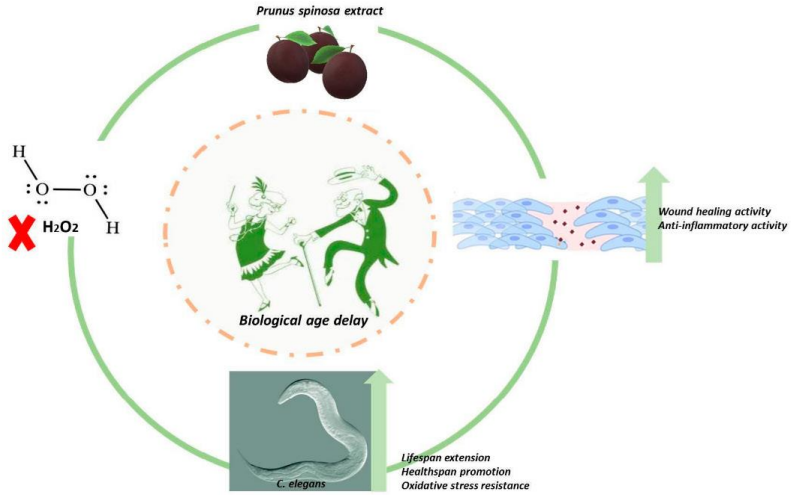

Figure 8. PSF extract delays biological age by acting as an antioxidant and anti-inflammatory agent. Beneficial effects promote in vitro endothelial cell functions (wound healing) and in vivo lifespan/healthspan of *C. elegans*.

In our study, PSF extract (abundant in polyphenolics) acted as an antioxidant and anti-inflammatory agent in vitro and in vivo, showing also a beneficial effect on lifespan and healthspan of *C. elegans*; moreover, PSF treatment enhanced the cellular response to wound healing, suggesting a potential activity of polyphenols to promote endothelial cell functions. In this regard, it would be very interesting to verify in a future study the hypothesis that PSF treatment may result in a significant modification of capillary-like tube formation (angiogenesis) by inducing important molecular markers responsible for the microcirculation and (maybe) vasodilation of endothelial cells, thus showing meaningful benefits on microvascular activities. To test the ability of the PSF polyphenols to affect microcirculation and vasodilation in endothelial cells, many experiments need to be carried out including: gene expression analyses of the vascular endothelial growth factor (VEGF, well known for its role in angiogenesis and wound repair), the endothelin 1 (ET-1), the endothelial nitric oxide synthase (eNOS), and the miR-146a-CREB3L1-FGFBP1 signaling axis. In the event that such a conjecture is confirmed, it would be possible to affirm that a dietary supplementation with foods containing PSF extract, properly prepared, could be an inexpensive, non-pharmacological approach for improving cardiovascular health not only in currently healthy individuals but also in populations with microvascular dysfunction.

5. Conclusions

Present findings provide further support to the view that plant polyphenols may affect inflammation and associated disorders not only as antioxidants but also as modulators of inflammatory redox signaling pathways with a positive effect on wound healing. In particular, our results suggest that, at a proper dilution, *Prunus spinosa* may have health benefits and could be a potential dietary supplement and alternative medicine with antioxidant, antiaging, and wound healing properties to be included in those lifestyle interventions useful in the treatment of acute inflammation and senescence associated diseases and/or tissue repair and regeneration. However, although our results might be of interest to prevent and/or treat aging-associated disorders and might suggest a way to improve the quality of life, further in-depth mechanistic and translational studies with other organisms, including humans, are needed to support these beneficial effects and to determine the clinical relevance.

Author Contributions: S.C., M.C., N.V. and M.C.A. conceptualized, designed the experiments and wrote the manuscript; D.F. provided the research materials; S.C., D.F., V.B., M.R., B.D.G., M.M. and L.G. performed the experiments; M.B.L.R. analyzed the data; M.C., S.R., N.V. and M.C.A. validated the data and edited the manuscript. All authors have read and agreed to the published version of the manuscript.

Funding: This research was funded by the University of Urbino Carlo Bo, Urbino (PU), Italy (grant number DISB_Progetti_valorizzazione_2018) and by German Research Foundation DFG (grant number VE633/8-1).

Institutional Review Board Statement: Not applicable.

Informed Consent Statement: Not applicable.

Data Availability Statement: Not applicable.

Acknowledgments: This work has been supported by DISB_Progetti_valorizzazione_2018, University of Urbino Carlo Bo, Urbino (PU), Italy. Natascia Ventura would like to acknowledge the German Research Foundation (DFG grant VE633/8-1).

Conflicts of Interest: The authors declare no conflict of interest.

References

1. Tiboni, M.; Coppari, S.; Casettari, L.; Guescini, M.; Colomba, M.; Fraternale, D.; Gorassini, A.; Verardo, G.; Ramakrishna, S.; Guidi, L.; et al. *Prunus spinosa* Extract Loaded in Biomimetic Nanoparticles Evokes In Vitro Anti-Inflammatory and Wound Healing Activities. *Nanomaterials* **2020**, *11*, 36. [CrossRef]
2. Franceschi, C.; Bonafè, M.; Valensin, S.; Olivieri, F.; De Luca, M.; Ottaviani, E.; De Benedictis, G. Inflamm-aging. An evolutionary perspective on immunosenescence. *Ann. N. Y. Acad. Sci.* **2000**, *908*, 244–254. [CrossRef] [PubMed]
3. Vasa-Nicotera, M.; Chen, H.; Tucci, P.; Yang, A.L.; Saintigny, G.; Menghini, R.; Mahè, C.; Agostini, M.; Knight, R.A.; Melino, G.; et al. MiR-146a is modulated in human endothelial cell with aging. *Atherosclerosis* **2011**, *217*, 326–330. [CrossRef]
4. Olivieri, F.; Lazzarini, R.; Recchioni, R.; Marcheselli, F.; Rippo, M.R.; Di Nuzzo, S.; Albertini, M.C.; Graciotti, L.; Babini, L.; Mariotti, S.; et al. MiR-146a as marker of senescence-associated pro-inflammatory status in cells involved in vascular remodelling. *Age (Omaha)* **2013**, *35*, 1157–1172. [CrossRef] [PubMed]
5. Nour, V.; Trandafir, I.; Cosmulescu, S. Bioactive compounds, antioxidant activity and nutritional quality of different culinary aromatic herbs. *Not. Bot. Horti Agrobot. Cluj-Napoca* **2017**, *45*, 179–184. [CrossRef]
6. Fraternale, D.; Giamperi, L.; Bucchini, A.; Sestili, P.; Paolillo, M.; Ricci, D. *Prunus spinosa* fresh fruit juice: Antioxidant activity in cell-free and cellular systems. *Nat. Prod. Commun.* **2009**, *4*, 1665–1670. [CrossRef] [PubMed]
7. Ganhão, R.; Estévez, M.; Kylli, P.; Heinonen, M.; Morcuende, D. Characterization of selected wild mediterranean fruits and comparative efficacy as inhibitors of oxidative reactions in emulsified raw pork burger patties. *J. Agric. Food Chem.* **2010**, *58*, 8854–8861. [CrossRef]
8. Radovanović, B.C.; Andelković, A.S.M.; Radovanović, A.B.; Andelković, M.Z. Antioxidant and antimicrobial activity of polyphenol extracts from wild berry fruits grown in Southeast Serbia. *Trop. J. Pharm. Res.* **2013**, *12*, 813–819. [CrossRef]
9. Karabegović, I.T.; Stojičević, S.S.; Veličković, D.T.; Todorović, Z.B.; Nikolić, N.Č.; Lazić, M.L. The effect of different extraction techniques on the composition and antioxidant activity of cherry laurel (Prunus laurocerasus) leaf and fruit extracts. *Ind. Crops Prod.* **2014**, *54*, 142–148. [CrossRef]
10. Veličković, J.M.; Kostić, D.A.; Stojanović, G.S.; Mitić, S.S.; Mitić, M.N.; Ranđelović, S.S.; Đorđević, A.S. Phenolic composition, antioxidant and antimicrobial activity of the extracts from *Prunus spinosa* L. fruit. *Hem. Ind.* **2014**, *68*, 297–303. [CrossRef]
11. Walraven, M.; Hinz, B. Therapeutic approaches to control tissue repair and fibrosis: Extracellular matrix as a game changer. *Matrix Biol.* **2018**, *71–72*, 205–224. [CrossRef]
12. Albertini, M.C.; Fraternale, D.; Semprucci, F.; Cecchini, S.; Colomba, M.; Rocchi, M.B.L.; Sisti, D.; Di Giacomo, B.; Mari, M.; Sabatini, L.; et al. Bioeffects of *Prunus spinosa* L. Fruit ethanol extract on reproduction and phenotypic plasticity of Trichoplax adhaerens Schulze, 1883 (Placozoa). *PeerJ* **2019**, *7*. [CrossRef]
13. Sabatini, L.; Fraternale, D.; Di Giacomo, B.; Mari, M.; Albertini, M.C.; Gordillo, B.; Rocchi, M.B.L.; Sisti, D.; Coppari, S.; Semprucci, F.; et al. Chemical composition, antioxidant, antimicrobial and anti-inflammatory activity of *Prunus spinosa* L. fruit ethanol extract. *J. Funct. Foods* **2020**, *67*, 103885. [CrossRef]
14. Neveu, V.; Perez-Jiménez, J.; Vos, F.; Crespy, V.; du Chaffaut, L.; Mennen, L.; Knox, C.; Eisner, R.; Cruz, J.; Wishart, D.; et al. Phenol-Explorer: An online comprehensive database on polyphenol contents in foods. *Database (Oxford)* **2010**, *2010*. [CrossRef] [PubMed]
15. Prattichizzo, F.; Giuliani, A.; Recchioni, R.; Bonafè, M.; Marcheselli, F.; De Carolis, S.; Campanati, A.; Giuliodori, K.; Rippo, M.R.; Brugè, F.; et al. Anti-TNF-α treatment modulates SASP and SASP-related microRNAs in endothelial cells and in circulating angiogenic cells. *Oncotarget* **2016**, *7*, 11945–11958. [CrossRef] [PubMed]

16. Angel-Morales, G.; Noratto, G.; Mertens-Talcott, S.U. Standardized curcuminoid extract (*Curcuma longa* L.) decreases gene expression related to inflammation and interacts with associated microRNAs in human umbilical vein endothelial cells (HUVEC). *Food Funct.* **2012**, *3*, 1286–1293. [CrossRef] [PubMed]
17. Fraternale, D.; Giamperi, L.; Bucchini, A.; Ricci, D.; Epifano, F.; Burini, G.; Curini, M. Chemical Composition, Antifungal and In Vitro Antioxidant Properties of Monarda didyma L. Essential Oil. *J. Essent. Oil Res. J. Essent. Oil Res* **2006**, *18*, 581–585. [CrossRef]
18. Kamath, R.S.; Ahringer, J. Genome-wide RNAi screening in Caenorhabditis elegans. *Methods* **2003**, *30*, 313–321. [CrossRef]
19. Han, S.K.; Lee, D.; Lee, H.; Kim, D.; Son, H.G.; Yang, J.S.; Lee, S.J.V.; Kim, S. OASIS 2: Online application for survival analysis 2 with features for the analysis of maximal lifespan and healthspan in aging research. *Oncotarget* **2016**, *7*, 56147–56152. [CrossRef] [PubMed]
20. Schiavi, A.; Maglioni, S.; Palikaras, K.; Shaik, A.; Strappazzon, F.; Brinkmann, V.; Torgovnick, A.; Castelein, N.; De Henau, S.; Braeckman, B.P.; et al. Iron-Starvation-Induced Mitophagy Mediates Lifespan Extension upon Mitochondrial Stress in C. elegans. *Curr. Biol.* **2015**, *25*, 1810–1822. [CrossRef]
21. Shaham, S. Methods in cell biology. *WormBook* **2006**. [CrossRef]
22. Diomede, L.; Romeo, M.; Rognoni, P.; Beeg, M.; Foray, C.; Ghibaudi, E.; Palladini, G.; Cherny, R.A.; Verga, L.; Capello, G.L.; et al. Cardiac Light Chain Amyloidosis: The Role of Metal Ions in Oxidative Stress and Mitochondrial Damage. *Antioxid. Redox Signal.* **2017**, *27*, 567–582. [CrossRef]
23. Diomede, L.; Rognoni, P.; Lavatelli, F.; Romeo, M.; Del Favero, E.; Cantù, L.; Ghibaudi, E.; Di Fonzo, A.; Corbelli, A.; Fiordaliso, F.; et al. A Caenorhabditis elegans-based assay recognizes immunoglobulin light chains causing heart amyloidosis. *Blood* **2014**, *123*, 3543–3552. [CrossRef] [PubMed]
24. Diomede, L.; Soria, C.; Romeo, M.; Giorgetti, S.; Marchese, L.; Mangione, P.P.; Porcari, R.; Zorzoli, I.; Salmona, M.; Bellotti, V.; et al. *C. elegans* Expressing Human β2-Microglobulin: A Novel Model for Studying the Relationship between the Molecular Assembly and the Toxic Phenotype. *PLoS ONE* **2012**, *7*, e52314. [CrossRef]
25. Deineka, V.I.; Deineka, L.A.; Sirotin, A.A. Anthocyans from fruit of certain plants of the genus Prunus. *Chem. Nat. Compd.* **2005**, *41*, 230–231. [CrossRef]
26. Ruiz, A.; Hermosín-Gutiérrez, I.; Vergara, C.; von Baer, D.; Zapata, M.; Hitschfeld, A.; Obando, L.; Mardones, C. Anthocyanin profiles in south Patagonian wild berries by HPLC-DAD-ESI-MS/MS. *Food Res. Int.* **2013**, *51*, 706–713. [CrossRef]
27. Wu, X.; Prior, R.L. Systematic identification and characterization of anthocyanins by HPLC-ESI-MS/MS in common foods in the United States: Fruits and berries. *J. Agric. Food Chem.* **2005**, *53*, 2589–2599. [CrossRef]
28. Zhuang, B.; Bi, Z.M.; Wang, Z.Y.; Duan, L.; Lai, C.J.S.; Liu, E.H. Chemical profiling and quantitation of bioactive compounds in Platycladi Cacumen by UPLC-Q-TOF-MS/MS and UPLC-DAD. *J. Pharm. Biomed. Anal.* **2018**, *154*, 207–215. [CrossRef] [PubMed]
29. Torgovnick, A.; Schiavi, A.; Maglioni, S.; Ventura, N. Gesundes Altern: Was können wir von Caenorhabditis elegans lernen? *Z. Gerontol. Geriatr.* **2013**, *46*, 623–628. [CrossRef]
30. Maglioni, S.; Arsalan, N.; Ventura, N. *C. elegans* screening strategies to identify pro-longevity interventions. *Mech. Ageing Dev.* **2016**, *157*, 60–69. [CrossRef] [PubMed]
31. Wilson, M.A.; Shukitt-Hale, B.; Kalt, W.; Ingram, D.K.; Joseph, J.A.; Wolkow, C.A. Blueberry polyphenols increase lifespan and thermotolerance in Caenorhabditis elegans. *Aging Cell* **2006**, *5*, 59–68. [CrossRef]
32. Wang, N.; Liu, J.; Xie, F.; Gao, X.; Ye, J.H.; Sun, L.Y.; Wei, R.; Ai, J. miR-124/ATF-6, a novel lifespan extension pathway of Astragalus polysaccharide in Caenorhabditis elegans. *J. Cell. Biochem.* **2015**, *116*, 242–251. [CrossRef]
33. Dallaire, A.; Garand, C.; Paquet, E.R.; Mitchell, S.J.; de Cabo, R.D.; Simard, M.J.; Lebel, M. Down regulation of miR-124 in both Werner syndrome DNA helicase mutant mice and mutant Caenorhabditis elegans wrn-1 reveals the importance of this microRNA in accelerated aging. *Aging (Albany NY)* **2012**, *4*, 636–647. [CrossRef]
34. Qu, M.; Luo, L.; Yang, Y.; Kong, Y.; Wang, D. Nanopolystyrene-induced microRNAs response in Caenorhabditis elegans after long-term and lose-dose exposure. *Sci. Total Environ.* **2019**, *697*, 134131. [CrossRef] [PubMed]
35. Hayflick, L. The limited in vitro lifetime of human diploid cell strains. *Exp. Cell Res.* **1965**, *37*, 614–636. [CrossRef]
36. Campisi, J. Cellular senescence as a tumor-suppressor mechanism. *Trends Cell Biol.* **2001**, *11*, S27–S31. [CrossRef]
37. Demaria, M.; Ohtani, N.; Youssef, S.A.; Rodier, F.; Toussaint, W.; Mitchell, J.R.; Laberge, R.M.; Vijg, J.; VanSteeg, H.; Dollé, M.E.T.; et al. An essential role for senescent cells in optimal wound healing through secretion of PDGF-AA. *Dev. Cell* **2014**, *31*, 722–733. [CrossRef]
38. Storer, M.; Mas, A.; Robert-Moreno, A.; Pecoraro, M.; Ortells, M.C.; Di Giacomo, V.; Yosef, R.; Pilpel, N.; Krizhanovsky, V.; Sharpe, J.; et al. Senescence is a developmental mechanism that contributes to embryonic growth and patterning. *Cell* **2013**, *155*, 1119. [CrossRef]
39. Boccardi, V.; Pelini, L.; Ercolani, S.; Ruggiero, C.; Mecocci, P. From cellular senescence to Alzheimer's disease: The role of telomere shortening. *Ageing Res. Rev.* **2015**, *22*, 1–8. [CrossRef] [PubMed]
40. Chinta, S.J.; Lieu, C.A.; DeMaria, M.; Laberge, R.-M.; Campisi, J.; Andersen, J.K. Environmental stress, ageing and glial cell senescence: A novel mechanistic link to Parkinson's disease? *J. Intern. Med.* **2013**, *273*, 429–436. [CrossRef] [PubMed]
41. Kostyuk, V.A.; Potapovich, A.I.; Suhan, T.O.; De Luca, C.; Korkina, L.G. Antioxidant and signal modulation properties of plant polyphenols in controlling vascular inflammation. *Eur. J. Pharmacol.* **2011**, *658*, 248–256. [CrossRef]
42. Benavente-García, O.; Castillo, J. Update on uses and properties of citrus flavonoids: New findings in anticancer, cardiovascular, and anti-inflammatory activity. *J. Agric. Food Chem.* **2008**, *56*, 6185–6205. [CrossRef] [PubMed]

43. Carmona-Gutierrez, D.; Zimmermann, A.; Kainz, K.; Pietrocola, F.; Chen, G.; Maglioni, S.; Schiavi, A.; Nah, J.; Mertel, S.; Beuschel, C.B.; et al. The flavonoid 4,4′-dimethoxychalcone promotes autophagy-dependent longevity across species. *Nat. Commun.* **2019**, *10*. [CrossRef] [PubMed]
44. Voinnet, O. MicroRNA and autophagy - C. elegans joins the crew. *EMBO Rep.* **2013**, *14*, 485–487. [CrossRef] [PubMed]
45. Zhu, H.-Y.; Bai, W.-D.; Liu, J.-Q.; Zheng, Z.; Guan, H.; Zhou, Q.; Su, L.-L.; Xie, S.-T.; Wang, Y.-C.; Li, J.; et al. Up-regulation of FGFBP1 signaling contributes to miR-146a-induced angiogenesis in human umbilical vein endothelial cells. *Sci. Rep.* **2016**. [CrossRef]
46. Buachan, P.; Chularojmontri, L.; Wattanapitayakul, S. Selected activities of Citrus maxima merr. fruits on human endothelial cells: Enhancing cell migration and delaying cellular aging. *Nutrients* **2014**, *6*, 1618–1634. [CrossRef] [PubMed]
47. Han, K.T.; Kim, D.W.; Kim, S.J.; Kim, S.J. Biological age is associated with the active use of nutrition data. *Int. J. Environ. Res. Public Health* **2018**, *15*, 2431. [CrossRef]

6. CURCUMIN, POLYDATIN AND QUERCETIN SYNERGISTIC ACTIVITY PROTECTS FROM HIGH-GLUCOSE-INDUCED INFLAMMATION AND OXIDATIVE STRESS

Age-Associated Diseases, characterized by a SASP pro-inflammatory phenotype, also concerns type 2 Diabetes Mellitus since it is associated with a chronic hyperglycemic state that promotes cellular senescence. The production of inflammatory markers (MCP-1, IL-1β and IL-8) and reactive oxygen species were evaluated in young and senescent HUVECs subjected to a high glucose environment to mimic the hyperglycemic state. Natural bioactive compounds, such as polydatin, curcumin and quercetin, demonstrated a protection on hyperglycemia inflammation and oxidative stress.

Original article published in:

Antioxidants. Volume 11(6), May2022, 1037 (doi.org/10.3390/antiox11061037).

antioxidants

Article

Curcumin, Polydatin and Quercetin Synergistic Activity Protects from High-Glucose-Induced Inflammation and Oxidative Stress

Giulia Matacchione [1,*], Debora Valli [1], Andrea Silvestrini [1], Angelica Giuliani [1], Jacopo Sabbatinelli [1], Chiara Giordani [1], Sofia Coppari [2], Maria Rita Rippo [1], Maria Cristina Albertini [2,†] and Fabiola Olivieri [1,3,†]

[1] Department of Clinical and Molecular Sciences, DISCLIMO, Università Politecnica Delle Marche, 60126 Ancona, Italy; debora.valli@libero.it (D.V.); a.silvestrini@pm.univpm.it (A.S.); angelica.giuliani@staff.univpm.it (A.G.); j.sabbatinelli@staff.univpm.it (J.S.); c.giordani@pm.univpm.it (C.G.); m.r.rippo@staff.univpm.it (M.R.R.); f.olivieri@staff.univpm.it (F.O.)
[2] Department of Biomolecular Sciences, University of Urbino Carlo Bo, 61029 Urbino, Italy; s.coppari3@campus.uniurb.it (S.C.); maria.albertini@uniurb.it (M.C.A.)
[3] Center of Clinical Pathology and Innovative Therapy, IRCCS INRCA, 60127 Ancona, Italy
* Correspondence: g.matacchione@pm.univpm.it; Tel.: +39-071-220-6243
† These authors contributed equally to this work.

Abstract: Chronic hyperglycemia, the diagnostic biomarker of Type 2 Diabetes Mellitus (T2DM), is a condition that fosters oxidative stress and proinflammatory signals, both involved in the promotion of cellular senescence. Senescent cells acquire a proinflammatory secretory phenotype, called SASP, exacerbating and perpetuating the detrimental effects of hyperglycemia. Bioactive compounds can exert antioxidant and anti-inflammatory properties. However, the synergistic anti-inflammatory and antioxidant effects of the most extensively investigated natural compounds have not been confirmed yet in senescent cells and in hyperglycemic conditions. Here, we exposed young and replicative senescent HUVEC (yHUVEC and sHUVEC) to a high-glucose (HG) condition (45 mM) and treated them with Polydatin (POL), Curcumin (CUR) and Quercetin (QRC), alone or in combination (MIX), to mirror the anti-inflammatory component OxiDef^{TM} contained in the novel nutraceutical Glicefen^{TM} (Mivell, Italy). In both yHUVEC and sHUVEC, the MIX significantly decreased the expression levels of inflammatory markers, such as MCP-1, IL-1β and IL-8, and ROS production. Importantly, in sHUVEC, a synergistic effect of the MIX was observed, suggesting its senomorphic activity. Moreover, the MIX was able to reduce the expression level of RAGE, a receptor involved in the activation of proinflammatory signaling. Overall, our data suggest that the consumption of nutraceuticals containing different natural compounds could be an adjuvant supplement to counteract proinflammatory and pro-oxidative signals induced by both hyperglycemic and senescence conditions.

Keywords: hyperglycemia; natural compounds; T2DM; aging; oxidative stress

Citation: Matacchione, G.; Valli, D.; Silvestrini, A.; Giuliani, A.; Sabbatinelli, J.; Giordani, C.; Coppari, S.; Rippo, M.R.; Albertini, M.C.; Olivieri, F. Curcumin, Polydatin and Quercetin Synergistic Activity Protects from High-Glucose-Induced Inflammation and Oxidative Stress. *Antioxidants* **2022**, *11*, 1037. https://doi.org/10.3390/antiox11061037

Academic Editor: Stanley Omaye

Received: 28 April 2022
Accepted: 19 May 2022
Published: 24 May 2022

1. Introduction

Chronic hyperglycemia, the diagnostic biomarker for Type 2 Diabetes Mellitus (T2DM), can foster a chronic low-grade proinflammatory status named inflammaging [1,2], nowadays recognized as the main risk factor for the development of the most common age-related diseases (ARDs) [3].

Aging is among the most effective risk factor of T2DM [4], as advanced age leads to the exacerbation of the inflammaging, promoted by the accumulation of senescent cells (SCs).

Cellular senescence is a process in which cells terminate to proliferate and acquire distinctive phenotypic and metabolic alterations, named senescence-associated secretory phenotype (SASP), with pro-inflammatory activity [5]. Indeed, in the last decade, the accumulation of SCs was identified in different tissues of T2DM patients and mouse models [6,7].

Though the main pathways involved in the proinflammatory activity of hyperglycemia were extensively investigated, the molecular mechanisms underpinning this activation are currently under investigation. A high glucose level can stimulate the production of reactive oxygen (ROS) and nitrogen species [8]. Hyperglycemia is also related to an increased production of advanced glycation end products (AGE), derived by non-enzymatic protein glycation, as observed in the serum/plasma of patients affected by T2DM [9]. AGEs can stimulate immune and non-immune cells, i.e., endothelial cells, to release a plethora of pro-inflammatory cytokines, through their binding to the cellular isoform of AGE receptor (RAGE). Human endothelial cells can be stimulated by AGEs and ROS, which activate NF-kB transcription factor and increase the synthesis and releases of inflammatory mediators such as tumor necrosis factor-alpha (TNF-α), interleukin-1β (IL-1β) and chemokines, such as monocyte/macrophage chemotactic protein-1 (MCP-1) and interleukin-8 (IL-8) [10]. Several studies have reported that a hyperglycemic condition markedly stimulate monocyte adhesion, vascular permeability, ROS formation and NF-kB activation in human endothelial cells [11–15]. Hyperglycemia is therefore considered an important causative factor in the development of micro- and macrovascular complications in patients affected by T2DM [4,16].

Among the compounds playing antioxidant and anti-inflammatory activities, polyphenols are the most extensively investigated both in animal models and in human clinical trials [17–19]. Clinical and epidemiological evidence strongly suggests that diets rich in polyphenols can reduce the risk of development of several age-related chronic diseases [20]. In this framework, the number of studies related to the usefulness of consuming compounds derived from natural sources has increased, with the purpose to create differentiated products with high added value. Here, we investigated the properties of three of the most extensively investigated natural compounds, i.e., Curcumin (CUR), Polydatin (POL) and Quercetin (QRC), alone and in combination (MIX), to mirror the anti-inflammatory component, named OxiDef^{TM}, of the novel nutraceutical Glicefen^{TM} (Mivell, Italy).

Curcumin, a yellow-orange lipophilic compound from *Curcuma longa*, and Polydatin, a precursor of Resveratrol, are recognized powerful modulators of inflammation [21,22]. Clinical trials and in vitro studies have reported the role of Curcumin in reducing the pro-inflammatory status occurring in T2DM patients and its complications [23,24]. Polydatin exhibits many biological functions, among which the inhibition of adipose tissue inflammation in high-fat-fed mice [25] and the improvement of diabetic conditions in streptozotocin-induced diabetic rats [26,27] as well as of DSS-induced colitis in mice [28].

Quercetin is a very promising bioactive compound, with anti-inflammatory and antioxidant effects in high-glucose-treated endothelial and mesangial cells [29–31], with anti-senescence effects [32] and with pro-health effects in animal models [33,34].

However, although each of these phytochemicals has been deeply studied alone, their synergistic anti-inflammatory activity has not been extensively investigated, in particular in human endothelial cells in conditions of senescence and hyperglycemia, about which no studies have been published [35,36]. In this study, we aimed to evaluate a possible synergistic activity of Curcumin, Polydatin and Quercetin bioactive compounds, by testing their anti-inflammatory and antioxidant activities in high-glucose-treated young and senescent human endothelial cells (HUVECs).

2. Materials and Methods

2.1. HUVEC

Human umbilical vein endothelial cells (HUVEC) are primary pooled cells that were obtained from Clonetics (Lonza, Switzerland). HUVEC were cultured in endothelial growth medium (EGM-2, Lonza, Switzerland), composed of endothelial basal medium (EBM-2, Lonza, Switzerland) and the SingleQuot Bullet Kit (Lonza, Switzerland). The cells were seeded at a density of 5000/cm^2 in T75 flasks (Corning Costar, Sigma Aldrich, St. Louis, MO, USA).

2.2. Characterization of Young and Senescent HUVEC Cells

Replicative senescence (RS) was reached by subsequent replicative passages (measured as cumulative population doubling, cPD). cPD was calculated as the sum of PD changes, calculated by the formula: $(\log_{10}(F) - \log_{10}(I))/\log_{10}$ [2], where F is the number of cells at the end of a passage, and I is the number of seeded cells. HUVECs were classified as young or senescent based on cPD, senescence-associated (SA)-β-Galactosidase activity and $p16^{ink4a}$ expression. SA-β-Gal activity was detected by using a Senescence Detection Kit (BioVision Inc., Milpitas, CA, USA), following the manufacturer's instructions.

2.3. Cell Viability Assay

We tested cell viability by using the MTT (3-(4,5-dimethylthiazol-2-yl)-2,5-diphenyltetrazolium bromide) assay. The cells were grown for 24 h and 72 h in 24-well plates at a density of 5000 cells/cm^2 before treatments with different doses of the natural compounds as well as in high glucose conditions (25–35–45 mM). Briefly, the MTT (1 mg/mL) solution was added, and the cells were incubated for 4 h; the obtained product, a formazan salt, was solubilized in dimethyl sulfoxide (DMSO) and measured by a microplate reader (MPT Reader, Invitrogen, Milano, Italy) at the optical density of 540 nm.

Cell viability was calculated according to the equation $(T/C) \times 100\%$, where T and C represent the mean optical density of the treated group and of the control group, respectively.

2.4. High-Glucose Treatments

To achieve hyperglycemic conditions (HG), HUVEC were treated with D-Glucose for 24 and 72 h. Three different concentrations (25 mM, 35 mM and 45 mM) were tested. HUVECs were grown in EGM-2 medium (D-Glucose 5 mM) as a control (NG).

2.5. Natural Compound Treatments

Curcumin (218580100) was purchased from Acros organic. Polydatin (P1878) and Quercetin (P0042) were purchased from TCI. All compounds were dissolved in DMSO at a 0.1% final concentration of DMSO in all the solutions. Based on the results of the viability assay, the cells were treated with 1 μM Curcumin, 10 μM Polydatin and 0.5 μM Quercetin, alone or in combination (MIX, 1 μM Curcumin, 10 μM Polydatin and 0.5 μM Quercetin). The MIX resembles the anti-inflammatory component OxiDef™ of the nutraceutical Glicefen™ (patent number:102021000032909). The treatments with the single compounds and the MIX consisted in a 2 h pretreatment, followed by a 24 h treatment for young HUVEC in HG conditions and a 72 h treatment for senescent HUVEC in HG conditions. The synergistic effect was calculated by measuring the anti-inflammatory effect (to be intended as a reduction of the expression of markers of inflammation with respect to their expression in inflamed HUVEC) of each single compound and of the MIX. We considered the MIX as synergistic if the effect of the MIX was greater than the sum of the effects of each compound acting separately.

2.6. RNA Isolation, mRNA and Mature miRNAs Expression by RT-qPCR

Total RNA was isolated by using the Norgen Biotek Kit (Thorold, ON, Canada), according to the manufacturer's instructions and stored at −80 °C until use. mRNA and miRNA expression was determined as previously described [37]. RT-qPCR analysis were standardized with RNU48 for miRNA expression and with GAPDH and β-actin for mRNA expression.

2.7. Western Blot Analysis

RIPA buffer (0.1% SDS, 150 mM NaCl, 1.0% Triton X-100, 10 mM Tris, 5 mM EDTA pH 8.0) with a protease and phosphatase inhibitor cocktail (Roche Applied Science, Indianapolis, IN, USA) was used to obtain the cell lysates. The Bradford assay was used to evaluate the protein concentration in each sample. Proteins (25 μg) were analyzed by SDS-PAGE, and then transferred to a nitrocellulose membrane (Bio-Rad, Hercules, CA,

USA). A blocking buffer (Bio-Rad, Hercules, CA, USA) was used to block the membrane that was then incubated overnight with primary antibodies.

Mouse anti-phospho-p38 (Cell Signaling), rabbit anti-phospho-NF-kB (Cell Signaling), mouse anti-PCNA (Cell Signaling) and mouse anti-β-actin (Cell Signaling) were used as primary antibodies.

We used secondary horseradish peroxidase-conjugated antibodies (anti-mouse or anti-rabbit) (The Jackson laboratory, Bar Harbor, ME, USA). A Uvitec Imager (UVItec, Cambridge, UK) was used to visualize the protein bands by using the Clarity ECL chemiluminescence substrate (Bio-Rad) that were then quantified using ImageJ software. Each measure was normalized with respect to β-actin.

2.8. ELISA Assay

Conditioned medium from the cell cultures was collected at the end of each incubation, centrifuged at 14.000 $\times$ RPM for 20 min and stored at -80 °C until use. IL-8 ELISA Kit (Invitrogen, Waltham, MA, USA) was used to measure the concentration of IL-8 released in the medium, according to the manufacturer's instructions.

2.9. DCFDA Assay

The 2′,7′ –dichlorofluorescin diacetate (DCFDA) assay is based on the quantification of 2′, 7′ –dichlorofluorescin (DCF) within cells, which indicates the presence of ROS. DCFDA enters the cells and is deacetylated by cellular esterases to a non-fluorescent compound, which is later oxidized by ROS into DCF. DCF is a highly fluorescent compound with maximum excitation/emission spectra at 495/529 nm. yHUVEC and sHUVEC were seeded in a dark, clear-bottom 96-well plate at 5000 cells/cm^2 in 100 µL of growth medium and allowed to grow for 24 h at 37 °C, 5% CO_2, 95% humidity. The treatments with the single compounds and the MIX consisted in a 2 h pretreatment, followed by a 4 h treatment for young HUVEC in HG conditions and a 48 h treatment for senescent HUVEC in HG conditions. Forty-five minutes prior to the completion of the treatment, 100 µL of 40 µM DCFDA diluted in the same media used for treatment (containing the experimental compounds) was added to each well. Fluorescence intensity was measured at the excitation wavelength of 485 nm and the emission wavelength of 535 nm on a Biotek plate reader.

2.10. Statistical Analysis

Data are shown as mean $\pm$ SD or frequency (%) of three independent biological replicates. Data of RT-qPCR, ELISA and densitometry were analyzed by using the paired sample T test. Data analysis was performed using IBM SPSS Statistics for Windows, version 25 (IBM Corp., Armonk, NY, USA). Statistical significance was defined as a two-tailed p-value < 0.05.

3. Results and Discussion

3.1. High-Glucose Treatment in yHUVEC and sHUVEC Induces Pro-Inflammatory Responses

HUVEC were considered (i) young (yHUVEC) when they were at replicative passage <6, (SA)-β-Gal activity was <20%, and p16^{ink4a} expression was significantly lower compared to its level in senescent HUVEC, (ii) senescent (sHUVEC) when at a replicative passage >15, (SA)-β- < Gal activity was >60%, and p16^{ink4a} expression was significantly higher than its level in yHUVEC (Figure 1A(i–iii)).

yHUVEC and sHUVEC were exposed to different concentrations of glucose (D-Glucose) (25, 35 and 45 mM) to identify potential side effects (decreased cell viability) and proinflammatory stimulation, after 24 and 72 h of treatment.

In all these experimental conditions, cell viability did not decrease under 70% compared to control cells both for yHUVEC and for sHUVEC cells (Figure 1B(i, ii)). When the inflammatory response to different D-Glucose concentrations was tested, pro-inflammatory cytokines (IL-1β and IL-6) and chemokines (MCP-1 and IL-8) were differently modulated in yHUVEC compared to sHUVEC. yHUVEC showed a significant up-regulation of MCP-1,

IL-1β and IL-8 after 24 h of treatment with 45 mM D-Glucose (Figure 1C(i)). The exposure of yHUVEC to all the tested concentrations of D-Glucose was associated with a significant up-regulation of IL-6, but only at 72 h (Figure 1D(i)). When yHUVEC were exposed to 45 mM D-Glucose, MCP-1 was significantly up-regulated at both 24 and 72 h (Figure 1C(i),D(i)).

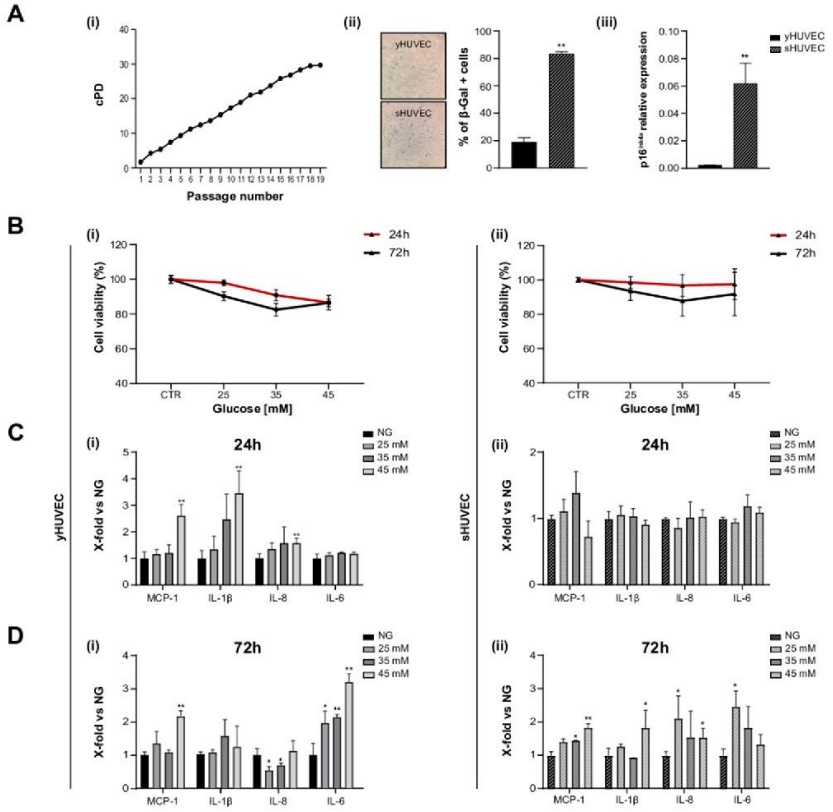

Figure 1. High glucose concentration induced inflammation in yHUVEC and sHUVEC. Characterization of sHUVEC by a cumulative population doubling curve (**i**), β-Gal activity (**ii**) and $p16^{ink4a}$ expression level (**iii**) (**A**). Effect of high-glucose treatments on cell viability. yHUVEC (**i**, left-hand side panel) and sHUVEC (**ii**, right-hand side panel) cells were treated with 25, 35 and 45 mM glucose for 24 and 72 h. Cell viability was determined by the MTT assay (**B**). Relative mRNA expression of MCP-1, IL-1β, IL-8 and IL-6 in yHUVEC (**i**, left-hand side panel) and sHUVEC (**ii**, right-hand side panel) in cells upon treatment with 25, 35 and 45 mM of glucose for 24 h (**C**) and 72 h (**D**). Results are expressed as mean ± SD of three independent biological replicates. Asterisks (*) indicate significance versus NG; * $p < 0.05$, ** $p < 0.01$. NG, normal glucose; HG, high glucose.

sHUVEC, did not show any modulation of the pro-inflammatory markers after 24 h (Figure 1C(ii)), but the levels of MCP-1, IL-1β and IL-8 were significantly increased after 72 h of exposure to 45 mM D-Glucose (Figure 1D(ii)).

These results allowed us to specifically select the D-Glucose treatment conditions, i.e., glucose concentration and time of exposure, effectively associated with an inflammatory response in yHUVEC and sHUVEC. All subsequent experiments were performed with 45 mM D-Glucose, treating young (24 h) and senescent cells (72 h) for different time.

It is not surprising that young and senescent cells are characterized by a different mean time of inflammatory responses when subjected to stressful stimuli. As an increased transcriptional activity of pro-inflammatory molecules is a key feature of senescent cells, it is reasonable to assume that young cells can rapidly increase the synthesis and release

of proinflammatory compounds in response to harmful stimuli, whereas senescent cells with SASPs require a longer treatment with stressogenic stimuli to be able to observe an intensive proinflammatory response [38].

3.2. Polydatin, Curcumin and Quercetin Effects on HUVECs Viability

After identifying the appropriate experimental conditions to mimic in vitro the inflammatory activation of endothelial cells induced by hyperglycemia, we tested the anti-inflammatory properties of Polydatin (POL), Curcumin (CUR) and Quercetin (QRC) natural compounds, either alone or mixed together (MIX). This experimental approach was applied to verify their potential synergistic effects. We previously reported that the combination of some natural compounds was able to improve their anti-inflammatory properties [37]. We firstly evaluated cell viability of yHUVEC (Figure 2A–D) and sHUVEC (Figure 2E–H) treated for 24 h and 72 h, respectively, with different concentrations of natural compounds alone. The concentrations to be used for subsequent experiments were selected based on cell viability > 70% compared to that of control HUVEC and resulted to be 10 μM POL, 1 μM CUR, 0.5 μM QRC, whether used individually or in combination (MIX).

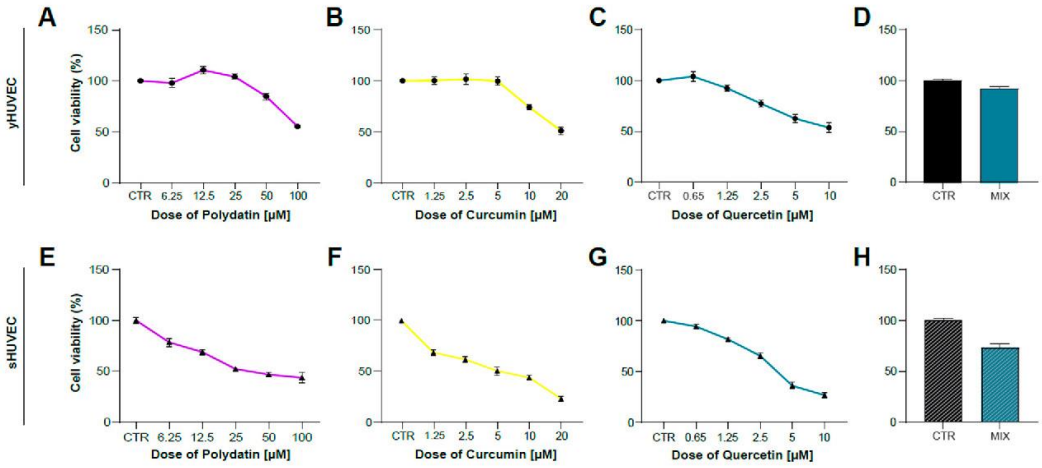

Figure 2. Dose–response curve of yHUVEC and sHUVEC to Polydatin, Curcumin, Quercetin and combination treatment. yHUVEC (**A**–**D**) and sHUVEC (**E**–**H**) were treated with different concentrations of Polydatin (from 6.25 μM to 100 μM), Curcumin (from 1.25 μM to 20 μM), Quercetin (from 0.65 μM to 10 μM), MIX or with DMSO alone as a control for the indicated times. The MTT assay was used to assess the effect of the treatments on cell viability. The results indicate the percentage of cell viability normalized to the viability of DMSO-treated cells (CTR) and presented as mean value ±SD from three independent biological replicates.

3.3. The Combined Natural Compounds Exert Anti-Inflammatory Activity on yHUVEC

To evaluate the anti-inflammatory activity of POL, CUR and QRC, yHUVEC were pre-treated for 2 h with 10 μM POL, 1 μM CUR, 0.5 μM QRC or the MIX (10 μM POL, 1 μM CUR and 0.5 μM QRC) and then treated for 24 h with D-Glucose (45 mM). We observed that the MIX significantly decreased the expression of MCP-1 and IL-8 but we did not observe a synergistic effect (Table 1), whereas CUR and POL alone significantly down-regulated MCP-1 and IL-8, respectively, compared to control yHUVEC (Figure 3A). These results were confirmed by the quantification of IL-8 chemokine release in the culture medium. High-glucose conditions were able to induce a significant up-regulation of IL-8 release, which was significantly reduced by the treatments with POL and the MIX (Figure 3B). IL-1β mRNA expression was not modulated by any of the three substances, either alone or in combination (Figure S1A).

Table 1. Effect of POL, CUR, QRC and MIX on gene expression versus expression after HG treatment in yHUVEC.

yHUVEC	MCP-1		IL-8		miR-126	
	Effect vs. HG (%)	Synergistic Effect *	Effect vs. HG (%)	Synergistic Effect *	Effect vs. HG (%)	Synergistic Effect *
POL	58	N	57	N	8	N
CUR	55		44		33	
QRC	54		27		84	
MIX	61		58		82	

N = None. * The effect of the three compounds (POL, CUR and QRC) taken together (MIX) is greater than the sum of their separate effect at the same doses.

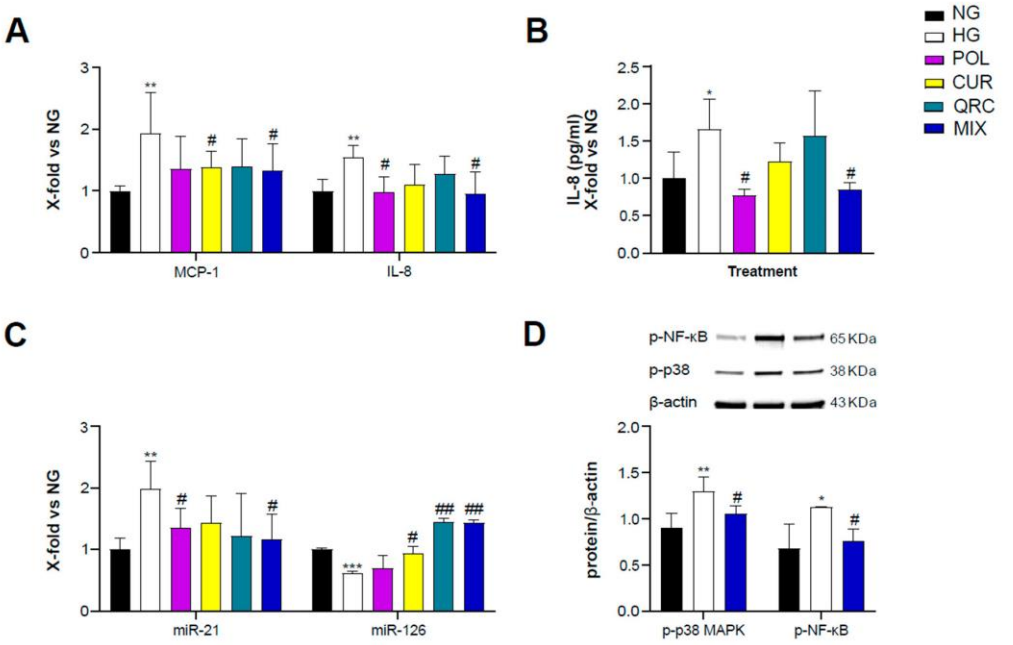

Figure 3. Effect of each compound following exposure to high glucose in yHUVEC. The cells were treated for 24 h with a single compound or with their combination. Relative mRNA expression of MCP-1 and IL-8 (**A**), concentration (pg/mL) of IL-8 in the culture medium (**B**), expression levels of miR-21 and miR-126 (**C**), representative western blot analysis showing p-p38 MAPK and p-NF-kB expression in yHUVEC treated with NG, HG or the MIX (**D**). β -actin levels were used as a control. The bands were quantified by ImageJ. All data are reported as fold change vs. untreated young HUVEC. The results are expressed as mean ±SD from three independent biological replicates. In all panels, asterisks (*) indicate significance versus NG; (#) indicates significance versus HG; one symbol, $p < 0.05$; two symbols, $p < 0.01$; three symbols, $p < 0.001$. NG, normal glucose; HG, high glucose; POL, polydatin; CUR, curcumin; QRC, quercetin; p-p38, phosphorylated-p38; p-NF-kB, phosphorylated-NF-kB; β -act, β -actin.

Since specific microRNAs such as miR-21 and miR-126 and miR-146a, belonging to the group of inflamma-miRs, are able to modulate inflammatory pathways and endothelial cell health [39–43] and are involved in the modulation of transcriptional programs related to the performance of endothelial cells [44], here we also analyzed their expression/modulation under HG and natural compounds treatment. miR-21 appeared significantly up-regulated in HG-exposed yHUVEC compared to control cells. Importantly, POL and MIX treatments

were both associated with a significant decrease of miR-21 levels, suggesting a reduction of the inflammatory response. A significant down-regulation of miR-126 was observed in HG-treated yHUVEC, and this phenomenon was significantly reverted by treatment with CUR, QRC and the MIX (Figure 3C), suggesting that these compounds can ameliorate the function of endothelial cells. In contrast, we observed increased miR-146a expression in yHUVEC exposed to HG, but the single substances and the MIX were ineffective in reducing it (Figure S1B).

Finally, we aimed to identify the pathways involved in the anti-inflammatory activity of the MIX. Among various intracellular proteins that can modulate inflammation, we selected p38 mitogen-activated protein kinases (MAPK), since it is one of the major players during inflammatory responses [45]. Indeed, p38 MAPK regulates the transcriptional activity of NF-kB by controlling the phosphorylation of the p65 subunit in a IKKγ-independent manner [46]. We found that the activation of p38 MAPK and the phosphorylation of NF-kB (p65 subunit) were increased in yHUVEC in high-glucose conditions compared to the control and significantly reduced by the MIX treatment (Figure 3D). This result suggests that the MIX could significantly restrain NF-kB activation.

3.4. Synergistic Anti-Inflammatory Effect of Natural Compounds on sHUVEC

As T2DM is an age-related disease, and aging is characterized by an increased burden of senescent cells, we aimed to address the anti-inflammatory effects of POL, CUR and QRC on senescent endothelial cells. sHUVEC were pre-treated for 2 h with all the natural compounds (10 µM POL, 1 µM CUR and 0.5 µM QRC or with their combination (MIX)), before adding glucose (45 mM D-Glucose) for 72 h exposure. First, sHUVEC were compared to yHUVEC. The expression of the main pro-inflammatory markers (IL-1β, IL-8, MCP-1, miR-21 and miR-146) confirmed that sHUVEC were characterized by an elevated inflammatory status at basal level (Figure 4A–C). Then, we noted that only the MIX was able to significantly reduce the expression of IL-1β, whereas CUR alone and the MIX significantly down-regulated IL-8 and MCP-1 expression compared to control cells (Figure 4A). Notably, we achieved a synergistic effect of the three natural compounds in reducing IL-1β and IL-8 expression (Table 2), as their combined action was greater than the sum of each individual compound's action [47].

Table 2. Effect of POL, CUR, QRC and the MIX on gene expression versus expression after HG treatment in sHUVEC.

sHUVEC	IL-1B		IL-8		miR-126	
	Effect vs. HG (%)	Synergistic Effect *	Effect vs. HG (%)	Synergistic Effect *	Effect vs. HG (%)	Synergistic Effect
POL	26	Y	28	Y	50	Y
CUR	34		50		5	
QRC	96		10		45	
MIX	163		102		145	

Y = Yes. * The effect of the three compounds (POL, CUR and QRC) taken together (MIX) is greater than the sum of their separate effect at the same doses.

Another interesting result is that POL e MIX treatments were able to significantly reduce the release of IL-8, which was increased in the medium of sHUVEC exposed to hyperglycemia (Figure 4B). These data suggest a senomorphic activity of these compounds, that is, a suppression of SASP effects without cell death. Senomorphic treatments provide an alternative pharmacological approach to target cellular senescence, since they suppress the detrimental effects of SASP components secreted by senescent cells without causing cell death.

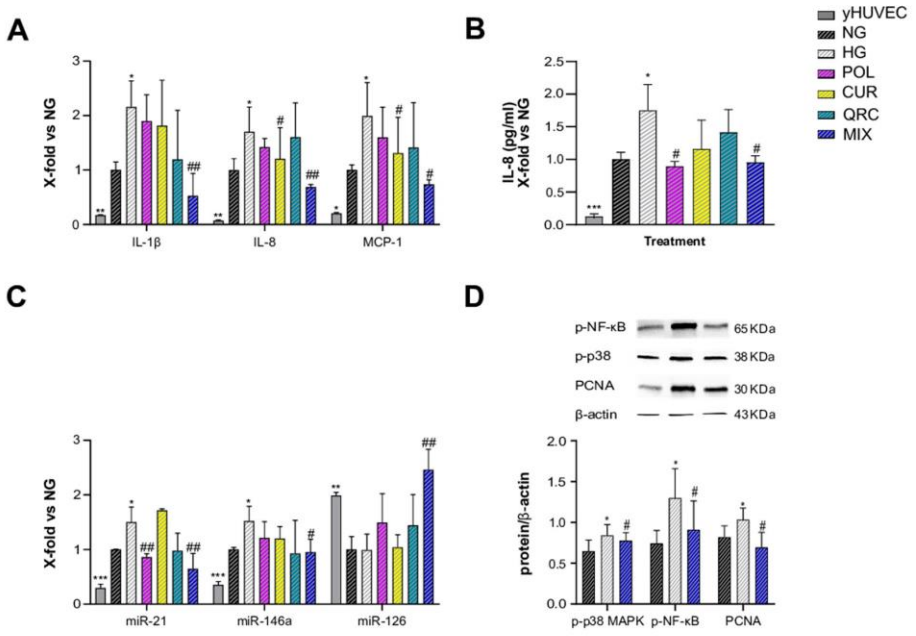

Figure 4. Effect of each compound following exposure to high glucose in sHUVEC. Cells were treated for 72 h with a single compound or with their combination. Relative mRNA expression of IL-1β, IL-8 and MCP-1 (**A**), concentration (pg/mL) of IL-8 in the culture medium (**B**), miRNA expression levels of miR-21, miR-146a and miR-126 (**C**), representative western blot analysis showing p-p38 MAPK, p-NF-kB and PCNA expression in sHUVEC cells treated with NG, HG or the MIX (**D**). β -actin levels were used as a control. The bands were quantified by ImageJ. All data are reported as fold change vs. untreated senescent HUVECs. The results are expressed as mean ±SD from three independent biological replicates. In all panels, asterisks (*) indicate significance versus NG; (#) indicates significance versus HG; one symbol, $p < 0.05$; two symbols, $p < 0.01$; three symbols $p < 0.001$. NG, normal glucose; HG, high glucose; POL, polydatin; CUR, curcumin; QRC, quercetin; p-p38, phosphorylated-p38; p-NF-kB, phosphorylated-NF-kB; PCNA, proliferating cell nuclear antigen; β -act, β -actin.

When the expression levels of miR-21, miR-146a and miR-126 were evaluated in sHUVEC, miR-21 showed a significant reduction in cells exposed to HG treated with POL, and, importantly, an even more relevant decrease was obtained with MIX treatment. A significant down-regulation was observed also for miR-146a in sHUVEC treated with the MIX. MiR-21 and miR-146a were previously identified as miRNAs able to restrain the activation of NF-kB, and therefore a reduction of their levels is indicative of an anti-inflammatory response [48]. Of note, even if we did not find any significant difference in the expression levels of miR-126 between sHUVEC cultured in high-glucose conditions and control cells cultured in normoglycemic medium, we obtained a synergistic effect of the MIX on the up-regulation of miR-126 expression compared to each tested compound (Figure 4C).

Lastly, increased activation of p38-MAPK and phosphorylation of p65-NF-kB were confirmed in sHUVEC exposed to HG, both modulated by the treatment with the MIX (Figure 4D). Besides, we also assessed the modulation of Proliferating Cell Nuclear Antigen (PCNA), as this molecule is involved in DNA damage repair [49]. In HG-sHUVEC. the level of PCNA was significant increased compared to control cells, indicating that a high glucose level can induce DNA damage. Of note, the treatment with the MIX significantly down-regulated the PCNA level (Figure 4D), thus suggesting a role of the natural compounds also in reducing DNA damage.

3.5. Antioxidants Activity of POL, CUR and QRC on yHUVEC and sHUVEC

It is well established that hyperglycemia leads to an increased production of reactive oxygen species (ROS) through several mechanisms [50]. Therapeutic strategies involving antioxidant natural molecules have become popular in the last decades. As expected, our experimental conditions showed a significant increase of ROS production in HG-exposed yHUVEC (Figure 5A) and sHUVEC (Figure 5C). Interestingly, only the treatment with QRC, and even more with MIX, induced a significant reduction of ROS levels in yHUVEC compared to the cells in HG conditions (Figure 5A). In sHUVEC, each of the three compounds, either alone or in combination, had a significant effect in reducing the production of ROS (Figure 5C).

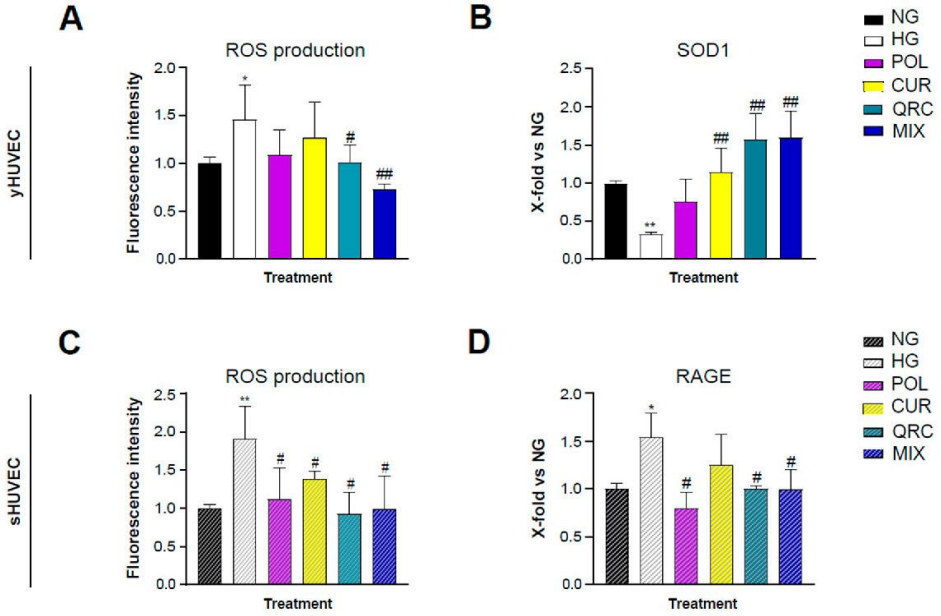

Figure 5. Effect of each natural compound on HG-induced ROS production in HUVEC. The cells were treated with a single compound or with their combination (MIX). Reactive oxygen species concentration was measured using the DCFDA assay in yHUVEC (**A**) and sHUVEC (**C**) cells. Relative mRNA expression of SOD1 (**B**) and RAGE (**D**) in yHUVEC and sHUVEC, respectively. All data are reported as fold change vs. untreated HUVEC cells. Results are expressed as mean ±SD from three independent biological replicates. In all panels, asterisks (*) indicate significance versus NG; (#) indicates significance versus HG; one symbol, $p < 0.05$; two symbols, $p < 0.01$. NG, normal glucose; HG, high glucose; POL, polydatin; CUR, curcumin; QRC, quercetin.

The expression of superoxide dismutase type 1 (SOD1) was also analyzed, since it is one of the main enzymes involved in ROS removal and conversion. SOD1 expression was significantly down-regulated in yHUVEC in HG compared to NG conditions. The treatment with CUR, QRC and MIX was associated with a substantial increase of SOD1 expression (Figure 5B). In sHUVEC, we did not find any modulation of SOD1 expression (data not shown). As in HUVECs the acquisition of the senescence phenotype is related to oxidative stress [51], we hypothesized that high-glucose conditions might not be able to induce a significative modification of SOD1 activity.

Thus, we evaluated the expression of RAGE, the receptor for AGE, whose formation is accelerated in high-glucose conditions and can promote activation of the NF-kB pathway and increased oxidative stress through its binding to RAGE [52]. Interestingly, we found that sHUVEC exposed to HG conditions expressed a significative higher level of RAGE

compared to control cells, which was significantly reduced at the mRNA level by POL, QRC and the MIX (Figure 5D).

4. Conclusions

Both in in vitro and in vivo models, a hyperglycemic status was demonstrated to deregulate the functionality of the endothelium, promoting the development of vascular complications and dysfunction [53]. Hyperglycemia is a diagnostic parameter for T2DM, a complex metabolic disorder characterized by glucidic and lipidic metabolism imbalance. At the cellular and molecular levels, a high-glucose condition is associated with increased ROS, responsible for vascular inflammation, nitric oxide (NO) synthesis inhibition, insulin resistance and protein and macromolecule glycation inducing the formation of AGEs.

Increasing evidence strongly suggests that nutritional supplement intake can contribute to improving endothelial dysfunction in T2DM patients.

In our study, we observed a synergistic effect of a specific combination of Polydatin, Curcumin and Quercetin (OxiDef^{TM}, Mivell), only in sHUVEC, in reducing the expression levels of IL-8 and IL-1β, two main SASP components, supporting the view that some natural compounds can act synergistically as "senomorphic", suppressing the most relevant markers of SASP and thus reducing the exacerbation and the spreading of SASP, that can fuel a systemic inflammatory chronic condition.

Overall, the most relevant and innovative results reported in our manuscript are the evaluation of the combination of two pro-inflammatory conditions: cellular senescence and hyperglycemia. This model mirrors the conditions that can be both present in vivo in diabetic patients, especially in those older and with poorer glycemic control, and therefore at higher risk of developing severe complications.

Our in vitro results strongly suggest testing OxiDef^{TM} as an adjuvant treatment in T2DM patients.

Supplementary Materials: The following supporting information can be downloaded at: https://www.mdpi.com/article/10.3390/antiox11061037/s1.

Author Contributions: Conceptualization, F.O. and G.M.; Methodology, D.V., A.S. and S.C.; Software, A.G. and C.G.; Data Curation, D.V. and J.S.; Writing—Original Draft Preparation, G.M.; Writing—Review & Editing, F.O., M.C.A. and M.R.R.; Supervision, M.C.A.; Project Administration, F.O. and G.M.; Funding Acquisition, F.O. All authors have read and agreed to the published version of the manuscript.

Funding: This study was supported by POR Marche FESR 2014/2020 funding I34I19007170007 from Regione Marche grants to FO, from Ricerca Corrente INRCA to FO and from Ricerca Scientifica di Ateneo (RSA) UNIVPM to FO.

Institutional Review Board Statement: Not Applicable.

Informed Consent Statement: Not Applicable.

Data Availability Statement: Data are contained within the article or supplementary material.

Conflicts of Interest: All authors declare no conflict of interest.

References

1. Franceschi, C.; Santoro, A.; Capri, M. The complex relationship between Immunosenescence and Inflammaging: Special issue on the New Biomedical Perspectives. *Semin. Immunopathol.* **2020**, *42*, 517–520. [CrossRef] [PubMed]
2. Prattichizzo, F.; De Nigris, V.; Mancuso, E.; Spiga, R.; Giuliani, A.; Matacchione, G.; Lazzarini, R.; Marcheselli, F.; Recchioni, R.; Testa, R.; et al. Short-term sustained hyperglycaemia fosters an archetypal senescence-associated secretory phenotype in endothelial cells and macrophages. *Redox Biol.* **2017**, *15*, 170–181. [CrossRef] [PubMed]
3. Fulop, T.; Witkowski, J.M.; Olivieri, F.; Larbi, A. The integration of inflammaging in age-related diseases. *Semin. Immunol.* **2018**, *40*, 17–35. [CrossRef] [PubMed]
4. Savji, N.; Rockman, C.B.; Skolnick, A.H.; Guo, Y.; Adelman, M.A.; Riles, T.; Berger, J.S. Association between advanced age and vascular disease in different arterial territories: A population database of over 3.6 million subjects. *J. Am. Coll. Cardiol.* **2013**, *61*, 1736–1743. [CrossRef]

5. Coppé, J.-P.; Desprez, P.-Y.; Krtolica, A.; Campisi, J. The Senescence-Associated Secretory Phenotype: The Dark Side of Tumor Suppression. *Annu. Rev. Pathol. Mech. Dis.* **2010**, *5*, 99–118. [CrossRef]
6. Wang, L.; Wang, B.; Gasek, N.S.; Zhou, Y.; Cohn, R.L.; Martin, D.E.; Zuo, W.; Flynn, W.F.; Guo, C.; Jellison, E.R.; et al. Targeting p21(Cip1) highly expressing cells in adipose tissue alleviates insulin resistance in obesity. *Cell Metab.* **2022**, *34*, 75–89.e8. [CrossRef]
7. Matacchione, G.; Perugini, J.; Di Mercurio, E.; Sabbatinelli, J.; Prattichizzo, F.; Senzacqua, M.; Storci, G.; Dani, C.; Lezoche, G.; Guerrieri, M.; et al. Senescent macrophages in the human adipose tissue as a source of inflammaging. *GeroScience* **2022**. [CrossRef]
8. Inoguchi, T.; Sonta, T.; Tsubouchi, H.; Etoh, T.; Kakimoto, M.; Sonoda, N.; Sato, N.; Sekiguchi, N.; Kobayashi, K.; Sumimoto, H.; et al. Protein Kinase C–Dependent Increase in Reactive Oxygen Species (ROS) Production in Vascular Tissues of Diabetes: Role of Vascular NAD(P)H Oxidase. *J. Am. Soc. Nephrol.* **2003**, *14* (Suppl. 3), S227–S232. [CrossRef]
9. Indyk, D.; Bronowicka-Szydełko, A.; Gamian, A.; Kuzan, A. Advanced glycation end products and their receptors in serum of patients with type 2 diabetes. *Sci. Rep.* **2021**, *11*, 13264. [CrossRef]
10. Deng, H.; Wang, S.; Li, L.; Zhou, Q.; Guo, W.; Wang, X.; Liu, M.; Liu, K.; Xiao, X. Puerarin prevents vascular endothelial injury through suppression of NF-kappaB activation in LPS-challenged human umbilical vein endothelial cells. *Biomed. Pharmacother.* **2018**, *104*, 261–267. [CrossRef]
11. Kwak, S.; Ku, S.-K.; Bae, J.-S. Fisetin inhibits high-glucose-induced vascular inflammation in vitro and in vivo. *Agents Actions* **2014**, *63*, 779–787. [CrossRef] [PubMed]
12. Lee, W.; Ku, S.K.; Lee, D.; Lee, T.; Bae, J.S. Emodin-6-O-beta-D–glucoside inhibits high-glucose-induced vascular inflammation. *Inflammation* **2014**, *37*, 306–313. [CrossRef] [PubMed]
13. Budamagunta, V.; Manohar-Sindhu, S.; Yang, Y.; He, Y.; Traktuev, D.O.; Foster, T.C.; Zhou, D. Senescence-associated hyper-activation to inflammatory stimuli in vitro. *Aging* **2021**, *13*, 19088–19107. [CrossRef] [PubMed]
14. Zhang, W.; Li, R.; Li, J.; Wang, W.; Tie, R.; Tian, F.; Liang, X.; Xing, W.; He, Y.; Yu, L.; et al. Alpha-Linolenic Acid Exerts an Endothelial Protective Effect against High Glucose Injury via PI3K/Akt Pathway. *PLoS ONE* **2013**, *8*, e68489. [CrossRef] [PubMed]
15. Yamagata, K.; Miyashita, A.; Matsufuji, H.; Chino, M. Dietary flavonoid apigenin inhibits high glucose and tumor necrosis factor α-induced adhesion molecule expression in human endothelial cells. *J. Nutr. Biochem.* **2010**, *21*, 116–124. [CrossRef]
16. Kim, A.; Yun, J.-M. Combination Treatments with Luteolin and Fisetin Enhance Anti-Inflammatory Effects in High Glucose-Treated THP-1 Cells Through Histone Acetyltransferase/Histone Deacetylase Regulation. *J. Med. Food* **2017**, *20*, 782–789. [CrossRef]
17. Gurău, F.; Baldoni, S.; Prattichizzo, F.; Espinosa, E.; Amenta, F.; Procopio, A.D.; Albertini, M.C.; Bonafè, M.; Olivieri, F. Anti-senescence compounds: A potential nutraceutical approach to healthy aging. *Ageing Res. Rev.* **2018**, *46*, 14–31. [CrossRef]
18. Stromsnes, K.; Correas, A.; Lehmann, J.; Gambini, J.; Olaso-Gonzalez, G. Anti-Inflammatory Properties of Diet: Role in Healthy Aging. *Biomedicines* **2021**, *9*, 922. [CrossRef]
19. Matacchione, G.; Gurău, F.; Baldoni, S.; Prattichizzo, F.; Silvestrini, A.; Giuliani, A.; Pugnaloni, A.; Espinosa, E.; Amenta, F.; Bonafè, M.; et al. Pleiotropic effects of polyphenols on glucose and lipid metabolism: Focus on clinical trials. *Ageing Res. Rev.* **2020**, *61*, 101074. [CrossRef]
20. Debelo, H.; Li, M.; Ferruzzi, M.G. Processing influences on food polyphenol profiles and biological activity. *Curr. Opin. Food Sci.* **2020**, *32*, 90–102. [CrossRef]
21. Ruan, H.; Huang, Q.; Wan, B.; Yang, M. Curcumin alleviates lipopolysaccharides-induced inflammation and apoptosis in vascular smooth muscle cells via inhibition of the NF-kappaB and JNK signaling pathways. *Inflammopharmacology* **2022**, *30*, 517–525. [CrossRef] [PubMed]
22. Weiskirchen, S.; Weiskirchen, R. Resveratrol: How Much Wine Do You Have to Drink to Stay Healthy? *Adv. Nutr.* **2016**, *7*, 706–718. [CrossRef] [PubMed]
23. Mokgalaboni, K.; Ntamo, Y.; Ziqubu, K.; Nyambuya, T.M.; Nkambule, B.B.; Mazibuko-Mbeje, S.E.; Gabuza, K.B.; Chellan, N.; Tiano, L.; Dludla, P.V. Curcumin supplementation improves biomarkers of oxidative stress and inflammation in conditions of obesity, type 2 diabetes and NAFLD: Updating the status of clinical evidence. *Food Funct.* **2021**, *12*, 12235–12249. [CrossRef] [PubMed]
24. Hou, K.; Chen, Y.; Zhu, D.; Chen, G.; Chen, F.; Xu, N.; Chen, R. Curcumin inhibits high glucose oxidative stress and apoptosis in pancreatic beta cells via CHOP/PCG-1a and pERK1/2. *Front. Biosci.* **2020**, *25*, 1974–1984.
25. Zheng, L.; Wu, J.; Mo, J.; Guo, L.; Wu, X.; Bao, Y. Polydatin Inhibits Adipose Tissue Inflammation and Ameliorates Lipid Metabolism in High-Fat-Fed Mice. *BioMed Res. Int.* **2019**, *2019*, 7196535. [CrossRef]
26. Abd El-Hameed, A.M.; Yousef, A.I.; Abd El-Twab, S.M.; El-Shahawy, A.A.G.; Abdel-Moneim, A. Hepatoprotective Effects of Polydatin-Loaded Chitosan Nanoparticles in Diabetic Rats: Modulation of Glucose Metabolism, Oxidative Stress, and Inflammation Biomarkers. *Biochemistry* **2021**, *86*, 179–189. [CrossRef]
27. Abd El-Hameed, A.M. Polydatin-loaded chitosan nanoparticles ameliorates early diabetic nephropathy by attenuating oxidative stress and inflammatory responses in streptozotocin-induced diabetic rat. *J. Diabetes Metab. Disord.* **2020**, *19*, 1599–1607. [CrossRef]
28. Chen, G.; Yang, Z.; Wen, D.; Guo, J.; Xiong, Q.; Li, P.; Zhao, L.; Wang, J.; Wu, C.; Dong, L. Polydatin has anti-inflammatory and antioxidant effects in LPS-induced macrophages and improves DSS-induced mice colitis. *Immun. Inflamm. Dis.* **2021**, *9*, 959–970. [CrossRef]

29. Wan, H.; Wang, Y.; Pan, Q.; Chen, X.; Chen, S.; Li, X.; Yao, W. Quercetin attenuates the proliferation, inflammation, and oxidative stress of high glucose-induced human mesangial cells by regulating the miR-485-5p/YAP1 pathway. *Int. J. Immunopathol. Pharmacol.* **2022**, *36*, 20587384211066440. [CrossRef]
30. Liu, L.; Huang, S.; Xu, M.; Gong, Y.; Li, D.; Wan, C.; Wu, H.; Tang, Q. Isoquercitrin protects HUVECs against high glucose-induced apoptosis through regulating p53 proteasomal degradation. *Int. J. Mol. Med.* **2021**, *48*, 122. [CrossRef]
31. Ozyel, B.; Le Gall, G.; Needs, P.W.; Kroon, P.A. Anti-Inflammatory Effects of Quercetin on High-Glucose and Pro-Inflammatory Cytokine Challenged Vascular Endothelial Cell Metabolism. *Mol. Nutr. Food Res.* **2021**, *65*, e2000777. [CrossRef] [PubMed]
32. Fan, T.; Du, Y.; Zhang, M.; Zhu, A.R.; Zhang, J. Senolytics Cocktail Dasatinib and Quercetin Alleviate Human Umbilical Vein Endothelial Cell Senescence via the TRAF6-MAPK-NF-kappaB Axis in a YTHDF2-Dependent Manner. *Gerontology* **2022**, 1–15. [CrossRef] [PubMed]
33. Zhao, B.; Zhang, Q.; Liang, X.; Xie, J.; Sun, Q. Quercetin reduces inflammation in a rat model of diabetic peripheral neuropathy by regulating the TLR4/MyD88/NF-kappaB signalling pathway. *Eur. J. Pharmacol.* **2021**, *912*, 174607. [CrossRef]
34. Feng, X.; Bu, F.; Huang, L.; Xu, W.; Wang, W.; Wu, Q. Preclinical evidence of the effect of quercetin on diabetic nephropathy: A meta-analysis of animal studies. *Eur. J. Pharmacol.* **2022**, *921*, 174868. [CrossRef] [PubMed]
35. Wagner, H. Synergy research: Approaching a new generation of phytopharmaceuticals. *Fitoterapia* **2011**, *82*, 34–37. [CrossRef]
36. Zhang, L.; Virgous, C.; Si, H. Synergistic anti-inflammatory effects and mechanisms of combined phytochemicals. *J. Nutr. Biochem.* **2019**, *69*, 19–30. [CrossRef] [PubMed]
37. Matacchione, G.; Gurău, F.; Silvestrini, A.; Tiboni, M.; Mancini, L.; Valli, D.; Rippo, M.R.; Recchioni, R.; Marcheselli, F.; Carnevali, O.; et al. Anti-SASP and anti-inflammatory activity of resveratrol, curcumin and beta-caryophyllene association on human endothelial and monocytic cells. *Biogerontology* **2021**, *22*, 297–313. [CrossRef] [PubMed]
38. Van Deursen, J.M. The role of senescent cells in ageing. *Nature* **2014**, *509*, 439–446. [CrossRef]
39. Dimmeler, S.; Nicotera, P. MicroRNAs in age-related diseases. *EMBO Mol. Med.* **2013**, *5*, 180–190. [CrossRef]
40. Harris, T.A.; Yamakuchi, M.; Ferlito, M.; Mendell, J.T.; Lowenstein, C.J. MicroRNA-126 regulates endothelial expression of vascular cell adhesion molecule 1. *Proc. Natl. Acad. Sci. USA* **2008**, *105*, 1516–1521. [CrossRef]
41. Tili, E.; Michaille, J.; Cimino, A.; Costinean, S.; Dumitru, C.D.; Adair, B.; Fabbri, M.; Alder, H.; Liu, C.G.; Calin, G.A.; et al. Modulation of miR-155 and miR-125b levels following lipopolysaccharide/TNF-alpha stimulation and their possible roles in regulating the response to endotoxin shock. *J. Immunol.* **2007**, *179*, 5082–5089. [CrossRef] [PubMed]
42. O'Connell, R.M.; Rao, D.S.; Chaudhuri, A.A.; Boldin, M.P.; Taganov, K.D.; Nicoll, J.; Paquette, R.L.; Baltimore, D. Sustained expression of microRNA-155 in hematopoietic stem cells causes a myeloproliferative disorder. *J. Exp. Med.* **2008**, *205*, 585–594. [CrossRef] [PubMed]
43. Olivieri, F.; Rippo, M.R.; Procopio, A.D.; Fazioli, F. Circulating inflamma-miRs in aging and age-related diseases. *Front. Genet.* **2013**, *4*, 121. [CrossRef] [PubMed]
44. Wang, S.; Aurora, A.B.; Johnson, B.A.; Qi, X.; McAnally, J.; Hill, J.A.; Richardson, J.A.; Bassel-Duby, R.; Olson, E.N. The Endothelial-Specific MicroRNA miR-126 Governs Vascular Integrity and Angiogenesis. *Dev. Cell* **2008**, *15*, 261–271. [CrossRef] [PubMed]
45. Yang, Y.; Kim, S.C.; Yu, T.; Yi, Y.-S.; Rhee, M.H.; Sung, G.-H.; Yoo, B.C.; Cho, J.Y. Functional Roles of p38 Mitogen-Activated Protein Kinase in Macrophage-Mediated Inflammatory Responses. *Mediat. Inflamm.* **2014**, *2014*, 352371. [CrossRef]
46. Jijon, H.; Allard, B.; Jobin, C. NF-kappaB inducing kinase activates NF-kappaB transcriptional activity independently of IkappaB kinase gamma through a p38 MAPK-dependent RelA phosphorylation pathway. *Cell Signal.* **2004**, *16*, 1023–1032. [CrossRef]
47. Sonam, K.S.; Guleria, S. Synergistic Antioxidant Activity of Natural Products. *Ann. Pharmacol. Pharm.* **2017**, *2*, 1086.
48. Olivieri, F.; Prattichizzo, F.; Giuliani, A.; Matacchione, G.; Rippo, M.R.; Sabbatinelli, J.; Bonafè, M. miR-21 and miR-146a: The microRNAs of inflammaging and age-related diseases. *Ageing Res. Rev.* **2021**, *70*, 101374. [CrossRef]
49. Moldovan, G.-L.; Pfander, B.; Jentsch, S. PCNA, the Maestro of the Replication Fork. *Cell* **2007**, *129*, 665–679. [CrossRef]
50. Bonnefont-Rousselot, D. Glucose and reactive oxygen species. *Curr. Opin. Clin. Nutr. Metab. Care* **2002**, *5*, 561–568. [CrossRef]
51. Bodega, G.; Alique, M.; Bohórquez, L.; Ciordia, S.; Mena, M.C.; Ramírez, M.R. The Antioxidant Machinery of Young and Senescent Human Umbilical Vein Endothelial Cells and Their Microvesicles. *Oxidative Med. Cell. Longev.* **2017**, *2017*, 7094781. [CrossRef] [PubMed]
52. Yamagishi, S.-I.; Fukami, K.; Matsui, T. Crosstalk between advanced glycation end products (AGEs)-receptor RAGE axis and dipeptidyl peptidase-4-incretin system in diabetic vascular complications. *Cardiovasc. Diabetol.* **2015**, *14*, 2. [CrossRef] [PubMed]
53. Patel, H.; Chen, J.; Das, K.C.; Kavdia, M. Hyperglycemia induces differential change in oxidative stress at gene expression and functional levels in HUVEC and HMVEC. *Cardiovasc. Diabetol.* **2013**, *12*, 142. [CrossRef] [PubMed]

7. CONCLUSIONS

Plant-derived secondary metabolites are active molecules with a diversity of biological properties beneficial to human health. For this reason, they have been long used for their clinical therapeutic application. It is actually known, that bioactive molecules influence the expression of genes and proteins, activating or inhibiting various metabolic pathways involved in different biological processes. For this reason, the aim of this research was the study of the functional properties of plant secondary metabolites, with particular attention to phenols of *P. Spinosa* L. extract, curcumin, polydatin and quercetin. Considering the increasing interest of natural extracts for the functionalization of biomaterials, *in silico* bioinformatics analyses can certainly be a first useful approach to identify the modulated pathways following the interaction between cell and substrate. Furthermore, the inclusion of natural molecules into electrospun scaffolds can support and improve material biocompatibility. This approach has important applications in disease treatment for different purposes including drug delivery (i.e. drugs, nucleic acids and hormones) and targeted and personalized medicine. The *P. Spinosa* extract can be a good candidate to the functionalization of biomaterials since *in vitro* and *in vivo* approaches identified appropriate functional characteristics that have been successfully applied in leucosome biomimetic nanosystems encapsulation for wound healing treatment. Biomimetic nanoparticles have also recently emerged as innovative drug delivery systems for highly effective and safe next-generation therapies.

Growing evidences strongly suggest that diet rich in polyphenols can reduce the inflammatory condition associated with the development of different diseases. In this study, inflamma-miRs contained in food were identified for their ability to modulate inflammatory processes.

Specifically, curcumin, polydatin and quercetin demonstrated antioxidant, anti-inflammatory and hypoglycemic abilities.

Overall, our data suggest that the use of secondary plant metabolites may be an adjuvant therapeutic treatment to counteract the pro-inflammatory and pro-oxidative conditions induced by aging and the associated diseases. These properties can also be exploited in biomedicine, both for the functionalization of biomaterials and for drug delivery.

8. References

1. Ghasemi-Mobarakeh L, Kolahreez D, Ramakrishna S, Williams D (2019) Key terminology in biomaterials and biocompatibility. Curr. Opin. Biomed. Eng. 10:45–50

2. Power KA, Fitzgerald KT, Gallagher WM (2010) Examination of cell-host-biomaterial interactions via high-throughput technologies: A re-appraisal. Biomaterials 31:6667–6674. https://doi.org/10.1016/j.biomaterials.2010.05.029

3. Liu X, Xu H, Zhang M, Yu DG (2021) Electrospun Medicated Nanofibers for Wound Healing: Review. Membranes (Basel) 11:. https://doi.org/10.3390/MEMBRANES11100770

4. Ping Neo Y, Ray S, Jin J, et al (2013) Encapsulation of food grade antioxidant in natural biopolymer by electrospinning technique: A physicochemical study based on zeinâ€“gallic acid system. Food Chem 136:1013–1021. https://doi.org/10.1016/j.foodchem.2012.09.010

5. Coppari S, Ramakrishna S, Teodori L, Albertini MC (2021) Cell signalling and biomaterials have a symbiotic relationship as demonstrated by a bioinformatics study: The role of surface topography. Curr Opin Biomed Eng 17:. https://doi.org/10.1016/j.cobme.2020.09.002

6. Bacakova L, Filova E, Parizek M, et al (2011) Modulation of cell adhesion, proliferation and differentiation on materials designed for body implants. Biotechnol. Adv. 29:739–767

7. Ma W, Ding Y, Zhang M, et al (2020) Nature-inspired chemistry toward hierarchical superhydrophobic, antibacterial and biocompatible nanofibrous membranes for effective UV-shielding, self-cleaning and oil-water separation. J Hazard Mater 384:121476. https://doi.org/10.1016/J.JHAZMAT.2019.121476

8. Guo J, Suma T, Richardson JJ, Ejima H (2019) Modular Assembly of Biomaterials Using Polyphenols as Building Blocks. ACS Biomater Sci Eng 5:5578–5596. https://doi.org/10.1021/ACSBIOMATERIALS.8B01507

9. Cazzola M, Ferraris S, Boschetto F, et al (2018) Green Tea Polyphenols Coupled with a Bioactive Titanium Alloy Surface: In Vitro Characterization of Osteoinductive Behavior through a KUSA A1 Cell Study. Int J Mol Sci 19:2255. https://doi.org/10.3390/IJMS19082255

10. Munin A, Edwards-Lévy F (2011) Encapsulation of natural polyphenolic compounds; a review. Pharmaceutics 3:793–829. https://doi.org/10.3390/PHARMACEUTICS3040793

11. Kumar N, Goel N (2019) Phenolic acids: Natural versatile molecules with promising therapeutic applications. Biotechnol Reports 24:. https://doi.org/10.1016/J.BTRE.2019.E00370

12. Cheng YC, Sheen JM, Hu WL, Hung YC (2017) Polyphenols and Oxidative Stress in Atherosclerosis-Related Ischemic Heart Disease and Stroke. Oxid Med Cell Longev 2017:. https://doi.org/10.1155/2017/8526438

13. Franceschi C, Garagnani P, Parini P, et al (2018) Inflammaging: a new immune-metabolic viewpoint for age-related diseases. Nat Rev Endocrinol 14:576–590. https://doi.org/10.1038/S41574-018-0059-4

14. Cuollo L, Antonangeli F, Santoni A, Soriani A (2020) The Senescence-Associated Secretory Phenotype (SASP) in the Challenging Future of Cancer Therapy and Age-Related Diseases. Biology (Basel) 9:1–16. https://doi.org/10.3390/BIOLOGY9120485

15. Choi SW, Lee JY, Kang KS (2017) miRNAs in stem cell aging and age-related disease. Mech Ageing Dev 168:20–29. https://doi.org/10.1016/J.MAD.2017.08.013

16. Lu H, Yao Y, Yang J, et al (2021) Microbiome–miRNA interactions in the progress from undifferentiated arthritis to rheumatoid arthritis: evidence, hypotheses, and opportunities. Rheumatol Int 41:1567. https://doi.org/10.1007/S00296-021-04798-3

17. Yoo JY, Groer M, Dutra SVO, et al (2020) Gut Microbiota and Immune System Interactions. Microorganisms 8:1–22. https://doi.org/10.3390/MICROORGANISMS8101587

18. Teodori L, Petrignani I, Giuliani A, et al (2019) Inflamm-aging microRNAs may integrate signals from food and gut microbiota by modulating common signalling

pathways. Mech Ageing Dev 182:. https://doi.org/10.1016/j.mad.2019.111127

19. Marques-Rocha JL, Samblas M, Milagro FI, et al (2015) Noncoding RNAs, cytokines, and inflammation-related diseases. FASEB J 29:3595–3611. https://doi.org/10.1096/FJ.14-260323

20. Tiboni M, Coppari S, Casettari L, et al (2020) Prunus spinosa Extract Loaded in Biomimetic Nanoparticles Evokes In Vitro Anti-Inflammatory and Wound Healing Activities. Nanomaterials 11:36. https://doi.org/10.3390/nano11010036

21. Lunyak V V., Amaro-Ortiz A, Gaur M (2017) Mesenchymal Stem Cells Secretory Responses: Senescence Messaging Secretome and Immunomodulation Perspective. Front Genet 8:220. https://doi.org/10.3389/FGENE.2017.00220

22. Krizhanovsky V, Yon M, Dickins RA, et al (2008) Senescence of activated stellate cells limits liver fibrosis. Cell 134:657–667. https://doi.org/10.1016/J.CELL.2008.06.049

23. Demaria M, Ohtani N, Youssef SA, et al (2014) An essential role for senescent cells in optimal wound healing through secretion of PDGF-AA. Dev Cell 31:722–733. https://doi.org/10.1016/J.DEVCEL.2014.11.012

24. Mosteiro L, Pantoja C, Alcazar N, et al (2016) Tissue damage and senescence provide critical signals for cellular reprogramming in vivo. Science 354:. https://doi.org/10.1126/SCIENCE.AAF4445

25. Acosta JC, Banito A, Wuestefeld T, et al (2013) A complex secretory program orchestrated by the inflammasome controls paracrine senescence. Nat Cell Biol 15:978–990. https://doi.org/10.1038/NCB2784

26. Eming SA, Krieg T, Davidson JM (2007) Inflammation in Wound Repair: Molecular and Cellular Mechanisms. J Invest Dermatol 127:514–525. https://doi.org/10.1038/SJ.JID.5700701

27. Gurău F, Baldoni S, Prattichizzo F, et al (2018) Anti-senescence compounds: A potential nutraceutical approach to healthy aging. Ageing Res Rev 46:14–31. https://doi.org/10.1016/J.ARR.2018.05.001

28. Ghitescu RE, Popa AM, Popa VI, et al (2015) Encapsulation of polyphenols into

pHEMA e-spun fibers and determination of their antioxidant activities. Int J Pharm 494:278–287. https://doi.org/10.1016/J.IJPHARM.2015.08.020

29. Li Y, Zhang J-J, Xu D-P, et al (2016) Bioactivities and Health Benefits of Wild Fruits. Int J Mol Sci 17:. https://doi.org/10.3390/IJMS17081258

30. Giampieri F, Alvarez-suarez JM, Battino M, et al (2014) Strawberry and Human Health : E ff ects beyond Antioxidant Activity

31. Pinacho R, Cavero RY, Astiasarán I, et al (2015) Phenolic compounds of blackthorn (Prunus spinosa L.) and influence of in vitro digestion on their antioxidant capacity. J Funct Foods 19:49–62. https://doi.org/10.1016/j.jff.2015.09.015

32. Radovanović BC, Andelković ASM, Radovanović AB, Andelković MZ (2013) Antioxidant and antimicrobial activity of polyphenol extracts from wild berry fruits grown in Southeast Serbia. Trop J Pharm Res 12:813–819. https://doi.org/10.4314/tjpr.v12i5.23

33. Olszewska M (2014) Flavonoids from the flowers of Prunus spinosa L

34. Albertini MC, Fraternale D, Semprucci F, et al (2019) Bioeffects of Prunus spinosa L . fruit ethanol extract on reproduction and phenotypic plasticity of Trichoplax. 1883:1–22. https://doi.org/10.7717/peerj.6789

35. Marchelak A, Owczarek A, Matczak M, et al (2017) Bioactivity Potential of Prunus spinosa L . Flower Extracts : Phytochemical Profiling , Cellular Safety , Pro-inflammatory Enzymes Inhibition and Protective Effects Against Oxidative Stress In Vitro. 8:. https://doi.org/10.3389/fphar.2017.00680

36. Fraternale D, Giamperi L, Bucchini A, et al (2009) Prunus spinosa fresh fruit juice: Antioxidant activity in cell-free and cellular systems. Nat Prod Commun 4:1665–1670. https://doi.org/10.1177/1934578x0900401211

37. Sabatini L, Fraternale D, Di Giacomo B, et al (2020) Chemical composition, antioxidant, antimicrobial and anti-inflammatory activity of Prunus spinosa L. fruit ethanol extract. J Funct Foods 67:103885. https://doi.org/10.1016/j.jff.2020.103885

38. Ruiz A, Hermosín-Gutiérrez I, Vergara C, et al (2013) Anthocyanin profiles in south Patagonian wild berries by HPLC-DAD-ESI-MS/MS. Food Res Int 51:706–713.

https://doi.org/10.1016/j.foodres.2013.01.043

39. Kesarwani K, Gupta R (2013) Bioavailability enhancers of herbal origin: An overview. Asian Pac J Trop Biomed 3:253. https://doi.org/10.1016/S2221-1691(13)60060-X

ACKNOWLEDGEMENTS

First, I would like to express my sincere gratitude to my advisor Prof. Maria Cristina Albertini for the helping, encouraging, and supporting me during these years. I also wish to express my gratitude to all the people that I had the opportunity to work with at the University of Urbino.